Founded 1925

Incorporated
by Royal Charter 1961

*To promote the advancement of radio, electronics and kindred subjects by the exchange of information in these branches of engineering*

Volume 51 No. 6

June 1981

# The Radio and Electronic Engineer

**The Journal of the Institution of Electronic and Radio Engineers**

## The Benevolent Eye in the Sky

Most of us have during recent years become aware of the contribution made by meteorological satellites to aiding the still imprecise science (or art?) of weather forecasting. The superimposition on the synoptic charts of pictures from satellites showing the cyclonic patterns of cloud over the Atlantic Ocean has brought reality to the forecasters' talk of 'warm' and 'cold' fronts. But there are other important applications which remote sensing satellites have made possible by enabling completely new kinds of observation to be made, which are just as innovatory as the meteorological pictures and can have just as great an effect on man's knowledge of his environment.

Over the past ten years, several series of satellites with remote sensing capabilities have been put into orbit and provide sources of almost overwhelming amounts of data telemetered back to Earth stations for processing. Particularly active in this work has been the National Remote Sensing Centre (NRSC) at RAE Farnborough which has developed a new technique using information from satellites to produce a more accurate picture than ever before of the whole of the UK, and indeed other parts of the World.

The picture, known as a digital mosaic, is derived from data transmitted by the *Landsat* remote sensing satellites. It combines a high degree of accuracy with wide geographical coverage and excellent resolution. Although it can be put to many uses, the mosaic is particularly important as the foundation of a precise digital data base which can be used for planning and environmental monitoring.

NRSC's technique can be applied to almost any satellite imagery, enabling changes in the landscape to be examined much more accurately than before, opening up new opportunities for mapping and monitoring land use, especially in underdeveloped countries. For example, the Centre has completed a hydrology project in Botswana using the new method, providing more accurate cartographic information than in available maps or where maps did not exist at all. An example of the technique's use in the UK is a recent analysis of images of the Bristol Channel which showed that sandbanks have shifted substantially since maps of the area were last revised.

The very wide range of uses for information gathered by remote sensing satellites includes:

Land use surveying; Monitoring inland and coastal waters for pollution and sedimentation; Surveying routes for railways, roads and pipelines; Evaluating crop types and yields; Agricultural monitoring of diseases and pests; Maintaining woodland inventories; Geological surveying for mineral and oil deposits.

The mosaic of the UK was formed from 43 separate 185 km × 185 km scenes acquired by the *Landsat* satellites which observe the surface of the Earth with a multi-spectral scanner which operates in four bands of the spectrum. Two of these are in the visible (Bands 4: 0·5 to 0·6 $\mu$m, and 5: 0·6 to 0·7 $\mu$m, roughly equivalent to green and red respectively) and two are in the near infra-red (Bands 6: 0·7 to 0·8 $\mu$m and 7: 0·8 to 1·1 $\mu$m). From an orbital height of 900 km, this sensor records a scene as an array of picture elements, or pixels, measuring 57 m × 79 m. The orbit of these spacecraft is such that the sensors cover the entire surface of the Earth between latitudes of 82 degrees N and 82 degrees S every 18 days.

*Landsat 3* also carries a return beam vidicon sensor which is similar in operation to a black and white television camera. This gives an improved spatial resolution of about 40 m, but observations are only made in one broad spectral band (0·5 to 0·75 $\mu$m).

The initial process required to construct a digital mosaic is the transformation of all images needed into the same geographical co-ordinate system, in this case the UK National Grid. This can be done accurately only if a number of ground control points can be located on each image: these are prominent points, such as airfield runway intersections, headlands and major road junctions, which can be clearly identified in both the image and the appropriate maps.

In forming the mosaic, 1200 ground control points were found by eye in the 43 *Landsat* scenes, with up to 120 in one image. Knowledge of their co-ordinates allowed the transformation to be derived for each scene, to an accuracy of 50 m with respect to the National Grid. A pixel size of 100 m × 100 m was selected, which allows the complete mosaic to be stored on a 300 megabyte computer disk store.

The sensor provides some overlap between adjacent scenes and use was made of this feature in constructing the mosaic. In the overlapping areas, histograms of the

data were examined in the computer, and contrast changes introduced to match the scenes. This technique eliminates the joins between scenes which are so often visible in photographic mosaics.

The result of this procedure was a digital image covering the whole of the UK, in each of the spectral bands. Separate photographic negatives were then produced using a Linoscan film-writing machine. A false colour composite image from bands 4, 5 and 7, was formed using the Plessey IDP 3000 digital interactive interpretation facility to adjust the colour balance. It is described as a false colour image because band 4 is arbitrarily produced as blue, band 5 as green and band 7 as red.

The size of the computing task involved in constructing the mosaic can be illustrated by stating that the 43 *Landsat* scenes contain a total of 327 million pixels in each of their four spectral bands, and that the final mosaic has 70 million pixels. No less than 17 magnetic tapes are needed to store it.

It is not possible to reproduce the fine detail of the mosaic in a small photograph, but the full resolution data is accessible in digital form, and photographs of small areas can be produced at full resolution. In the November/December issue of *The Radio and Electronic Engineer* a paper on certain aspects of comparable work in Sweden was published which was accompanied by colour illustrations such as are essential in realizing the full potential of the multi-spectral scanner.

The NRSC is one of a number of similar organizations making use of this potentially invaluable space technique. It was set up within the Space Department at RAE Farnborough on 1st April 1980 and its role is:

to provide a system for the supply of remote sensing data and imagery;
to provide facilities for research into, and development of, data processing, analysis and interpretive techniques;
to act as a focal point for the development of remote sensing techniques and their application;
to provide educational and training facilities in remote sensing techniques.

The Centre is funded by a number of Government bodies, including: Department of Industry; Department of the Environment; Ministry of Agriculture, Fisheries and Food; Overseas Development Administration; Natural Environment Research Council; and the Scottish Development Department. Its work is determined by a Programme Board, comprising representatives of those bodies contributing to the Centre.

The Centre is concerned with research into techniques of remote sensing, data processing, analysis and interpretation for a wide variety of applications on behalf of or in conjunction with users. Among the fields of application which are the subject of current work are forestry, cartography, coastal sedimentation and morphology, wave dynamics, exploration geology and land cover survey.

Remote sensing from satellites is obviously an impressive technique using highly involved electronic systems which were initially developed to meet military surveillance requirements: its potentialities for aiding the peaceful needs of the human race have hardly begun but will certainly be of the very greatest significance.

F. W. S.

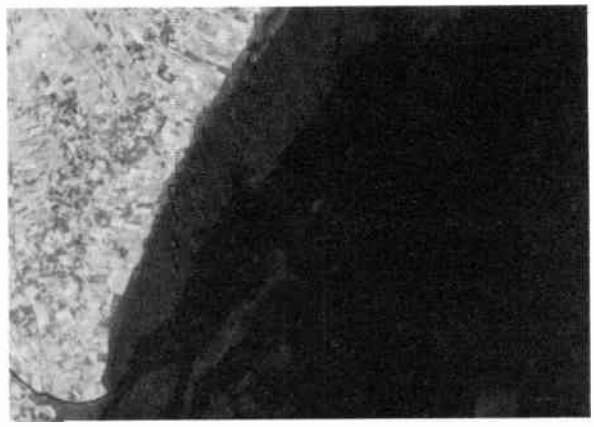

(a) Original band 5 red image with a contrast stretch.

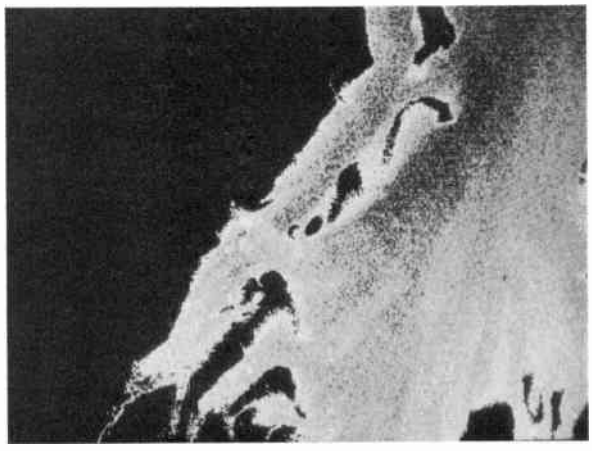

(b) Density sliced version of (a) with the darkest tones representing deep water and the lighter tones shallow or sediment-laden water.

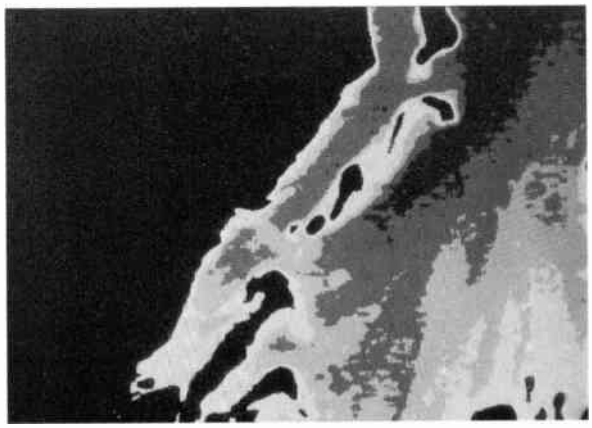

(c) Same density slice as (b) but applied after digital filtering to remove striping and noise within the image. A 7 × 7 equal-weight convolution filter has been used.

The IDP 3000 digital interactive image processing system was used to produce these black and white images of part of The Wash, from data collected by *Landsat 1* on 26th June 1976.

# Notice to all Corporate Members of the Institution of Electronic and Radio Engineers

## NOMINATIONS FOR ELECTION TO THE 1981–82 COUNCIL OF THE INSTITUTION

In accordance with Bye-law 49, the Council has nominated the following members for election at the Annual General Meeting to be held on Thursday, 29th October 1981:

**President**

*For Election:* H. E. Drew, C.B.

**Vice-Presidents**

Under Bye-law 46, all Vice-Presidents retire each year but may be re-elected provided they do not serve thereby for more than three years in succession.

*For Re-election:* Professor J. R. James, B.Sc., Ph.D., D.Sc.; P. K. Patwardhan, M.Sc., Ph.D.

*For Election:* Colonel W. Barker; L. A. Bonvini; Major-General H. E. Roper, C.B., B.Sc.(Eng.) D. L. A. Smith, B.Sc.(Eng.); Group Captain J. M. Walker, R.A.F.

**Honorary Treasurer**

*For Re-election:* S. R. Wilkins

**Ordinary Members of Council**

Under Bye-law 48, Ordinary Members of Council are elected for three years and may not hold that office for more than three years in succession.

FELLOWS

*The following must retire:* Sir Robert Clayton, C.B.E., M.A., F.Eng.; C. S. den Brinker, M.Sc.; Major-General H. E. Roper, C.B., B.Sc.(Eng.); D. L. A. Smith, B.Sc.(Eng.)

*For election:* L. W. Barclay, B.Sc.; G. A. McKenzie; V. Maller, M.A.; Professor K. G. Nichols, B. Sc., M.Sc.

MEMBERS

*The following must retire:* C. J. Lilly

*For election:* P. Atkinson, B.Sc.(Eng.)

HONORARY FELLOW OR COMPANION

*The following must retire:* H. J. Kroch, O.B.E.

*For election:* R. B. Michaelson

The remaining members of Council will continue to serve in accordance with the period of office laid down in Bye-law 48.

Within twenty-eight days after the publication of the names of the persons nominated by the Council for the vacancies about to occur any ten or more Corporate Members may nominate any one other duly qualified person to fill any of these vacancies by causing to be delivered to the Secretary a nomination in writing signed by them together with the written consent of the person nominated undertaking to accept office if elected, but each nominator shall be debarred from nominating any other person for the same vacancy (Bye-law 50).

By Order of the Council
S. M. DAVIDSON
*Secretary*

*1st June 1981*

# Members' Appointments

## CORPORATE MEMBERS

**B. V. Northall G.C.I.A.** (Fellow 1981, Member 1955) who was an Assistant Staff Engineer with the Post Office, retired last year and is now a self-employed consultant. Mr Northall received the City & Guilds Insignia Award in 1963 for his thesis entitled 'Factors affecting the design of an audio frequency magnetic recording system'; he is currently chairman of the City and Guilds Insignia Award Association. He is a member of the IERE Specialized Group Committees dealing with Components and Circuits and with Recording.

**Professor G. D. Simms, O.B.E., M.Sc., Ph.D., F.Eng.** (Fellow 1966) has been appointed chairman of the BBC Engineering Advisory Committee in succession to Sir Robert Cockburn, K.B.E., C.B. The Committee is a small group of eminent scientists and engineers which advises the BBC on its engineering R & D and seeks to correlate it with similar activities in industry and elsewhere. Professor Sims has been Vice Chancellor of the University of Sheffield since 1974; he was previously Head of the Department of Electronics at the University of Southampton. He has contributed several papers to the Institution on microwave techniques and on educational matters. Professor Sims was a member of the Annan Committee on the Future of Broadcasting and since 1977 he has been a member of Sir Harold Wilson's Interim Action Committee on the British Film Industry.

**M. A. Ali** (Member 1969, Graduate 1966) who was been with ITT since 1962, initially with Standard Telephones & Cables, is now a senior member of the Technical Staff at the ITT Advanced Technology Centre, Shelton, Conn., concerned with component engineering and circuit applications.

**D. M. Allen, B.E.** (Member 1980) who was seconded to the Asian-Pacific Broadcasting Union from the Broadcasting Corporation of New Zealand four years ago, has relinquished his post as Senior Engineer at the Technical Centre in Kuala Lumpur. He has taken up a position as a video field engineer.

**Wing Cdr. G. M. Apte, B.Sc.** (Member 1969) has been posted to London as the Deputy Air Adviser (Technical) at the High Commission of India.

**K. C. Ball, M.A.** (Member 1980, Graduate 1972) has taken up an appointment as Senior Experimental Officer in the Chemistry Department at Manchester University; he was previously at the Government Communications Headquarters.

**W. B. Bishop-Miller, B.A.** (Member 1973, Graduate 1968) has taken up the post of Head of the Department of Engineering at Salisbury College of Technology. He was formerly Head of the Department of Engineering and Science at Barrow-in-Furness College of Further Education.

**Major K. G. Bonser, M.Sc., REME** (Member 1978, Graduate 1969) is now Planning Officer at 35 Central Workshops, R.E.M.E., Melton Mowbray. He has recently successfully completed the M.Sc. course in g.w. systems at the Royal Military College of Science.

**G. M. Cornell, B.Sc.** (Member 1970, Graduate 1967) has been appointed a Principal Lecturer in the Department of Electrical Engineering at Plymouth College of Further Education. He was previously a Senior Lecturer at Reading College of Technology. Mr Cornell has served on the Thames Valley Section Committee of the Institution since 1969, holding the offices of both the Honorary Treasurer and Honorary Secretary. During this period he represented the IERE on the Thames Valley Branch of the Council of Engineering Institutions. Since 1973 Mr Cornell has been an Assistant Examiner for CEI.

**Colonel E. D. Doyle** (Member 1957, Associate 1948) has recently been appointed Director of Signals in the Irish Army.

**D. T. Hambley** (Member 1973, Graduate 1968) is now a Senior Engineer with Marconi Space and Defence Systems, Hillend, Fife; he was previously with Gould Advance Instruments in a similar capacity.

**J. M. Keble** (Member 1973, Graduate 1967) has taken up an apointment as a Senior Technical Writer with the public relations agency, Newstech Communications of Henley. Mr Keble who was Technical Officer of the Institution concerned with learned society activities from 1973 to 1979, has for the past two years been on the editorial staff of *Communications International*.

**A. C. J. Kirkham, M.Sc.** (Member 1971) has been appointed Chief Electricity Meter Examiner in the Electricity Division of the Department of Energy, having occupied the post of Deputy Chief Electricity Meter Examiner since August 1979. From 1965-73 Mr Kirkham was a Lecturer specializing in measurements at Hatfield Polytechnic

**Lee Pui Kwong, B.Sc.** (Member 1980) who was an engineer with Cable & Wireless Systems in Hong Kong, has taken up an appointment as Telecommunication Engineer with the Government Public Works in Hong Kong.

**Sqn Ldr P. A. G. Leach, RAF** (Member 1971) has returned to the UK after two years as Officer Commanding No. 12 Signals Unit, RAF, in Cyprus, and has joined the Staff of the Director of Signals (Air) at the Ministry of Defence.

**J. D. Munday** (Member 1969, Graduate 1967) has recently been appointed Chief Executive of Cable & Wireless Bahrain. Mr Munday has been with the company since 1955 and his previous post was with EMIRTEL in Dubai, UAE.

**B. W. Potter** (Member 1969, Graduate 1964) who has been with the BBC since 1943, latterly as Head of Programme Services and Engineering Wales, has left the Corporation to take up a post as Studio Technical Systems Advisor in the Network Operations and Maintenance Department of the Independent Broadcasting Authority at Crawley Court.

**K. K. Surti, B.E., M.E.E., Ph.D.** (Member 1978) has been appointed professor of electrical engineering at the University of New Haven, Connecticut. He has been at the University since 1965 when he was appointed an Instructor in the Department of Electrical Engineering.

**G. W. Taylor, B.A.** (Member 1970, Graduate 1965) is now president of Racal-Dana Instruments, of Irvine, California. Mr Taylor joined the Racal Electronics Group in 1963, becoming technical director of Racal Instruments in 1974. Since the merger of Dana Instruments with Racal Instruments in 1977 he has been involved in coordinating engineering products of the two companies and has been deputy managing director for the past year.

**R. S. Titchmarsh** (Member 1964) has been appointed managing director of Johne & Reilhofer (UK), the recently formed British subsidiary of the West German manufacturer of industrial telemetry equipment, Johne & Reilhofer. For the past 17 years Mr Titchmarsh has been with Marconi Instruments, lately managing the subsidiary Marconi Messtechnik of Munich.

**M. E. Walker** (Member 1969, Graduate 1962) has taken up an appointment as reliability engineer with EASAMS of Camberley, Surrey. Since 1969 he has been with Rex Thompson & Partners of Farnborough, Hants, as senior consultant.

**M. R. Weale** (Member 1978, Graduate 1963) has recently taken up an appointment as principal engineer at the engineering research station of the British Gas Corporation's research and development division, Killingworth, Newcastle-on-Tyne. Since 1969 he has been a radio systems engineer with the East Midland region of British Gas.

**C. R. Wheeler** (Member 1972, Graduate 1969) who has been working with Smith Kline Instruments, Sunny Valley, California, as manager of product engineering has been appointed manager of product qualifications in Racal-Vadic, Sunnyvale.

**J. Willerton** (Member 1973, Graduate 1964) is currently quality assurance officer in charge for AQAD at British Aerospace at Brough, N. Humberside. He was previously a projects liaison officer for the directorate at Hawker Siddeley Aviation, Kingston upon Thames.

# Multi-disciplinary Engineering in the Process Industries

*This paper sets out the views of a group of people, mainly Industry Training Board staff, with interests across a wide range of process industries.*
*The aim of the paper is to draw attention to the professional engineering needs of the process industries and ensure the continuation and further development of education and training to meet their requirements.*
*It examines:*

- *the changes, particularly in technology, which are affecting the process industries.*
- *the implications for the role of their engineering personnel.*
- *whether a new approach is needed to the education and training of such personnel.*

## Introduction

The state of the British economy demands that manufacturing industry must increase its productivity. Amongst other things this means making the best use of existing plant, machinery and labour, making the most of new investment and taking advantage of advances in technology. The contribution of engineering personnel is fundamental to the achievement of these aims.

This paper has been produced:

- to provide evidence of wide interest and concern for the creation of the necessary engineering skills
- to draw the attention of those concerned with, and influential in, education and training for professional engineers to the particular needs of process industries
- to increase the support for the work of the educational establishments providing specific courses for the process industries and assistance in improving their acceptability and relevance
- to encourage the development of a more structured approach to the further/higher education, training and development of professional engineers in the process industries
- to provide a basis for further discussion and development of these and attendant issues.

Although the paper concentrates on professional engineers, the importance of the need for multi-disciplinary skills and knowledge among technicians and craftsmen acting in their support role to engineers is also recognized.

Manufacturing industry in Britain may be classified in a number of ways. For the purposes of this paper it has been divided into broad categories:

- industries producing machinery, equipment and other discrete items
- industries using process production.

Process production entails changing or modifying the nature, composition and form of materials and, typically, the use of chemical or biochemical reactions under controlled conditions. Its characteristics may include:

- continuous production
- high energy consumption
- materials handling problems
- capital intensive plant
- sophisticated control systems, sometimes with automatic correction.

Examples of process industries are:

- the generation of electricity and gas
- the separation of hydrocarbons and chemicals by fractional distillation
- the extraction, refining and forming of metals
- the production of glass, paper, plastics, paint, rubber and cement
- the manufacturing and processing of food and drink.

There are a number of similarities among them including:

- operating characteristics
- resources and processes used
- the range of engineering skills and knowledge required for successful operation and maintenance of highly capital-intensive plant.

Productivity is particularly dependent on effective plant utilization. The role of professional engineers in such circumstances is crucial, whether they are engaged in design, specification, construction or in plant maintenance.

In the past the differences between process industries and equipment manufacturing industries have been fairly clear. However, developments in automation and control systems are likely to result in the distinctions between traditional process industries and those concerned with the mass production of such goods as cars or washing machines becoming increasingly blurred.

## Changes affecting the process industries

Process production in many industries is continuous or semi-continuous, which precludes the treatment of its various parts as separate entities. Instead these industries have had to develop an approach based on the system as a whole. This has been facilitated by developments in engineering. Production systems may now embrace a combination of mechanical, hydraulic, pneumatic, electrical and electronic sub-systems which are interdependent and therefore cannot be treated in isolation. Further advances in this direction can be expected to result from the introduction of new techniques in instrumentation and control. Use of automation is likely to increase and this will be combined with higher speeds of operation in some processes.

Economic, social and legislative factors are also contributing to the changes in the process industries. These include the need:

- to use energy in the most economic manner
- to improve conversion efficiencies to reduce the effects of both the scarcity and the rising cost of raw materials
- to ensure the requirements of the Health and Safety at Work etc. Act, 1974 are met
- to avoid major hazards to the environment
- to maximize the use of plant and equipment at a time when the cost of financing investment is rising.

## The implications for engineers in the process industries

Engineers face a major challenge in developing the potential of advances in technology to meet demands for quality and quantity of production, cost targets and delivery dates, all within the constraints listed above. They have a key role in optimizing production strategy whether they are engaged in the design, specification, construction or maintenance of plant.

In order to meet this challenge, the process industries will need:

- to make full and effective use of proven technology and to keep abreast of that still at the development stage
- to have an understanding of a range of engineering disciplines rather than an exclusive knowledge of a particular one
- to adopt a systems approach to the overall production process and its control
- to be able to work across the boundaries which have arisen from the traditional single discipline approach to engineering.

Production systems increasingly rely on the effective take-up of available technology. However, the demands of that technology will not always be compatible with those of the organization which exists to supply and support the system and to market its products. Engineers are required to interpret the demands of both in such a way as to achieve the optimum production strategy. They therefore occupy a position where their professional judgements can markedly affect business decisions.

They will need the ability and willingness to match the use of engineering technology to the needs of the organization and to its capacity to absorb change. In so doing, they may need to deal with:

- effective deployment, utilization and training of various personnel including technicians, craftsmen and others concerned with process operations
- employee relations and other general management considerations, including health and safety
- management of change arising from the implementation of technical developments and new technology
- the relationship between the production system and the organization of manufacture as a whole, particularly as it affects overall costs and profitability.

These requirements indicate that a proportion of the engineers employed in the industries must have multi-disciplinary skills and knowledge if they are to be able to take the necessary integrated approach.

They will need:

- an education and training encompassing a range of engineering disciplines appropriate to the process industries
- a sound understanding of the manufacturing process itself
- the capacity for systems thinking
- the ability to acquire a high level of interpersonal and communications skills.

The complexities of the equipment used in process industries will still demand the specialist knowledge of engineers educated and trained in a single discipline. Multidisciplinary engineers will need to know when it is appropriate to seek the help of these specialists and to be able to communicate to them the way in which the specialist discipline impinges on the operation of the system as an integrated whole. It will undoubtedly help the specialist if he too has a basic appreciation of the manufacturing process and understands the systems approach.

## The education and training of engineers

At present there is a widely held view that, apart possibly from those trained in chemical engineering, engineers are primarily prepared for a career in the industries which produce machinery and equipment. This approach tends to result in engineers who are trained in a single discipline, usually mechanical, electrical or production engineering. The particular discipline is studied in considerable depth and often backed up by formal or informal training and experience which tends to consolidate the specialism, rather than develop a broader knowledge which brings into perspective the inter-relationship existing between the various disciplines in a continuous production process. The process industries have a significant interest in the education and training of engineers which, it seems, is being neglected in favour of an approach related more to tradition and history than to present-day conditions.

The departmental structure in many universities and other institutions of higher education may inhibit, and in some cases positively discourage, an inter-disciplinary approach from the very start of an engineer's education and training. This tends to be consolidated by the specialist nature of the engineers' professional institutions.

The approach described above seems to have led to two important consequences:

- inadequate provision for the education and training of multi-disciplinary engineers both at first appointment and post-experience level.
- a stock of engineers already employed in the process industries who do not have the skills and knowledge required to appreciate a systems approach.

A few universities, polytechnics and colleges have recognized the need for both an alternative to the traditional pattern of engineering education and an increased provision for post-experience training to develop the skills and knowledge of those engineers whose education and training has followed the conventional course. However, at present they are in the minority. If the balance between the supply of multi-disciplinary and single discipline engineers is to be redressed, then it will be necessary to increase substantially the provision for the education and training of the former group.

If this is to be achieved, the process industries must develop and present a more effective case for change. This will require a concerted approach which at present is lacking, largely due to the number of diverse bodies which can claim to represent them. In contrast the equipment building and batch manufacturing industries which are the major users of the engineer educated and trained in one discipline have a unified voice which enables them to present their needs clearly and forcefully.

## Conclusion

It seems that the process industries urgently require an increase in the supply of multi-disciplinary engineers whose skills would be transferable across a large variety of processes and industries. Isolated efforts are being made in individual companies and elsewhere to develop engineers from a single discipline base, but these are usually specific to particular situations. Nevertheless they have resulted in the development of a valuable though fragmented and widely distributed body of knowledge and experience which could and should be brought together.

The publication of the Finniston Report 'Engineering our Future', has stimulated much public discussion on the education and training of professional engineers. Government, industry and educational and professional institutions are actively considering what changes, if any, should be made to present structures.

It is vitally important that the process industries should take this opportunity to make their requirements for multi-disciplinary engineers known. A joint effort should be made to ensure that this need is not neglected in favour of options which can be more easily met.

# A New I.C. for Viewdata Applications

Some two years ago Mullard introduced a dedicated integrated circuit for viewdata-type applications. Designed specifically as a microprocessor peripheral, it is known as LUCY (a corruption of Line Coupling Unit Asynchronous receiver/transmitter). Despite considerable developments of the facilities of the i.c. itself (the SAA5070), circuit density is so high that the i.c. package count for basic viewdata acquisition is reduced to four, including the LUCY chip itself and the microprocessor on which it is based. The chip area is 30 sq. mm in 4.8$\mu$m geometry, and it contains 12,000 active devices.

To appreciate the role of LUCY it is necessary to understand the earlier role and applications of microprocessors in viewdata decoder designs as interpreted by Mullard.

From the outset it has been impossible to define a specific list of features which a viewdata decoder should provide. Markets have been identified for both low-cost minimum-feature applications and for full editing terminals with complete keyboard facilities and simple word-processing. For this reason every viewdata decoder introduced to date has included a microprocessor to give flexibility of design, using software changes alone.

Despite its flexibility, the processor is limited in that it can only be involved in one particular task at any instant in time. The decoder system can be instructed from many information sources (e.g. data from telephone line, keyboard, cassette recorder) at unpredictable times. This means the processor has continuously to switch from its internal system 'housekeeping' to scan its external system-inputs for incoming information.

To ease this pressure, the processor in earlier systems was surrounded by a host of peripheral chips for, among other tasks, converting f.s.k. into digital information (modem function) and asynchronous serial data into parallel data and vice-versa (UART function). Even then, software space and processor time had to be used to generate rather standard functions for such things as dialling. Experience has shown that within the confines of using low-cost processors to keep the overall system cost as low as possible, the engineer never had quite enough software space to provide all the features needed.

The function of the LUCY chip is to combine a large majority of the peripheral chips used in earlier systems and to take the pressure off the processor in terms of both software and time. In addition it provides other features not previously incorporated into viewdata decoders. Thus LUCY can be considered as a device which is an interface between the processor and the 'outside world' (e.g. telephone line, keyboard, cassette recorder).

Each input and output point has a register where data can be accumulated and temporarily stored. All registers are connected to a common 8-bit parallel data highway (the bus) which links them to the processor. The registers are individually connected to one of two status registers, again linked to the bus. When a particular register has accumulated and stored incoming information for the processor, it passes the identity of that register on to the status register.

In this way the processor has to examine the status registers only occasionally and can instantly determine if and where there is information upon which it should act. This information can then be released on to the bus by instruction from the processor through an address register. There is also command and mode registers through which the processor can instruct and control the 'data' registers prior to data being sent from the processor to the 'outside world'.

While the chip is 'dedicated', many of its operations can be varied by the processor through the mode register. For example, it can accommodate 7-bit data with even or odd parity or 8-bit data with no parity. Also the output data for a telephone line can be selected for transmission at either 75 baud (Prestel standard) or at 1200 baud for communicating terminals or data-base bulk updating.

An improved cassette record/replay facility is also provided. This is based on the self-clocking 'Kansas City' standard which gives greater protection against problems of tape speed variations. Also, because connection is to a common bus, data can be recorded from various sources including telephone line and page memory. In addition there are 1·5-second and 60-second timers which the processor can access for such functions as dialling and time out.

Thus it can be seen that the LUCY chip is important as an alternative resource for carrying out all the routine tasks associated with viewdata. In addition it provides facilities which allow the user greater freedom to control various features through more efficient software. LUCY also allows the system to be designed with significantly fewer i.c.s and a reduced board area, thus saving both cost and space.

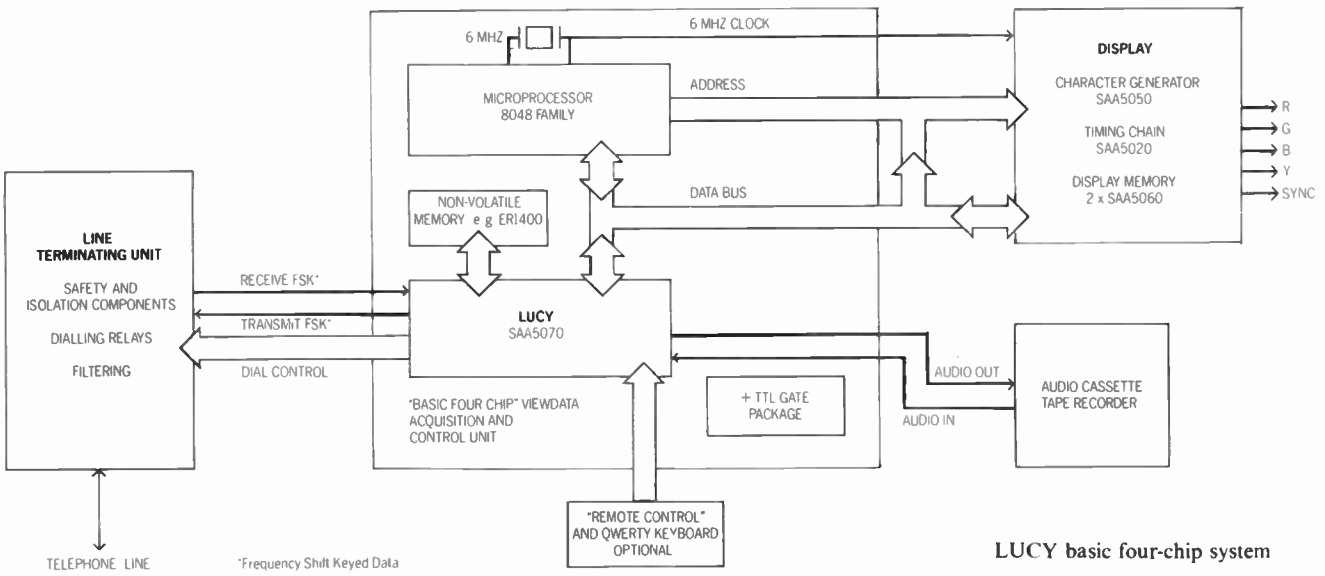


LUCY basic four-chip system

# Letter to the Editor

*From:* **A. C. Evans**, C.Eng., M.I.E.R.E.

**An Electronic IERE Journal?**

The question raised on the Editorial page of the March issue of the Journal is '*How* would you like to receive the Journal in this way?' My answer is 'I would like it very much and by any reasonable method.' The actual access method would, hopefully, not be limited to one, but initially it could be so, e.g. Prestel/Viewdata. The prime information that should be available is abstracts of new papers which could even be issued prior to publication of the full paper. Even if this were the sole information initially, it would allow simple searching for papers on particular topics over a reasonable period of time. For some while, of course, an 'electronic *Radio and Electronic Engineer*' will duplicate the existing medium, but I would suggest that with a willingness to pilot such a scheme, some 'internal' benefit would be possible to offset the small, but possibly significant resources that would need to be allocated initially, but hopefully with internal and 'popular' support this would be well justified.

In the longer term, I would see the possibility to charge for the different publishing mediums so that printing and distribution costs could be kept down, and increasing revenue could be raised by a small charge on the electronic medium. Initial availability of terminals might be seen as a problem, but with current terminal cost trends, namely Viewdata adaptors under £100 in the near future, this is unlikely to last for long.

As a 'parting shot', I do not notice many 'Letters to Editor' in either of the regular Institution publications, and I wonder why this is? At the head of the Editorial page of the Journal there is a quotation from the Institution's charter indicating that the Institution's aims are achieved by 'the exchange of information'. The current bias of direction is heavily in favour of the authors and presenters of papers. Unless particularly well organized and well chaired, a live meeting can be less than encouraging to a potential contributor from the floor. 'Letters to Editors' can be a lively interchange between readers and authors but they seldom are. An electronic publishing medium would be much more capable of 'exchange of information' if others could join in on a 'Letters to Editor/author' basis.

On your Editorial page there are two question marks and even a direct question to the reader, and so I hope that this letter is only one reply of many!

33 Elmdene Road
Kenilworth
Warwickshire CV8 2BW

ANDREW C. EVANS

*2nd April 1981*

[Mr Evans and other readers may be interested to know that a joint pilot venture launched by the *British Medical Journal* and Glaxo Laboratories with fifty 22 inch Prestel sets supplied by Granada TV Rental, will offer medical information on a 'closed user' circuit to selected postgraduate medical centres and group practices in the UK during a two-year trial period. A particular point of interest is that the *BMJ* input will include advance details of the contents of the Journal as well as locum vacancies and educational programmes based on case studies supplied by Consultants.—EDITOR]

# Standard Frequency and Time Service

*Communication from the National Physical Laboratory*

**Relative Phase Readings in Microseconds NPL—Station**

(Readings at 1500 UTC)

| FEBRUARY 1981 | MSF 60 kHz | GBR 16 kHz | Droitwich 200 kHz |
|---|---|---|---|
| 1 | 2·1 | 12·8 | 5·7 |
| 2 | 2·2 | 12.5 | 6.5 |
| 3 | 2·3 | • | 6·7 |
| 4 | 2·6 | • | 7·3 |
| 5 | 2.5 | 11.6 | 8·1 |
| 6 | 2·5 | 12·3 | 8.9 |
| 7 | 2·6 | 12·2 | 9·6 |
| 8 | 2·8 | 12·3 | • |
| 9 | 2·7 | 12·3 | 11·0 |
| 10 | 2·7 | 13·3 | 11·6 |
| 11 | 2·6 | 13·4 | 12·2 |
| 12 | 2·5 | 12·3 | 12·9 |
| 13 | 2·5 | 11·7 | 13·6 |
| 14 | 2·8 | 9·3 | 14·4 |
| 15 | 2·5 | 11·8 | • |
| 16 | 2·4 | 12·7 | 18·8 |
| 17 | 2·4 | 12·7 | 19·5 |
| 18 | 2·5 | 12·8 | 20·2 |
| 19 | 2·4 | 11·6 | 20·8 |
| 20 | 2·4 | 11·0 | 21·3 |
| 21 | 2·4 | 13·3 | 21·8 |
| 22 | 2·4 | 11·7 | 22·4 |
| 23 | 2·5 | 12·1 | 23·2 |
| 24 | 2·4 | 11·6 | 23·8 |
| 25 | 2·4 | 11·3 | 24·4 |
| 26 | 2·5 | 11·2 | 25·0 |
| 27 | 2·5 | 11·2 | 25·5 |
| 28 | 2·5 | 11·3 | 26·1 |

| MARCH 1981 | MSF 60 kHz | GBR 16 kHz | Droitwich* 200 kHz |
|---|---|---|---|
| 1 | 2·5 | 11·2 | 26·7 |
| 2 | 2·5 | 11·6 | 27·4 |
| 3 | 2·4 | 11·0 | 27·9 |
| 4 | 2·3 | 11·7 | 28·4 |
| 5 | 2·3 | 11.4 | 29·0 |
| 6 | 2·1 | 11·6 | 29·7 |
| 7 | 2·2 | 11·3 | 30.2 |
| 8 | 2.4 | 11·5 | 30.8 |
| 9 | 2·3 | 11·1 | 31·4 |
| 10 | 2·2 | 11·3 | 31·9 |
| 11 | 2·1 | 11·3 | 32·4 |
| 12 | 2·2 | 11·1 | 32·9 |
| 13 | 2·2 | 11·0 | 33·4 |
| 14 | 2·1 | 11·3 | 33·9 |
| 15 | 2·1 | 11·3 | 34·4 |
| 16 | 2·2 | 11.4 | 34·8 |
| 17 | 2·3 | 11·2 | 35·3 |
| 18 | 2·3 | 11·0 | 35·7 |
| 19 | 2·3 | 11·0 | 36·2 |
| 20 | 2·3 | 10·8 | 36·7 |
| 21 | 2·3 | 10·8 | 37·1 |
| 22 | 2·5 | – | – |
| 23 | 2·3 | 10·0 | 38·1 |
| 24 | 2·3 | 10·7 | 38·7 |
| 25 | 2·5 | 10·6 | 39·2 |
| 26 | 2·5 | 12·3 | 39·7 |
| 27 | 2·5 | 10·2 | 40·1 |
| 28 | 2·4 | 10·0 | 40·6 |
| 29 | 2·6 | 10·1 | 40·9 |
| 30 | 2·6 | 9·5 | 41·3 |
| 31 | 2·5 | 10·5 | 41·6 |

Notes: (a) Relative to UTC scale ($UTC_{NPL}$–Station) = +10 at 1500 UT, 1st January 1977.
(b) The convention followed is that a decrease in phase reading represents an increase in frequency.
(c) 1 μs represents a frequency change of 1 part in $10^{11}$ per day.
*It may be assumed that the satellite stations on 200 kHz at Westerglen and Burghead will follow the day to day changes in these phase values.

UDC 621.396.73.029.64:621.396.946
*Indexing Terms:* Telecommunication links, satellite, Radiosystems, mobile

# A manpack satellite communications earth station

**C. H. JONES,** B.Sc., C.Eng., M.I.E.E.*

**SUMMARY**

Recent advances in technology have enabled a family of small microwave satellite communication terminals to be constructed. This paper describes one of these, a prototype manpack equipment which can be carried by a single person. It was completed in mid-1978 and has since been demonstrated on numerous occasions.

Using a suitable satellite, such equipment can be used to establish a link with a main SATCOM base station; alternatively manpack/manpack links are possible provided there is a base station rebroadcast. Traffic facilities are either 50 baud duplex telegraph or analogue speech.

* *Royal Signals and Radar Establishment, Defford, Worcestershire WR8 9DV*

*The Radio and Electronic Engineer, Vol. 51, No. 6, pp. 259–271, June 1981*

## 1 Introduction

Recently there has been increased interest in the use of s.h.f. satellite links for mobile purposes, resulting in the development of small, easily deployed microwave stations. These are often vehicle-mounted and handle a limited traffic load, for example speech plus telegraph links. Aerial dishes are about 1·5 to 2 metres diameter, transmitter power is about 30 to 60 watts and primary power is taken either from mains, local generators or vehicle batteries.

The first prototype manpack station was built to demonstrate that s.h.f. technology now allowed an equipment which could be carried by a single person as a back pack and provide a duplex 50 baud telegraph duplex link or a low quality duplex analogue speech channel to a main base station via a suitable satellite. The equipment can be quickly deployed from its transportable to operational state and due to its relatively wide aerial beam width it is easy to acquire a geostationary satellite using the built-in compass, inclinometer and signal strength meter.

Even with the limitations of a laboratory-constructed prototype equipment, considerable experience has been obtained from its use in field conditions. From its inception close liaison has been maintained with possible users, and it has been frequently shown that the equipment can be deployed and a link set up in under 2 minutes.

The first prototype was designed for fixed frequency operation within the s.h.f. SATCOM band for simplicity and to take advantage of the high-gain of the *Skynet II* satellite repeater which happened to be used for the tests. Subsequent stations can be expected to be used in conjunction with high-gain spot beams of future s.h.f. satellites and should reduce the required transmitter power of the manpack, with increased battery life and weight reduction. The use of a higher gain satellite will also increase the traffic capabilities of the link, e.g. making high-quality speech possible.

**Table 1**

Manpack technical specification

| | |
|---|---|
| Station size | 45 cm × 45 cm × 20 cm plus back carrier |
| Maximum e.i.r.p. | 31 dBW |
| Aerial dish diameter | 45 cm |
| Aerial gain | 28·5 dB at 8 GHz |
| Aerial beam width | 6 degrees approximately |
| Station $G/T$ | 2 dB°K |
| Receiver noise temperature | 400°K at aerial feed |
| Frequency tuning | separate spot frequencies for transmitter and receiver within the *Skynet II* band |
| Modulation (telegraph) | differentially encoded phase reverse keying (d.e.p.r.k.) |
| Traffic | 50 baud telegraph or analogue speech |
| Bit error rate at 50 baud | better than $10^{-4}$ |
| Battery consumption | 30 W (duplex operation) |
| Station weight | 17 kg including battery and telegraph terminal |

0033–7722/81/060259+13 $1.50/1

## 2 Manpack Equipment

At the inception of this project, enquiries of possible users indicated that the complete equipment should not weigh more than about 17 kg (38 lb) in order to be carried on the back by a single person, leaving the hands and arms free. The width of the load should not be wider than the shoulders and this limited the package to about 45 cm × 45 cm × 20 cm. Pictures of the prototype equipment in its stowed and deployed modes are shown in Fig. 1.

The aerial is a shallow dish 45 cm in diameter forming one surface of the case and having a detachable ring focus feed as detailed in Appendix 1. The feed also contains a polarizer vane to produce circularly polarized propagation. Behind the dish is a single diplexer and transmission and reception waveguide filters. The dish is fabricated of fibre glass with a conducting surface, the other components and the case are of light alloy.

A simplified block diagram of the electrical circuitry is shown in Fig. 2. Every attempt has been made to keep the equipment simple and of lowest possible power consumption. To this end the output frequency of a single master oscillator, consisting of a temperature-compensated crystal-controlled source to eliminate the warm-up time and power consumption of an oven, is multiplied up to the transmission frequency and also to that for the receiver first local oscillator. This gives separate spot frequencies for transmission and reception, limited receiver tuning being achieved by replacement of a further crystal oscillator used with the second down-mixer. The synchronous 50 baud transmitted data stream, differentially encoded to eliminate phase ambiguity, phase-reverse keys the transmitted carrier as detailed later. The output is subsequently amplified for transmission using a high efficiency travelling-wave tube amplifier or power f.e.t. amplifier. The receiver chain has a f.e.t. low-noise amplifier and an image rejection filter, followed by the first mixer and intermediate frequency amplifier. The equivalent noise temperature of the receiver is calculated in Appendix 2. The first intermediate frequency is successively down-mixed, to eliminate interfering intermodulation products, before entering the telegraph modem.

The modem differentially encodes the data stream prior to transmission. On reception it reconstitutes and decodes the data in the face of carrier frequency tolerance and Doppler shift at the minimum signal-to-noise condition. Generation and presentation of the data is by means of a telegraph input/output terminal containing a QWERTY keyboard, a hard-copy printer, a limited message display and a data store.

With the limited transmitter e.i.r.p. of this prototype station and present reliance on the *Skynet II* repeater of this research, a digital speech link is not yet feasible, though it has been possible to include an experimental analogue speech link as described later.

A further limitation in the use of the first prototype manpack is its restricted battery life. Weight and volume restrictions dictated a battery capacity of about 4 AH giving a useful discharge time of up to 4 hours when providing a duplex telegraph link. With future circuit improvements and next generation satellites it is anticipated that this discharge time will be much extended.

## 3 Modulation

It can be shown[3] that a modulation technique using phase reverse keying (p.r.k.) requires approximately 3 dB less S/N level over an equivalent two-level frequency shift keying (f.s.k.) system at a common error probability rate of $10^{-4}$. Both systems are deteriorated by a further 1 dB at this error rate when the modulation is differentially encoded.

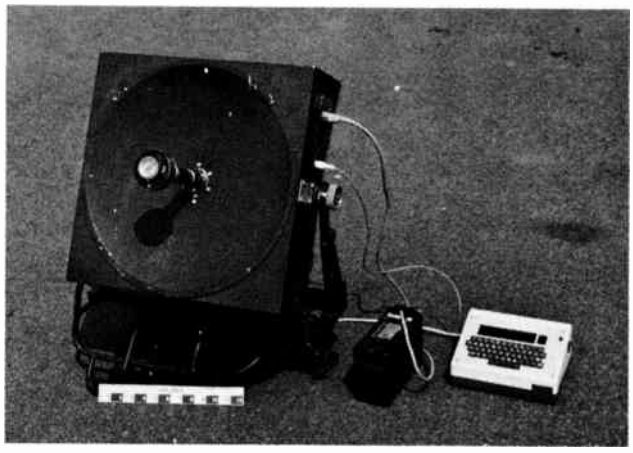

**Fig. 1.** The Manpack (left) stowed, and (above) deployed.

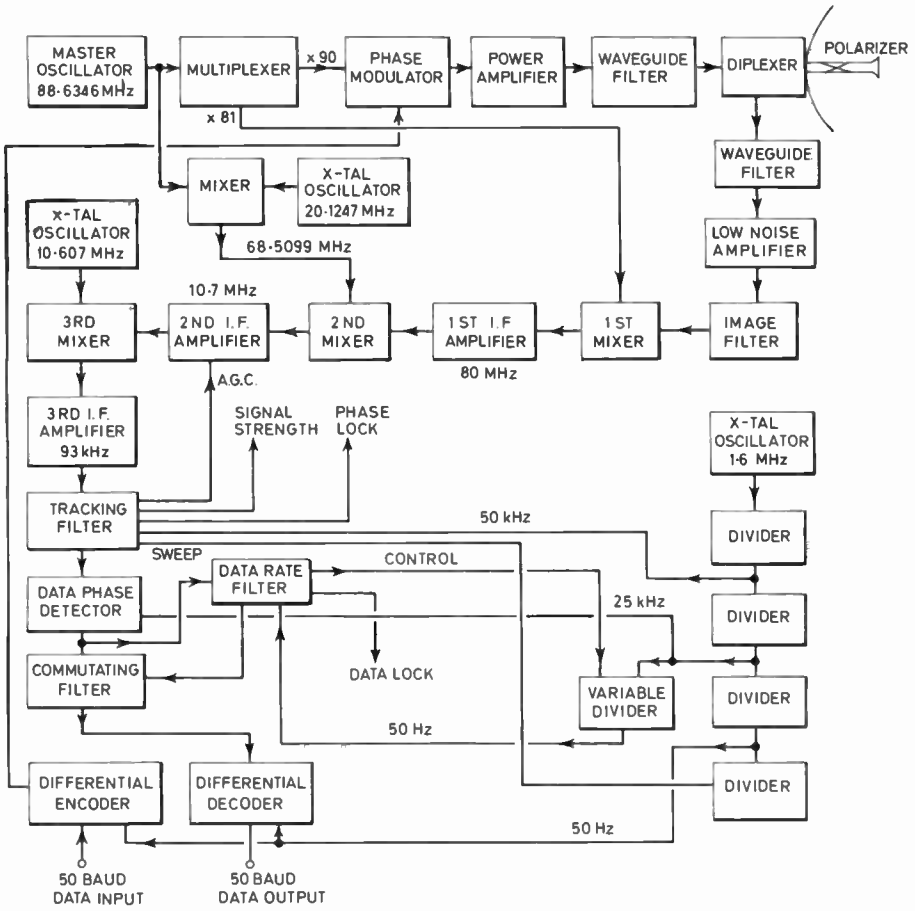


**Fig. 2.** Manpack electrical block diagram.

The p.r.k. modulation method is used on the Manpack to take advantage of the better noise performance. The ability to use a high density of low-power consumption digital circuit modules (c.m.o.s.) in this method is also an advantage over the analogue circuit requirements of f.s.k.

The modulation is applied directly to the low-level transmitter carrier at X-band via a low-insertion-loss switched phase-shifter.

## 4 Power Amplifier

Still the most efficient method of power amplification at X-band is the travelling-wave tube (t.w.t.). In spite of its high voltage supply requirements it makes an attractive solution for the Manpack. With its typical overall efficiency of 20%, it is a useful yard stick with which to compare suitable solid state amplifiers.

Work in industry has resulted in a suitable prototype field effect transistor amplifier. This device has volume and weight less than that of the t.w.t. and power supply previously used, but does require a very efficient power inverter/regulator to give an overall figure better than 10%. Both of the above amplifiers have been evaluated in the prototype Manpack equipment.

## 5 The Manpack Master Oscillator

The master oscillator, being common to both transmitter and receiver, defines the frequency and phase stability of the whole system as detailed in Appendix 3.3.

### 5.1 Frequency Stability

Since the largest multiplication ($\times 90$) is used for transmission this link defines the stability required. Taking the maximum carrier error to be not greater than 1 kHz:

$$\text{Stability} = 10^3 \times (90 \times 88{\cdot}6346 \times 10^6)^{-1}$$
$$= 1{\cdot}25 \times 10^{-7}$$

to be maintained over a temperature range not less than 0°C to +50°C.

This is easily achieved with an ovened crystal oscillator, but with the disadvantage of a high power drain for the oven and a long stabilizing time after switch on. These disadvantages have been overcome in the prototype equipment with the use of a temperature compensated crystal oscillator (t.c.x.o.). The sample used just achieves this stability over the above minimum temperature range with virtually no warm-up time and minimal power consumption.

### 5.2 Phase Stability

The Manpack modulation system as detailed above uses p.r.k. Here excursions of phase noise of 90 degrees or more, which occur during the period of an information digit, have a high probability of causing corruption. Since most satellite systems operate in the presence of a poor signal/noise condition to conserve satellite power, extra noise resulting from the phase instability of the Manpack is a disadvantage. As well as noise at the data rate causing digit corruption, components much nearer the carrier and within the bandwidth of the modem tracking filter can cause loss of acquisition. This second case is very important since most crystal oscillator sources have a falling noise characteristic away from the carrier.[4] Such measurements are very specialized and are normally only specified for very high quality frequency sources. As well as lacking this characterization, lesser quality sources can suffer from 'frequency stepping' and 'phase walking' which are random variations of the output due to the cut and quality of the quartz used.

The t.c.x.o. purchased for experiment was completely unspecified for its phase behaviour, but subsequent measurements have indicated that the phase noise amplitudes at frequencies of interest do not exceed 10 degrees peak-to-peak after multiplication.

## 6 Manpack Frequency Multiplier

The multiplier was manufactured especially for the Manpack by industry, based on designs for lightweight satellite repeaters. The unit consists of a common front-end multiplier followed by parallel multiplier stages to give two outputs, one of 90 times the input frequency for the transmitter and the other 81 times the input frequency for the receiver first down-mixer.

## 7 Second Mixer and Local Oscillator

Here the output of the first i.f. amplifier, at a frequency specified in Appendix 3.3 is down-mixed to 10·7 MHz. The frequency tolerance of this resulting signal due to its originating transmitter, Doppler effects within the transmission path, plus local oscillator frequency errors in this receiver, do not exceed $\pm 5$ kHz. These are subsequently corrected by the modem tracking filter detailed in Appendix 4. The local oscillator frequency required is $79{\cdot}2099 - 10{\cdot}7 = 68{\cdot}5099$ MHz.

The tolerance of this frequency is to be not worse than 1 part in $10^6$ over the operating temperature range to minimize its contribution to the above error. Unfortunately crystals cut for this frequency are difficult to obtain quickly and cheaply to such a tolerance. To overcome this, the above master oscillator is mixed with the output from a second oscillator using a fundamental mode crystal cut for: $88{\cdot}6346 - 68{\cdot}5099 = 20{\cdot}1247$ MHz

A simple filter and amplifier extracts the required lower sideband component to form the new local oscillator. Filtering is essential as the first stage of the following second i.f. amplifier is broadbanded. The resulting noise bandwidth here is defined by the previous first i.f. amplifier which is nominally 10 MHz centred on 80 MHz.

## 8 Second I.F. Amplifier

This sub-unit consists of several modules connected in series. The first is a broadband amplifier stage with provision for a.g.c., matched into a narrow band crystal filter to define the overall band width of the sub-unit. This is followed by two high-gain broadband modules to give an overall specification as follows:

| | |
|---|---|
| Overall gain (no a.g.c.) | +50 dB |
| Centre frequency | 10·7 MHz |
| Bandwidth (3 dB) | $\pm 6$ kHz |
| A.g.c. range | 70 dB |
| Input and output impedance | 50 Ω |

## 9 Third Mixer, Local Oscillator and Amplifier

This local oscillator is crystal-controlled at 10·607 MHz giving a nominal mixer output of 93 kHz. The stability requirement here is not so stringent as those for the first and second local oscillators since the frequency is so much lower. As the noise level at the input to this mixer is now approaching 0 dBm, the local oscillator power output is made typically +7 dBm to maintain the conversion efficiency of the mixer. The resulting i.f. band of 93 kHz $\pm$ 6 kHz is chosen so as not to interact with the modem timing frequencies which are harmonically related to 100 kHz.

The following third i.f. voltage amplifier uses an operational amplifier with negative feed back to define the gain. This is typically 160 times to ensure that under normal conditions the above a.g.c. is operative so that signal strength variations may be reduced at the following modem.

## 10 Tracking Filter with Acquisition Sweep and Lock Indication

The nominal 93 kHz modulated signal from the third i.f. amplifier suffers from inherent carrier frequency errors and Doppler variations which are contained within its bandwidth of $\pm 6$ kHz. This signal is made phase coherent with a local carrier enabling the p.r.k. modulation to be detected. Coherence is achieved by means of a tracking filter containing a frequency translation loop. (Fig. 3).

### 10.1 The Frequency Translation Loop

In designing a loop for the above application it is essential that it be of the second order to ensure that it will remain close to its locked state in the event of breaks in signal. Hence when the signal is restored, reacquisition is rapid.

The components and operation of the loop are as follows. The output from the voltage controlled oscillator (v.c.o.) is mixed with the input signal to produce a constant intermediate frequency of 25 kHz.

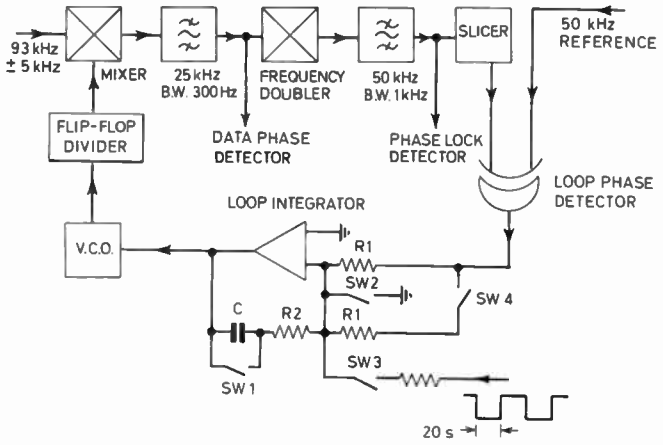


**Fig. 3.** Tracking filter.
Logic operated switches:
SW1 SW2 Integrator discharge operated at the end of each frequency sweep.
SW3 Sweep control, opened when phase lock is achieved.
SW4 This switch is closed when sweep is operative, but open when phase lock is achieved to increase the loop bandwidth.

This is band-limited to remove unwanted mixer products and to improve the signal-to-noise ratio over that of the input. After amplification the carrier is recovered by frequency doubling to remove the p.r.k. modulation. Since the doubling process results in large amplitude variations at the modulation rate as detailed in Appendix 4, the carrier is also filtered and amplified before feeding the lock indication phase detector and the hard limiter prior to the loop phase detector. The loop phase detector is an exclusive-OR gate which digitally combines the output of the limiter with an internally-generated, low jitter 50 kHz square wave. The loop error voltage, being the time average of the two resulting logic states is derived by the following integrator. This, as described in Appendix 4, combines a high-input-impedance operational amplifier, since the integration times are relatively long, and a lag-lead CR feedback network to realize an active filter stage. The lag-lead network enables the loop frequency and damping to be optimized.[5] The amplifier ensures a high loop gain for good tracking.

The frequency of the v.c.o. is corrected by the integrated error signal so that a loop phase lock is achieved. The oscillator is a free-running CR ramp generator which is simple to control and to correct for thermal variations. The slope of the ramp can lead to excessive phase jitter, so it is run at twice the required rate to 'clock' a binary divider stage within the loop to provide a suitable low jitter signal at the correct frequency.

### 10.2 Loop Acquisition and Error Rate Performance

Practical iterative measurements of the loop behaviour using the integrator time-constant determined in Appendix 4 showed that the latter gave the best acquisition behaviour for the whole system including a satellite link. It was also found that if the time-constant was doubled the error rate improved but the loop acquisition deteriorated. Hence, in the complete modem, the shorter time-constant is in circuit during the acquisition process, then doubled automatically when acquisition is achieved.

### 10.3 Loop Frequency Sweep

To accommodate frequency tolerances in the Manpack system as well as Doppler shift, a hold-in range for the loop of not less than $\pm 5$ kHz is required. Since this is well outside the loop lock-in or pull-in ability, the v.c.o. is swept over this range until lock is achieved. It can be shown[5] that there is a 99% probability of loop acquisition if the sweep rate does not exceed:

$$\tfrac{1}{2}\left(\frac{\omega_n^2}{2\pi}\right) \text{Hz} \cdot \text{s}^{-1}$$

where $\omega_n$ is the loop natural frequency

In this application this is approximately 40 seconds. The sweep voltage is produced by applying alternate positive and negative step functions of period 20 seconds, derived from the modem timing unit, to the input of the loop integrator. Between each alternate sweep, the integrator is discharged for 4 seconds to give a zero voltage-mean frequency reference. When acquisition is achieved the lock indication signal removes the sweep.

### 10.4 Loop Phase Lock Indication

When loop acquisition has been achieved it is convenient to have a digital indication of phase lock. In the Manpack it is used for the following:

(i) Operator indication of phase lock.
(ii) Removal of loop frequency sweep.
(iii) Removal of digital inhibit from signal processing circuits.

The indicator voltage is derived as follows. The filtered and amplified but unlimited output of the loop frequency doubler is detected using a quadrature phase detector against an internal frequency reference.

The detector output is noise which averages to near zero when the loop is unlocked, becoming a logic 1 when lock is achieved. The detector output is integrated and amplitude-sliced to give a reliable transition between the two states.

It is essential that this lock signal should not be affected by short loop disturbances or breaks in signal which would otherwise reintroduce the long reacquisition process. To ensure that this does not occur, the slicer is followed by a digital timing circuit which maintains the lock condition for about 10 seconds after true loop lock has been lost.

## 11 Aerial Pointing and Signal Strength Detection

It has been stated earlier that the Manpack can acquire the appropriate satellite signal by use of the supplied compass and inclinometer and known values of azimuth

and elevation angles for the particular satellite in use. Even though the aerial beam width is relatively wide it is essential that further fine pointing adjustment be made if full use is to be made of the limited transmitter e.i.r.p. Optimum pointing is indicated by a peak reading on the signal strength meter when the latter is switched to either of the following two pointing modes.

### 11.1 Wideband Signal Strength Detector and A.G.C. Mode

This uses a peak detector and amplifier operating within the 12 kHz noise bandwidth at the input of the modem. The resulting d.c. level controls the gain of the second i.f. amplifier forming a non-coherent a.g.c. loop. When used for pointing, the a.g.c. loop is broken and the amplifier gain adjusted manually. The output of the detector then deflects the signal strength meter. Pointing by this method is used when a very strong signal is available or a box search is being made for the satellite.

### 11.2 Narrowband Signal Strength Detector Mode

This uses a similar circuit to that above except that it detects the signal in the 300 Hz bandwidth within the tracking filter loop and is used only for aerial pointing. As above the gain of the second i.f. amplifier is adjusted manually to give an appropriate meter reading. Since the loop behaviour masks the peaking process, the loop is broken and the frequency of the v.c.o. adjusted manually until the meter indicates a response from the received signal. This is then maximized by fine adjustment to the aerial pointing.

## 12 Data Detection and Reconstitution

The 50 baud data recovery is achieved by phase detection of the narrowband 25 kHz loop signal relative to a local reference. The phase detector is a full-wave switching circuit combining an active filter to remove switching components. It is essential that amplitude linearity and signal balance be maintained here if the high noise and inter-symbol interference present is to be reduced by the following 'integrate-and-dump' filter. To give its optimum performance this filter, consisting of a long integrating-time-constant relative to the data bit period, charges during the data bit interval and is discharged in a short time between bits at the data rate. Correctly phased timing for this process is derived from the data clock stream synthesized from the received noisy data.

To derive the data clock, the detected data stream is applied to a full-wave differentiator to produce narrow, constant width, undirectional pulses. In the absence of noise these correspond in phase to the transitions of the incoming data clock, nominally at 50 pulses per second, with their presence or absence dependent on the data pattern. This stream is compared in phase with a continuous 50 p/s stream of similar width, generated from the modem master timing unit by successive stages of division. The phase of the latter is advanced or retarded by addition or deletion of pulses in the higher frequency divider stages until coincidence is achieved between the two waveforms. During the search for phase coincidence, on average the noise pulses causing phase advance are balanced by those affecting phase retardation, leaving a bias in favour of the true data signal pulse. When data synchronism is achieved, a digit level is produced which operates a data lock indicator.

The resulting output from the integrate-and-dump filter is a series of irregular ramps, due to the integrated noise and signal, of unit bit length. The polarity of the mean slope of each ramp is dependent on the sense of the transmitted bit. This is converted to a jitter-free digital form by hard limiting and retiming to a secondary clock in quadrature with the recovered data clock.

## 13 Data Differential Encoding and Decoding Circuits

The modem is primarily used for the handling of telegraph traffic which requires mark-and-space integrity over the link. This ensures correct interpretation of the transmitted code at the receiver. Since this integrity cannot be ensured every time the link is made or interrupted, the data stream is differentially encoded prior to transmission and subsequently decoded after reception.

The simple mnemonic for differential encoding/decoding is as follows:

| Input data stream | Differential encoded stream |
|---|---|
| Positive level | No change in previous bit |
| Negative level | Opposite to previous bit |

Provision is also made for retiming externally generated data to the phase of the internal modem clock. When used with a dedicated keyboard and character generator, as is usual with the Manpack, these timed directly from the modem clock. The encoder input can be driven from standard TTL levels or from a V24 interface and is protected from gross overload. The encoder output is fed directly to the transmitter carrier phase modulator unit.

Differential decoding of the digit stream is a converse logical process to that of encoding. The output is buffered to drive either a TTL or V24 interface and is short-circuit protected.

## 14 Master Timing Unit

The internal timing throughout the modem is based on a 1·6 MHz crystal oscillator. This forms part of a digital dividing network providing the following:

50 kHz for loop phase detection and lock indication.

25 kHz for data detection.

50 Hz for data timing.

Nominal 50 Hz for data rate recovery in conjunction with controllable dividers.

40 second period signals for phase loop frequency sweep control.

### 15 The Speech Link

It can be shown that for a digital speech link an error rate of 1 in 20 is acceptable due to the highly redundant nature of analogue speech.

i.e. $E/N_0 = 2$ dB [see Appendix 4(a)]

When digitized at, say, 16 k bit/s (42 dB):

$C/KT = 2+42 = 44$ dB Hz

This $S/N$ ratio cannot be achieved with the present Manpack when used in conjunction with *Skynet II*, though it will be readily achieved within the spot beam of later satellites. The maximum value that is practically possible using the *Skynet II* satellite is not more than about 39 dB·Hz subject to no noise margin and sole access to the satellite narrow band channel. This is an artificial situation, but since it can be achieved experimentally under certain circumstances, evaluation of an analogue speech link has been possible. For transmission the analogue speech waveform is hard limited to give infinite compression. This is applied directly to the final carrier phase modulator in place of the data stream. The result is analogue phase modulation with infinitely clipped audio speech. The spectrum during the speech phonemes consists of upper and lower side bands with suppressed carrier. For the intervals between phonemes carrier only is transmitted. In reception the speech signal is treated as data up to the output of the data detector. The carrier bursts and the low frequency speech components ensure the operation of the loop frequency doubler and hence maintenance of phase lock. After the data detector the speech is reconstituted by means of a simple filter. The bandwidth of the resulting speech is limited by that of the pre-detector filter whose bandwidth is approximately doubled for this application.

Users have noted that, even though there is a relatively high noise background level, the ear quickly accustoms itself to this and good communication can be achieved. Experiments have shown that the noise background has an advantageous softening effect on the link speech distortion giving talker recognition, while reduction of this noise makes the ensuing distortion less acceptable to the listener.

### 16 Base Station Installation

The modem for the base station end of the Manpack link (Fig. 4) uses similar sub-units to those in the Manpack. These are assembled in a rack mounted form with an integral mains power supply. Identical control and data input/output facilities to those on the Manpack are provided with the addition of an extra meter to monitor

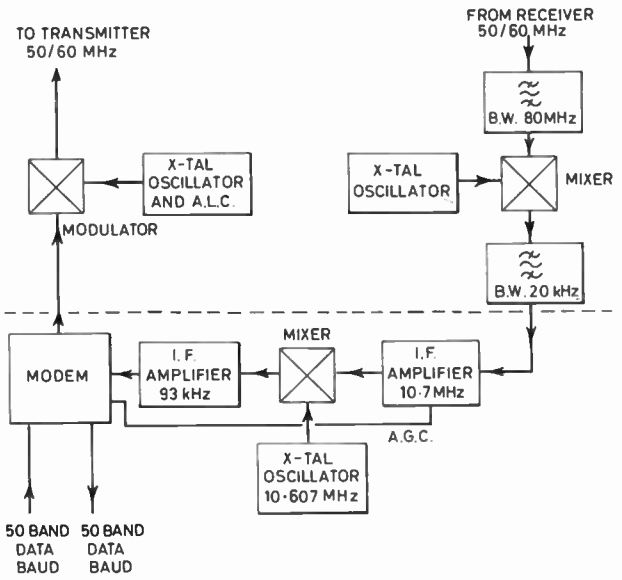


**Fig. 4.** Base station modem installation block diagram. All components shown below the line are identical to those used in the Manpack. Those above the line are for Master Station use.

the v.c.o. control voltage. The latter gives further indication of the link behaviour and overall system drift.

The interfaces with the base station are at intermediate frequencies in the range 50 to 60 MHz. For transmission the sub-carrier is locally generated by a crystal oscillator of appropriate stability. Since any variation in output level affects the radiated power of the station it is followed by an automatic level control amplifier. This also helps to buffer the oscillator from the fluctuating load of the following modulator. The latter is a suitable balanced diode mixer to give a modulated carrier output of 0 dBm in 50 Ω. The differentially encoded data stream drives the i.f. port of the mixer via a push-pull driver stage. This ensures that fast reversals of phase are achieved at the appropriate mixer current drive.

On reception, the modulated carrier is band-limited to approximately 8 MHz by means of a band-pass filter. It is then down-mixed to an i.f. of 10·7 MHz using a further balanced mixer and crystal oscillator of suitable stability. To ensure that the following i.f. amplifier is not overloaded by inter-modulation products or external interfering signals, it is preceded by a crystal filter of bandwidth 20 kHz.

Following this, the subsequent down-mixing and modem are identical to that used in the Manpack.

### 17 Telegraph Input/Output Devices

Several commercially available units have been purchased and subsequently modified and adapted to examine the present requirements for the Manpack. These have included a unit with a conventional keyboard layout and 16 character l.e.d. display. Its internal memory is able to store a message of 64 characters and also transmit and receive messages simultaneously. A second device has a 'pocket calculator' type keyboard and a more restricted display than that above, but of

otherwise similar performance. From the experience gained from these, a prototype terminal has been constructed in industry especially for the Manpack application. Its main features are as follows:

Conventionally spaced QWERTY keyboard for upper case letters and numbers

Hard copy of the received message, also of that transmitted if required.

Display of the last two or three current characters for checking the transmitted data when typing without a hard copy record.

Storage of received messages, when hard copy is not required, with subsequent recall.

Facility to erase the last current character during composition prior to transmission.

Protection of keyboard and printer when stowed.

Operation from the Manpack clock and power supply.

Small volume, power consumption and weight.

Since the heart of the instrument is a microprocessor, it may be subsequently reprogrammed to satisfy any further requirements or changes in facilities.

## 18 Mechanical and Electrical Construction

With the overall requirements for low weight, volume and power consumption, the following methods have been used for the prototype equipment.

### 18.1 Mechanical Construction

The case is fabricated from thin light alloy sheet suitably reinforced and braced. It separates as two similar wedge shaped halves, with a rubber seal between the two for waterproofing. One half of the case contains all the electrical and mechanical assemblies, while the other forms a lid. The larger surface of the former is also the aerial dish. For ease of construction this is 'layed up' in fibre glass and bolted into a circular cutout in the case. The surface of the dish is zinc coated as part of the 'laying-up' process to give it a conducting surface. Within this half of the case and directly behind the dish is a large detachable sub-panel on which all the electrical sub-assemblies are mounted. This enables the volume directly behind the dish to be used.

The back carrier is a military radio type of steel tube, modified to stow the above case when in transit and provide extended supports for the case trunnions plus three point ground contact when deployed. Future development of the carrier to use light alloy tube and provide azimuth adjustment may give some reduction in weight.

Many of the sub-assemblies are bought-in commercially available items specially chosen for their low power consumption and weight. The waveguide components are all fabricated in light alloy with no relaxation in their r.f. specification over that of their conventional brass or copper equivalent. The special sub-units constructed 'in-house' follow good mechanical and electrical practice, producing rugged, well-screened modules in light alloy. The low frequency circuits of the modem are assembled on printed circuit cards within a frame for easy removal.

### 18.2 Electrical Construction

To reduce power consumption, as many as possible of the Manpack circuits are operated from $\pm 6$ V. This is especially the case of the modem which also simplifies the production of the V24 data interface. The modem circuits make large use of the low power consumption c.m.o.s. range of integrated circuit modules. These are for digital processes with operational amplifiers for analogue circuits and for interfacing between the two. Several of the proprietary modules incorporated such as the f.e.t. power amplifier and some i.f. amplifiers are specified to operate from $+12$ V.

The power source proposed for the Manpack is a nickel/cadmium secondary battery of 4AH capacity having a useful voltage range on discharge between 28 and 22 V. This has to be converted to the stable values required by individual modules.

The present total battery drain is 30 W which could be reduced in subsequent models by the use of improved efficiency voltage regulators and lower power consumption proprietary sub-units now under evaluation. Two further methods of power conservation are also being considered for future Manpacks. The first is the inhibiting of the Manpack transmitter between messages. This will require a more sophisticated carrier acquisition circuit in the base station modem to reduce the signal acquisition time to less than the period of the message preamble time. This will not introduce any further complications in to the Manpack.

The second power reduction will be implemented when the high-gain spot beam satellites are used. This will enable the required Manpack e.i.r.p. to be reduced by up to 6 dB for telegraph links.

## 19 Manpack Tests and Trials

### 19.1 Confirmation of Theoretical Design Parameters via the Satellite Links

(i) The station e.i.r.p. was measured as 31 dBW using the power balance measurement technique at the RSRE 40ft Earth Station.

(ii) The $C/KT$ at the RSRE 40ft Earth Station receiver was measured as within 0·5 dB of the calculated value of 39 dB · Hz, when receiving the above signal from the manpack, the latter having sole access to the *Skynet II* 2 MHz channel.

(iii) The bit error rate at both the manpack receiver and base station receiver was better than $10^{-4}$ for a receiver $C/KT$ of approximately 30 dB · Hz. Precision in this measurement is difficult, since to get a meaningful error rate this must be measured over a considerable interval during which the

value of $C/KT$ may vary because of link variations outside the control of the experimenter. Measurements on the modem in isolation gave error rate figures better than $10^{-5}$ at this simulated noise level.

### 19.2 Familiarization in the Field

Such tests indicated ergonomic limitations in the equipment which could be improved in future models. For example when deploying the present equipment the case must first be separated from the carrier before reassembling in its operating position. Then the back carrier, which form a rudimentary tripod when deployed, has to be moved on the ground until the aerial azimuth is optimized. In practice this proved difficult on rough uneven ground and some form of limited travel turntable seems desirable.

### 19.3 Indoor Tests

Links were set up with the equipment deployed indoors 'on the office desk' and aimed out of a convenient window. Typically it was found that an increased path attenuation of about 4 dB results when transmitting through a closed window. This was reduced to about 1 dB when the glass was replaced with perspex.

## 20 Conclusions

Laboratory and field investigations have shown that s.h.f. Manpack stations are practicable. A first prototype research model has been constructed and demonstrated working both telegraph and low-quality speech.

The work has highlighted the importance of having satellite repeaters operating at relatively high gain in order to serve terminals with low e.i.r.p., e.g. manpacks. *Skynet II* is satisfactory in this respect but it should be noted that some existing satellite repeaters operated to serve trunk links between large land stations are not.

With the prototype station the satellite e.i.r.p. needed for duplex telegraph operation was approximately 5 W; 10 W was needed for analogue speech and it was estimated 100 W would be needed for a standard digital speech link. The latter figure is high with respect to the total e.i.r.p. available from *Skynet II* (350 W) but not at all unreasonable compared with the 10 kW or more available in the spot/area beams of the next generation satellites.

## 21 Acknowledgments

This paper is published by permission of the Director, R.S.R.E. Copyright Controller HMSO, London 1981.

## 22 References

1 Silver, S. (Ed.), 'Microwave Antenna Theory and Design', Section 12.5 (McGraw-Hill, New York, 1949).
2 Jasik, H. (Ed.), 'Antenna Engineering Handbook', Section 25–31 (McGraw-Hill, New York, 1961).
3 Stein, S. and Jones, J. J., 'Modern Communication Principles', Section 12–1 (McGraw-Hill, New York, 1967).
4 Jones, C. H., 'A test equipment for the measurement of phase and frequency instability in v.h.f. and s.h.f. sources', *The Radio and Electronic Engineer*, **49**, no. 4, pp. 187–196, April 1979.
5 Gardner, F. M., 'Phase-lock Techniques' (Wiley, New York, 1967).

## 23 Appendix 1: High Efficiency Feed for a Small Diameter Aerial

Parabolic dish, circularly polarized aerials for use at X-band with Cassegrain or splash plate feeds are not normally considered below about $1\frac{1}{2}$ metres in diameter. This is due to the relatively large blocking area presented by the feed causing reduction of gain and poor sidelobe rejection. Blocking can be overcome by the use of an offset feed, but this results in a complex mechanical assembly, a longer feed, and a line of propagation not along the parabola axis. Hence for the Manpack a modified splash plate feed and dish has been developed.

It can be shown[1] that the theoretical gain of a uniformly illuminated parabolic dish is:

$$G = \left(\frac{\pi D}{\lambda}\right)^2 \tag{1}$$

At 8 GHz for a dish diameter ($D$) of 45 cm:

$$G\,\text{dB} = 10\log\left(\frac{\pi \cdot 45}{3{\cdot}75}\right)^2 = 31{\cdot}5\ \text{dB} \tag{2}$$

Using a conventional parabolic dish (diam/focal length = 2·5) and splash plate, the measured gain:

$$G = 26{\cdot}5\ \text{dB} \tag{3}$$

and efficiency:

$$\eta = -(31{\cdot}5 - 26{\cdot}5) = -5\ \text{dB} = 31{\cdot}6\% \tag{4}$$

It has been found practically that this low gain and efficiency is markedly improved by the use of a ring-focus feed.[2] This consists of an open-ended circular waveguide with a reflecting plate, as shown in Fig. 5, producing a phase centre lying along a circle between the end of the guide and the plate. As a consequence, the simple paraboloid is unsatisfactory for the main reflector and is replaced by a figure of revolution generated by revolving

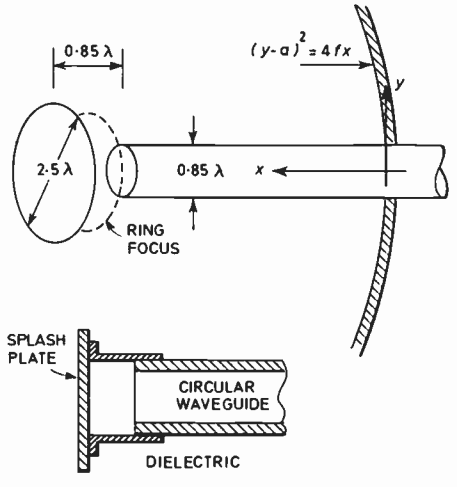


Fig. 5. Ring-focus aerial.

**Table 2**

| Focal Length | Diameter | Frequency | Gain | Bandwidth −3 dB | Side-lobe Rejection | Efficiency % |
|---|---|---|---|---|---|---|
| 18 cm | 45 cm | 8 GHz | 28·2 dB | 4·75 deg | 15·5 dB | 46·8 |
| | | 7·275 GHz | 28·0 dB | 5·6 deg | 20 dB | 44·7 |

the following parabola about the $x$-axis:

$$(y-a)^2 = 4fx \tag{5}$$

where $a$ is the radius of the above phase centre. The 'hole' in the centre of this surface is satisfactory as a plane. It has been suggested that the gain of this type of feed is probably better than any other simple rear feed system, though the sidelobe discrimination is not as good as a conventional system.

Measurements of the proposed Manpack dish and ring-feed are as in Table 2.

Since the transmission and reception use opposing hand circular polarization, the circular waveguide feed contains a suitable dielectric polarizer blade. The feed and polarizer are easily detached from the dish, by means of a located bayonet socket, for subsequent storage when the equipment is transported. Also associated with the feed, but behind the dish, are a diplexer to separate the resulting receiver and transmitter modes, and transmitter plus receiver waveguide filters. The bandwidth of the latter are both 50 MHz on the above nominal frequencies, and their insertion losses are less than 0·5 dB. The loss of the complete feed, diplexer and filter path is estimated to be not greater than 0·75 dB.

## 24 Appendix 2: Receiver Noise Calculations

The relevant parts of the Manpack receiver which contribute to the total system noise are shown in Fig. 6

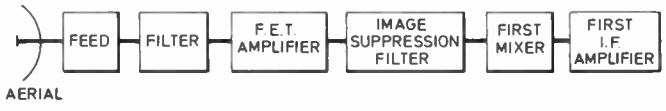


**Fig. 6.**

The components which have the greatest effect on the overall receiver noise temperature are those producing attenuation before the first amplifier plus the first amplifier and mixer. The aim is to reduce the pre-amplifier attenuation to as low a value as possible followed by an amplifier having the highest gain and lowest noise temperature possible. For the Manpack, due to its compact form, it is possible to reduce the attenuation to a very low order. The amplifier is a compromise between the uncooled parametric type with its low noise temperature but relatively low gain, and the f.e.t. amplifier, having normally higher gain but, in present models, higher noise temperature. The following shows the overall system noise balance referred to the aerial.

AERIAL

At an ambient temperature ($T_{amb}$) of 300 K, the aerial temperature is taken as:

$$T_{eq} = 40\ \text{K} \tag{6}$$

FEED

Taking the attenuation as 0·25 dB ($L_{feed}$)

$$T_{eq} = T_{amb}(L_{feed}-1)$$
$$= 300\,(1{\cdot}06-1) = 18\ \text{K} \tag{7}$$

FILTER

Attenuation is taken as 0·5 dB ($L_{filter}$)

$$T_{eq} = T_{amb}\,L_{feed}\,(L_{filter}-1)$$
$$= 300\times 1{\cdot}06(1{\cdot}12-1) = 39\ \text{K} \tag{8}$$

F.E.T. AMPLIFIER

Gain ($G_{amp}$) = 27 dB

Noise temperature ($T_N$) = 250 K (9)

$$T_{eq} = 250\times 1{\cdot}06\times 1{\cdot}12 = 297\ \text{K} \tag{10}$$

IMAGE SUPPRESSION FILTER

Pass-band attenuation $L_{ISF}$ = 0·5 dB

$$T_{eq} = T_{amb}\frac{1}{G_{amp}}(L_{ISF}-1)\,L_{filter}\,L_{feed}$$

This is negligible for all normal values of $G_{amp}$.

MIXER

Noise figure ($NF$) = 8 dB

Insertion loss ($L_{mix}$) = 6·5 dB

$$T_{mix} = T_{amb}\,(NF-1) = 300\,(6{\cdot}3-1) = 1593\ \text{K} \tag{11}$$

Referred to aerial:

$$T_{eq} = T_{mix}\frac{1}{G_{amp}}(L_{mix}-1)\,L_{filter}\,L_{feed}$$

For $G_{amp}$ = 27 dB

$$T_{eq} = 13\ \text{K} \tag{12}$$

FIRST I.F. AMPLIFIER

Noise figure ($NF$) = 3·2 dB

$$T_{amp} = T_{amb}\,(NF-1) = 300\,(2{\cdot}1-1) = 330\ \text{K} \quad (13)$$

Referred to aerial:

$$T_{eq} = T_{amp}\frac{1}{G_{amp}}\,L_{mix}\,L_{filter}\,L_{feed}$$

For $G_{amp}$ = 27 dB

$$T_{eq} = 1{\cdot}77\ \text{K} \quad (14)$$

RECEIVER EQUIVALENT NOISE TEMPERATURE

$$T_{eq} = 40+18+39+297+13+1{\cdot}77 = 409\ \text{K} \quad (15)$$

## 25 Appendix 3: Satellite Frequency and Power Allocation

1. Satellite Parameters

It will be evident from Fig. 2 that the prototype Manpack has been designed to operate on fixed frequencies for both transmission and reception. These frequencies are allocated for experimental use in conjunction with the narrow path way of the *Skynet II* satellite. This satellite has the advantage of greater repeater gain over that of other available Earth cover satellites. Unfortunately, *Skynet II* is a hard limiting repeater and power balancing between accesses is normally required. By operating the Manpack in the narrow pathway where only relatively low power accesses are permitted, large variations of ground received signals, due to changing traffic loads are reduced.

The relevant parameters of the *Skynet II* narrow pathway are as follows:

| | |
|---|---|
| Nominal bandwidth | 2·0 MHz |
| Effective noise bandwidth | 2·5 MHz |
| Nominal e.i.r.p. | 55·5 dBm, i.e. 355 W |
| Receiver noise temperature | 3000 K |
| Aerial gain | 16 dB |
| Transmitter frequency range | 7259·3 MHz |
| | 7257·3 MHz |
| Receiver frequency range | 7978·02 MHz |
| | 7976·02 MHz |
| Translation frequency | 718·72 MHz |

2. R.F. Power Requirements

It can be shown that the front-end noise generated by *Skynet II* is:

$$KT = K\cdot 3000\ \text{W}\cdot\text{Hz}^{-1} \text{ or } -194\ \text{dBW}\cdot\text{Hz}^{-1}$$

Since the Manpack has a maximum e.i.r.p. of 31 dBW (2 W via a 28 dB aerial) the signal received from the Manpack at the repeater input:

$$C|_{dB} = \text{manpack e.i.r.p.} - \text{path loss} + \text{satellite aerial gain}$$
$$= 31-201{\cdot}5+16 = -154{\cdot}5\ \text{dBW} \quad (17)$$

$C/KT|_{dB}$ at output of a linear repeater:

$$= 194-154{\cdot}5 = +39{\cdot}5\ \text{dB Hz} \quad (18)$$

This is received by the base station which is noise-limited by the satellite. Hence the $C/KT$ at the base station is also this value. In practice the repeater is hard limiting. The satellite front-end noise power is 2·5 MHz noise bandwidth:

$$N|_{dB} = -194+64 = -130\ \text{dBW} \quad (19)$$

Hence at the same point:

$$C/KTB|_{dB} = -(154{\cdot}5-130) = -24{\cdot}5\ \text{dB} \quad (20)$$

This can be shown to suppress the signal of (18) due to satellite limiter action by about 1 dB. Therefore,

$$\text{true } C/KT|_{dB} \simeq 38{\cdot}5\ \text{dB}\cdot\text{Hz} \quad (21)$$

which has been confirmed by practical measurement within 0·5 dB. Practical measurements have also shown that this condition can also be achieved at the manpack receiver with a base station e.i.r.p. of approximately 49 dBW, i.e. 0·25 W and aerial gain of 55 dB.

The individual power requirements from the satellite to produce the conditions of (21) at both the manpack and base station receivers are derived as follows:

Let $C/KT$ at receiver be $A$ dB . Hz

| | |
|---|---|
| receiver noise temperature | $T$ dB |
| aerial gain | $G$ dB |
| Boltzmann constant | $-198{\cdot}6\ \text{dBm}\cdot\text{K}^{-1}$ |

Then total receiver noise = $(-198{\cdot}6+T)\ \text{dBm}\cdot\text{Hz}^{-1}$

required modem signal = $(A-198{\cdot}6+T)$ dBm
signal before aerial = $A-198{\cdot}6+T-G$
signal at satellite = $(A-198{\cdot}6+T-G)+$path loss (22)

(a) For manpack let $A$ = 38·5 dB·Hz
$T$ = 26 dB
$G$ = 28 dB
path loss = 202 dB

Therefore satellite e.i.r.p. = $38{\cdot}5-198{\cdot}6+26-28+202$
= 39·9 dBm, i.e. 10 W (23)

(b) For base station let $A$ = 38·5 dB Hz
$T$ = 23 dB
$G$ = 55 dB
path loss = 202 dB

satellite e.i.r.p. = $38{\cdot}5-198{\cdot}6+23-55+202$
= 9·9 dBm, i.e. 10 mW (24)

In an operational telegraph duplex link the value of $A$ can be reduced by at least 3 dB in each case with the design error rate not exceeded under most weather and traffic conditions. This will now require less than 1½% of the total satellite power available in the *Skynet II* narrow pathway.

3. Satellite Frequency Allocation and its Effect on Ground Station First I.F.

The allocated frequencies for the link are:

| | |
|---|---|
| Manpack Tx | 7977·114 MHz |
| Base station Rx | 7258·39 MHz |
| Base station Tx | 7977·3325 MHz |
| Manpack Rx | 7258·6125 MHz |

It will be seen from Fig. 3 that the master oscillator, which is followed by a ×90 multiplier, will have an output at:

$$\frac{7977{\cdot}114}{90} = 88{\cdot}634 \text{ MHz} \qquad (25)$$

to achieve the required Manpack transmitter frequency.

Since the oscillator is also multiplied by 81 to produce the receiver first local oscillator, the resultant first intermediate frequency becomes:

$$7258{\cdot}6125 - (81 \times 88{\cdot}6346) = 79{\cdot}2099 \text{ MHz} \qquad (26)$$

## 26 Appendix 4: Modem Carrier Recovery Circuit Design

1. Input $S/N$ Conditions

It can be shown for a differentially encoded p.r.k. system that the required signal-to-noise ratio per baud ($E/N_0$) for a given error rate is theoretically as follows:

| Error rate | $E/N_0$ dB |
|---|---|
| $10^{-5}$ | 10·5 |
| $10^{-4}$ | 9 |
| $10^{-3}$ | 8 |
| $10^{-2}$ | 6 |
| $10^{-1{\cdot}3}$(1in 20) | 2 |

The normal operating error rate condition for telegraphy is $10^{-4}$ with $E/N_0$ of 9 dB.

It is essential that the tracking loop maintains lock for $E/N_0$ down to 6 dB. Hence at a data rate of 50 baud:

$$\text{minimum } C/KT = 6+17 = 23 \text{ dB}\cdot\text{Hz} \qquad (27)$$

The noise bandwidth at the input to the loop as defined by the second i.f. amplifier is 12 kHz (41 dB).

Therefore input $S/N$ for modem to just hold phase-lock:

$$= 23-41 = -18 \text{ dB} \qquad (28)$$

2. Loop $S/N$ Conditions

To design a tracking filter it is considered that the $S/N$ in the loop should be +6 dB for normal operation, falling to +3 dB for acquisition to be just possible.[5] For the loop to be stable and not affected by false locks, any i.f. filtering within the loop must not be too narrow. The post mixer filter uses a simple parallel tuned circuit of noise bandwidth 300 Hz.

$$\text{Resulting } S/N = -18+10\log\frac{12000}{300} = -2 \text{ dB} \qquad (29)$$

This bandwidth is sufficient to pass the 50 baud modulation spectrum. A deterioration of this $S/N$ is introduced by the following frequency doubler as follows:

$$\text{Let signal input} = S$$
$$\text{noise input} = N$$
$$\text{total input to doubler} = S+N$$
$$\text{output due to doubler} = S^2+2SN+N^2$$
$$\text{output } \frac{\text{signal}}{\text{noise}} = \frac{S^2}{2SN+N^2}$$

For an input $S/N$ of −2 dB

$$\text{output } S/N = -7{\cdot}5 \text{ dB} \qquad (30)$$

To achieve the minimum overall loop $S/N$ of +3 dB, the loop bandwidth is derived as follows:

required improvement in $S/N$ due to integrator:

$$= 7{\cdot}5+3 = 10{\cdot}5 \text{ dB} \quad (\times 11{\cdot}2)$$

$$\text{loop bandwidth} = \frac{300}{11{\cdot}2} = 26{\cdot}8 \text{ Hz} \qquad (31)$$

This is a single sideband width.

3. Further Effects of Frequency Doubling

Let the input to the doubler be:

$A \sin(\omega t+\phi)$ where $\phi$ is the instantaneous phase of the modulation.

The output expression can be expanded to be of the form:

$$K+(L\cos\phi)\cos 2\omega t+(M\sin 2\phi)\sin 2\omega t \qquad (32)$$

where $K$, $L$ and $M$ are constants.

When the modulation phase changes switch instantaneously between 0 and $\pi$, the output becomes:

$$K+L\cos 2\omega t \qquad (33)$$

consisting of a d.c. component plus a modulation free carrier of constant amplitude.

With restricted bandwidth the phase switches in a finite time. Hence the output is still a carrier of twice the input frequency, but the amplitude varies as a function of the switching time of the modulation. Since this can lead to possible breaks in the carrier, it is followed by a tuned circuit of sufficient $Q$ to 'fly wheel' over such intervals without unstabilizing the loop. A bandwidth of 1 kHz ($Q = 50$) is found to be satisfactory.

4. Loop Parameters and Integrator Time-constants

To calculate the integrator time-constants the following parameters are defined[5]

limiter suppression factor at lock threshold:

$$\alpha = \left(\frac{S/N}{4/\pi + S/N}\right)^{\frac{1}{2}}$$

For $S/N$ at input to loop limiter of $-7{\cdot}5$ dB

$$\alpha = 0{\cdot}35$$

phase detector gain factor $(K_d) = \frac{6}{2\pi}$ V·rad$^{-1}$

v.c.o. gain constant $(K_0) = \frac{\pi}{2} 10^4$ rad·s$^{-1}$ V$^{-1}$

loop damping factor $(\zeta) = 0{\cdot}5$

loop bandwidth $(B_L) = 26{\cdot}8$ Hz

$$B_L = \frac{\omega_n}{2}\left(\zeta + \frac{1}{4\zeta}\right)$$

natural frequency $(\omega_n) = 53{\cdot}6$ rad·s$^{-1}$.

Total hold-in range $(\Delta\omega_H) = 2\pi \cdot 10^4$ rad·s$^{-1}$.

Maximum static loop error $(\varepsilon_v) = 0{\cdot}1$ rad.

Also

$$\varepsilon_v = \frac{\Delta\omega_H}{\text{loop gain } (s^{-1})}$$

Therefore minimum loop gain $= 2\pi \times 10^5$ s$^{-1}$
$= \alpha A K_d K_0$

where $A$ is the voltage gain of the loop amplifier.

Therefore $A \not< 20$

In practice this value is greatly exceeded.

The integrator time-constants:

$$\tau_1 = \alpha\frac{K_d K_0}{2\omega_n^2} = 1{\cdot}83 \text{ s} \quad (34)$$

$$\tau_2 = \frac{2\zeta}{\omega_n} = 0{\cdot}019 \text{ s} \quad (35)$$

Since $\tau_1 = R_1 C$ and $\tau_2 = R_2 C$

$R_1 = 1$ MΩ $R_2 = 10$ kΩ and $C = 2{\cdot}2$ μF (36)

*Manuscript received by the Institution on 2nd October 1981.*
*(Paper No 1989/Comm 218)*

UDC 621.372.54

*Indexing terms:* Digital signal processing, Transversal filters, Binary p.n. sequences, Pulse compression, Ambiguity diagrams

# The design and performance of transversal filters for the sidelobe reduction of pulses compressed from combined Barker phase codes

**G. B. MORGAN,** B.Sc., Ph.D., M.Inst.P., C.Eng., M.I.E.E.*

**P. DASSANAYAKE,** B.Sc., M.Sc., Ph.D.*

and

**Ø. A. LIBERG,** B.Sc., Ph.D.*

**SUMMARY**

The high temporal sidelobes of compressed combined Barker codes can be reduced using minimum-square-error transversal spiking filters. Very large (40 to 60 dB) peak-to-sidelobe ratios may be obtained for words up to 169 bits long using transversal filters which are only several hundred bits long. The effect of a Doppler frequency shift of the signal is analysed and a cross-ambiguity diagram is presented for a 52-bit word and a 200-bit filter. The influence of noise and manufacturing tolerance is also considered, and, finally, improvements due to a further shaping of the output are detailed.

* *Department of Physics, Electronics and Electrical Engineering, University of Wales Institute of Science and Technology, King Edward VII Avenue, Cardiff CF1 3NU.*

*The Radio and Electronic Engineer, Vol. 51, No. 6, pp. 272–280, June 1981*

## 1 Introduction

The advances in digital circuitry and other electronic technologies[1] over the last decade, or so, have enhanced interest in phase-coded signals for pulse compression and spread spectrum techniques. When used in ranging and detecting systems, or digital communication systems, pulse compression can give considerable gain in signal-to-noise ratios and interference rejection, whilst in radar-type systems there is also an improvement in signal-to-clutter ratios. Digital words are cheap to generate and process, and so are of interest in low cost, low power solid-state systems. Codes can also be rapidly changed on a pulse-to-pulse basis, a feature that could be tactically important in some systems. However the designers of such systems are faced with the problem of finding binary words that give an appreciable compression ratio with acceptable temporal sidelobe levels.

While the well-known Barker codes[2,3] (see Table 1) are optimum from the point of view of low sidelobes, they are not satisfactory because they are limited to a compression ratio of thirteen or less. The longer pseudo-random binary words can offer higher compression ratios ($2^n - 1$, where $n$ is an integer), but require long mismatched receivers to get acceptable sidelobe levels.[4] Long words, of up to 169 bits, can also be obtained by combined Barker codes, but the peak-to-sidelobe ratios are not acceptable. Table 2 shows the matched filter performance for several combined Barker codes. The ratio of the peak-signal-to-peak-sidelobe voltage is given, as well as the ratio of the signal energy to self clutter (total sidelobe energy) for various combined Barker codes. Combined Barker codes using the shorter sub-codes have the lower peak-to-sidelobe ratios, because the peak-to-sidelobe ratio is determined by the sub-code within them. For most applications the peak-to-sidelobe ratios should be of the order 40 dB or more so that the combined Barker codes are not suitable, unless means are available to improve the peak-to-sidelobe ratios.

This paper reports on the performance of a transversal filter whose coefficients are chosen to reduce sidelobe energy. The effect of Doppler shifted signals is discussed, together with the influence of random noise. Finally manufacturing tolerances are considered and a new improved sidelobe suppression criterion for the design of filters is presented, together with its performance.

**Table 1**
Barker codes

| Code length (bits) | Code elements |
|---|---|
| 2 | + −, + + |
| 3 | + + − |
| 4 | + + − +, + + + − |
| 5 | + + + − + |
| 7 | + + + − − + − |
| 11 | + + + − − − + − − + − |
| 13 | + + + + + − − + + − + − + |

0033–7722/81/060272+09 £1.50/0

**Table 2**
Matched filter performance for combined Barker words

| Code length (bits) | Code structure | Peak signal voltage / Peak sidelobe voltage | Peak signal energy / Total sidelobe energy |
|---|---|---|---|
| 39 | 13 of 3-bit sub-code | 9·5 dB | 5·10 dB |
| 52 | 13 of 4-bit sub-code | 11·8 dB | 5·6 dB |
| 65 | 13 of 5-bit sub-code | 14·0 dB | 6·15 dB |
| 91 | 13 of 7-bit sub-code | 16·9 dB | 6·9 dB |
| 143 | 13 of 11-bit sub-code | 20·8 dB | 8·0 dB |
| 169 | 13 of 13-bit sub-code | 22·2 dB | |

## 2 The Optimum Spiking Filter

One of the techniques used to reduce sidelobes is to weight the receiver, as described for example in References 4 and 5, and references therein. This Section summarizes the theory of the choice of filter weighting coefficients.

Let $a_t = a_0, a_1, \ldots, a_m$ be the input p.n. word to the transversal filter shown in the diagram of Fig. 1 and let $b_t = b_0, b_1, \ldots, b_n$ be the filter impulse response. Then the filter output $c_t$ is given by the convolution

$$c_t = a_t * b_t$$

which in terms of $z$ transforms can be written

$$B(z) = C(z)/A(z).$$

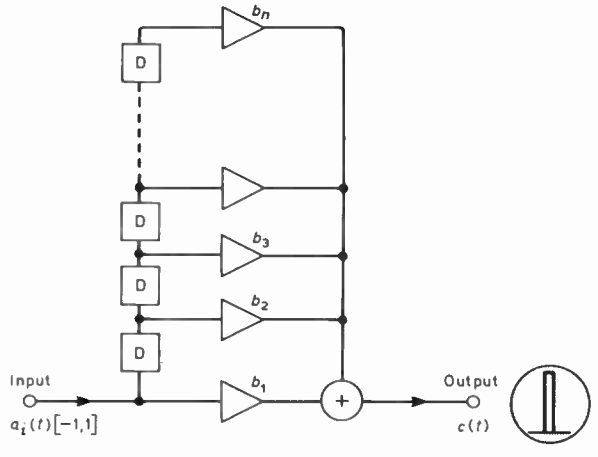


**Fig. 1.** Block diagram of $n$ bit transversal filter. It consists of delay stages D and taps with coefficients $b_k$ where $k = 1$ to $n$.

Ideally, since it is required that the peak-to-sidelobe ratio should be a maximum, $c_t$ should be an impulse function, so that $C(z) = 1$ and $B(z) = |A(z)|^{-1}$.

However, when $A(z)$ represents a binary sequence, $B(z)$ does not represent a physically realizable (i.e. closed form) impulse response, so that approximate solutions have to be found.

Rice[6] has shown that a closer approximation to the inverse filter can be obtained by employing the minimum square error criterion, the degree of approximation obtained depending upon the length (in bits) of the inverse filter. In this method the desired output, $d_t$ of the filter is specified explicitly as

$$d_t = d_1, d_2, \ldots, d_{m+n}$$

and the filter impulse response $b_t$ is evaluated so as to minimize the square error, $E$, given by

$$E = \sum_{t=0}^{m+n} (d_t - c_t)^2$$

Since

$$c_t = \sum_{k=0}^{n} b_k a_{t-k} \quad \text{for } t = 0, 1, \ldots, m+n$$
$$= 0$$

otherwise,

$$E = \sum_{t=0}^{m+n} |d_t - \sum_{k=0}^{n} b_k a_{t-k}|^2$$

Thus the condition for $E$ to be a minimum is given by

$$\sum_{k=0}^{n} b_k \left| \sum_{t=0}^{m+n} a_{t-k} a_{t-j} \right| = \sum_{t=0}^{m+n} d_t a_{t-j}$$

$$j = 0, 1, \ldots, n$$

which can be written in the form

$$\sum_{k=0}^{n} b_k r_{j-k} = s_j,$$

where

$$r_{j-k} = \sum_{t=0}^{m+n} a_{t-k} a_{t-j}$$

is the autocorrelation of the input $a_t$ and

$$s_j = \sum_{t=0}^{m+n} d_t a_{t-j}$$

is the cross-correlation of the input $a_t$ and the desired output $d_t$.

The filter that corresponds to a particular $d_t$ at which $E$ is minimum is called the optimum spike filter.[7]

Computer programs have been written to evaluate the optimum spike filters and their performance for several combined Barker codes. Appendix 1 gives an example of the values of the filter coefficients obtained for the 52-bit word and a filter length of 200 bits. Figures 2 and 3 illustrate the performance of the optimum spike filter for

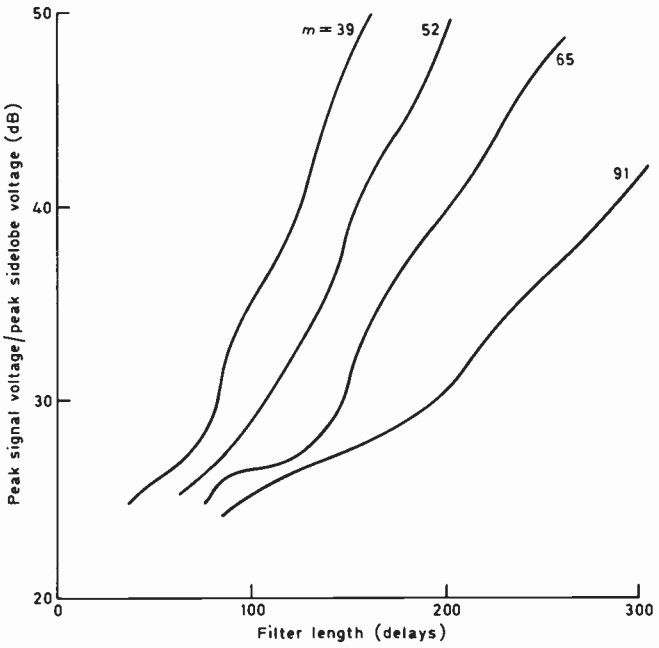


Fig. 2. Optimal spiking filter peak-to-sidelobe ratios for combined Barker words of length 39, 52, 65 and 91 bits as a function of filter length.

words of length 39, 52, 65 and 91. Figure 2 shows the enhancement in peak-to-sidelobe ratio (P/SL) obtainable with increasing filter length. In the case of a 39-bit word, a 30 dB peak-to-sidelobe ratio could be obtained with a filter of length 80 delay stages and a 40 dB peak-to-sidelobe ratio with a filter of 123 stages. For a 65-bit word 40 dB sidelobes require a 200-bit filter.

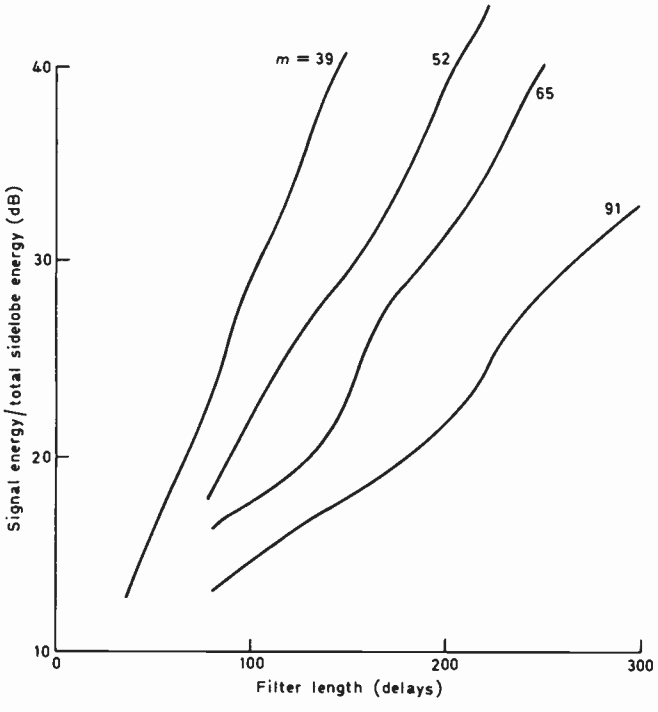


Fig. 3. Signal-to-selfclutter ratios for combined Barker words and spiking filter as a function of filter length, for words of length 39, 52, 65 and 91 bits.

Figure 3 shows the enhancement in the signal-to-selfclutter ratio (S/CL) obtainable with the spike filter. It can be seen that there is a steady improvement in the signal-to-selfclutter ratio with increasing filter length. This is to be expected, as the filter design criterion is one that essentially minimizes the selfclutter.

The price that has to be paid for these improvements in the values of the peak-to-sidelobe and signal-to-selfclutter ratios, apart from the added complexity, is the loss in signal detectability due to receiver mismatch. Typically, degradations are 1 to 1·5 dB.

### 3 The Effect of Doppler Shift on Phase Codes

The suitability of a particular radar waveform to determine target range and range rate may be described by means of its ambiguity diagram.[2] This is a three-dimensional representation of the modulus of the output from a filter matched to the signal in question, as a function of time-delay and Doppler shift. It can be shown that the correlator output is given by

$$\chi(T_R, f_D) = \left| \int_{-\infty}^{\infty} U(t)U^*(t - T_R) \exp(j2\pi f_D t)\, dt \right|$$

where $U(t)$ is the complex waveform modulation envelope, $T_R$ is the estimate of echo time and $f_D$ is the Doppler frequency shift. The asterisk denotes complex conjugate.

Of the large number of possible words and filters investigated data are presented for a 52-bit word, since such a word is a good compromise between showing the differences in the computed ambiguity and cross-ambiguity diagrams, and the present computing facilities. The ambiguity diagram for the 52-bit non-continuous combined Barker word is shown in Fig. 4. In view of the mirror symmetry about both axes only the second quadrant is presented, showing the negative time and positive frequency-axes. $T$ is the bit-duration in seconds.

It is considered that this quadrant gives the best detail of the sidelobe structure, which otherwise would be obscured by the main lobe at the origin. The modulus of the autocorrelation function of this 52-bit word can be seen in the foreground of the diagram. It can also be seen that the high sidelobes which appear far into the Doppler domain will produce strong selfclutter and ambiguous target range and range rate.

A transversal filter may be designed to reduce any particular patch of sidelobes at the expense of other regions. In the present case a mismatched filter was designed to give sidelobes which were 40 dB down on the central peak for zero Doppler shift, the design criterion being to minimize selfclutter energy. For every filter length a search was made to find the position of the compressed pulse that provided the minimum selfclutter energy, evaluated at zero Doppler shift. It can be shown[8] that the minimum square error is most likely to be found within the central region of the filter convolution output.

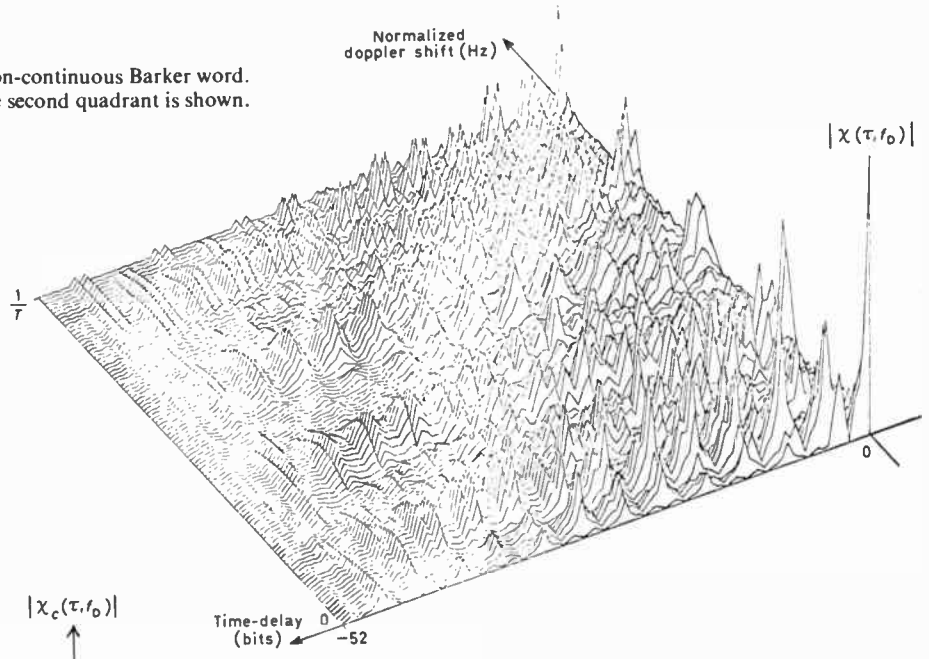


Fig. 4. Ambiguity diagram for the 52-bit non-continuous Barker word. As it is symmetrical about the axes only the second quadrant is shown.

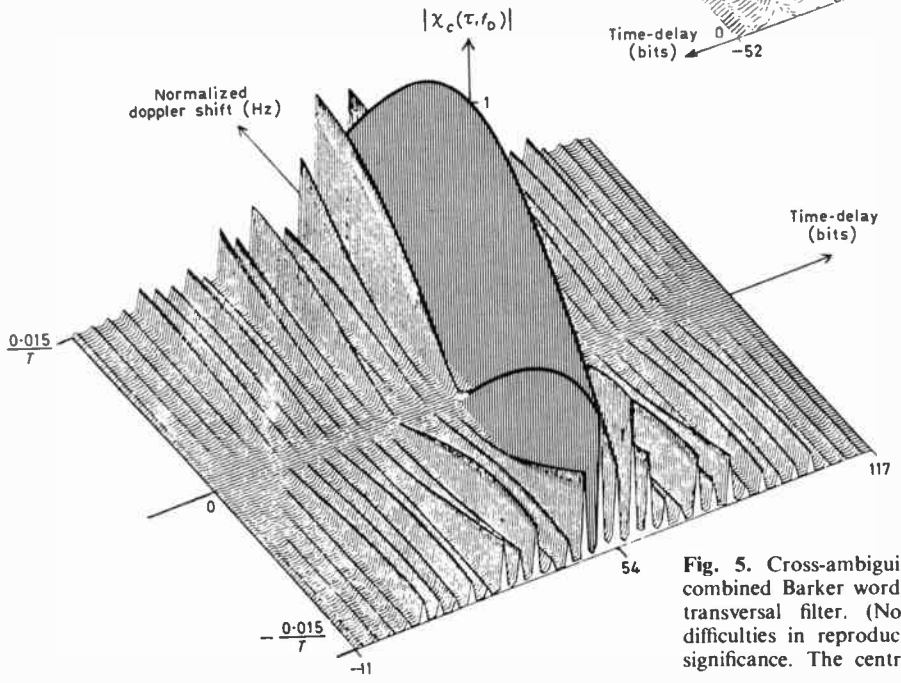


Fig. 5. Cross-ambiguity diagram for the 52-bit non-continuous combined Barker word and a 200-bit length minimum square error transversal filter. (Note.—Apparent 'high-lights' are caused by difficulties in reproducing an automatic plot and have no special significance. The centre lobes have been simulated for the same reason.)

In the present case it was found that a 200-bit filter was sufficiently long to give $-40{\cdot}7$ dB sidelobes, which is considered to be a sidelobe level in keeping with an entire radar system. The loss in signal detectability in white, Gaussian noise, relative to that of a matched filter, was computed to be 1·86 dB.

The effect of this mismatched filter may be seen by an inspection of the cross-ambiguity-diagram given in Fig. 5. For a word that is $52T$ seconds long the output from the filter starts at $-52T$. It can be seen that the main peak occurs at a time $54T$. Only the central portion of the cross-ambiguity diagram is plotted due to the limit on the number of discrete data points that the graphic package could handle. The time scale is plotted from $-11T$ to $117T$ s while the frequency scale is from 0 to $\pm 0{\cdot}015/T$ Hz. Notice that the frequency axis is expanded relative to that of Fig. 4 since only small Doppler shifts relative to signal bandwidth are physically relevant.

A comparison of the data present in Figs. 4 and 5 shows that filters designed to have low temporal sidelobes for zero Doppler also give an improvement relative to a matched filter for Doppler shifts below 0·5% of the signal bandwidth (see Fig. 6). The nominal Doppler bin width has widened by 8·6% measured at the half-power points. Hence the resolution in target range rate is slightly reduced.

A numerical example illustrates the joint resolution properties in range and range rate. For a nominal resolution cell which has $\Delta f_D = 0{\cdot}019/T$ and

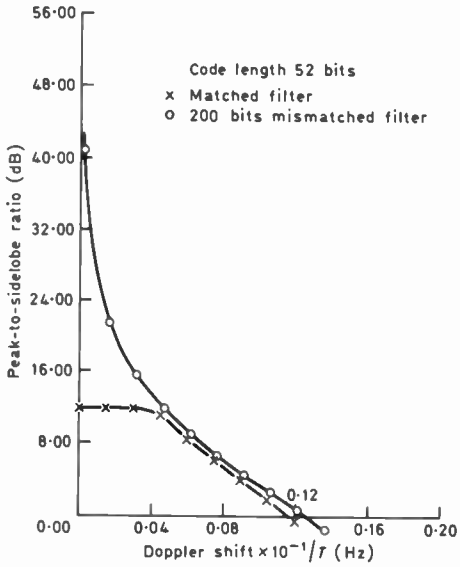


Fig. 6. Peak-to-sidelobe ratio versus Doppler frequency shift for a 52-bit combined Barker code showing the difference between the 200-bit minimum square error filter and the matched filter.

$\Delta T_R = 0{\cdot}60T$, and assuming that the carrier frequency $f_0$ is 6 GHz and $T = 0{\cdot}5$ μs, the minimum radial velocity that can be resolved by the system is $V_R = \Delta f_D C/2f_0 = 950$ m/s. The corresponding nominal resolution in echo-time is 45 m.

Similar studies have also been undertaken for other non-continuous Barker and combined words. For 65 and 91-bit words −40 dB temporal sidelobes can be obtained with transversal filters that are respectively 205 and 280 bits long. The longer combined Barker words require much longer filters.

It is concluded that the transversal filtering of combined Barker sequences to produce pulse compression is well worthwhile for slow moving targets, but for fast targets there is neither advantage, nor serious disadvantage.

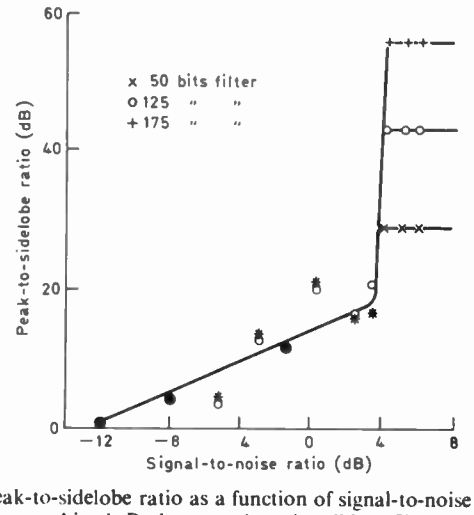


Fig. 7. Peak-to-sidelobe ratio as a function of signal-to-noise ratio for the 39-bit combined Barker word and spiking filters which are respectively 50, 125 and 175 bits long. A decision circuit is used prior to signal compression.

## 4 The Effect of Signal-to-noise Ratios on the Compressed Pulses

Having designed mismatched filters for sidelobe reduction, it is necessary to investigate their compression properties when noise contaminates the signal, since in radar systems the signal-to-noise ratios are small and bit errors occur.

The noise was taken to be random and Gaussian-distributed, and in this case a 39-bit combined Barker code was investigated in order to economize on computing time. Three filters of different lengths (50, 125 and 175 bits) were considered and two cases of processing the signal were analysed. In the first case the signal bits plus noise, produced by a random number generating program, were converted into a binary word, with a certain number of bit errors, and then compressed in the transversal filter. The conversion of the signal plus noise into a p.n. bit stream was done by determining if the signal plus noise at a certain signal bit position was above or below a threshold of zero. If the sum of the signal plus noise was positive it was taken to be a + 1,

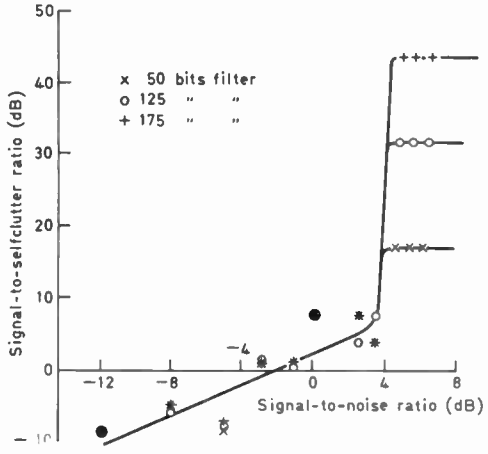


Fig. 8. As Fig. 7, but for signal-to-selfclutter ratio.

whilst if negative it was taken to be a −1. In the second case the digital signal plus noise was input to the transversal filter, i.e. there was no decision made to convert the signal plus noise waveform into a p.n. bit stream.

The effect of signal-to-noise ratio on the peak-to-sidelobe ratio for the first case may be seen in Fig. 7, whilst corresponding data for signal-to-self-clutter ratios are given in Fig. 8. An inspection of these figures shows that the signal-to-noise ratios must be greater than 4 dB if high peak-to-sidelobe ratios are required. With no decision circuit prior to the transversal filter no threshold improvement was observed in the peak-to-sidelobe ratio and signal-to-self-clutter ratios as the signal-to-noise ratios were increased. This may be seen by an inspection of Fig. 9 where the peak-to-sidelobe ratio is plotted as a function of signal to noise ratios. Subsequent calculations of the probability of a code being correctly identified in noise showed that for the 39-bit combined Barker code—28 dB sidelobes could be obtained with

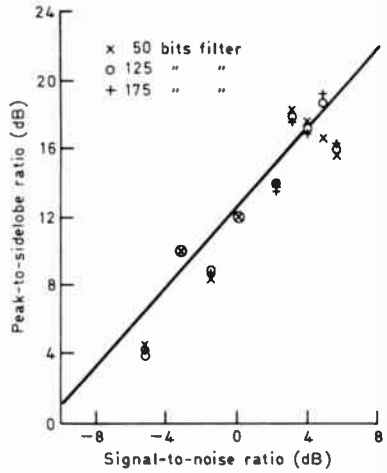


Fig. 9. As Fig. 7, but with no bit-decision-circuit prior to signal compression.

the 50-bit filter provided that the signal-to-noise ratio was greater than about 11 dB. The 53 dB sidelobes produced by the 175-bit filter required a signal to noise ratio of about 12·5 dB. Thus, any system using digital pulse compression must have a bit decision circuit prior to signal compression.

## 5 Effect of Coefficient Tolerance on Filter Performance

Digital circuits using analogue weighting coefficients, surface acoustic wave devices[9] and charge transfer devices[10,11] offer fairly simple and inexpensive means of implementing transversal filters, so that the effect of manufacturing tolerances on the performance of these filters is of interest. Digital filtering using binary multiplication also suffers from coefficient errors due to the truncation of the words, but at the present time gallium arsenide digital integrated circuits are expensive and relatively slow (8-bit multiplication requiring several nanoseconds), so that errors in this type of filter were not considered.

The tolerances on the values of the filter coefficients depend on the exact technology used, but the effect of errors in the resistors of shift register and bucket brigade filters, and electrode dimensions in surface acoustic wave and charge-coupled devices is most likely to follow a Gaussian distribution. Mask misalignments (skewing and/or lateral displacements) can cause further errors in the coefficients. (Further details of performance limitations in c.c.d. technology may be seen in similar studies.[10,11])

### 5.1 Effect of Gaussian Errors in the Weighting Coefficients

Results are presented for a combined Barker word which was 52 bits long and had a theoretical peak-to-sidelobe ratio of 48 dB for a 200-bit delay filter, and 67 dB for a 300-bit delay filter. Values of the coefficients of the 200-bit filter (given in Appendix 1) show the general feature of this filter is that the coefficients are low at the input and output of the filter, and are high at the centre. The standard error in the coefficients was varied from 0 to

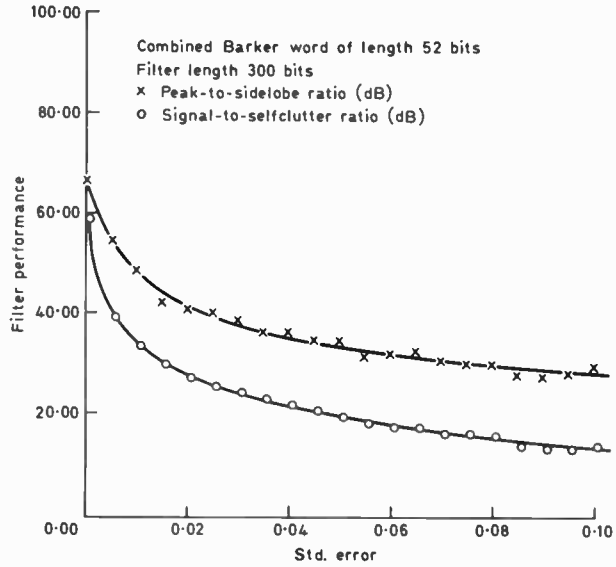


Fig. 10. The effect of Gaussian errors in the filter coefficients on the peak-to-sidelobe ratio and the signal-to-selfclutter ratio. The filter length is 300 bits and the word is a 52-bit combined Barker word.

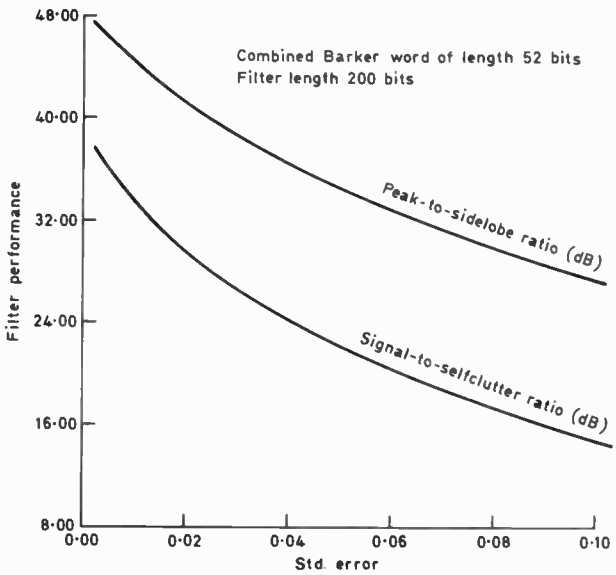


Fig. 11. As Fig. 10, but for a 200-bit filter.

0·1, and in each case the peak-to-sidelobe ratio and signal-to-selfclutter ratio was calculated. A comparison of Figs. 10 and 11 shows that to obtain the high peak-to-sidelobe ratio associated with the longer filter more accurate setting of the coefficients was necessary. For example, a standard error of 2% in the coefficients of the 300-bit delay filter decreases the sidelobe level from −67 dB to −40 dB, whilst a 2% standard error in the 200-bit filter means that the level of the sidelobes falls from about 48 dB below the peak to 40 dB. The same effect can be observed when the signal-to-selfclutter ratio is inspected, showing that a high degree of sidelobe suppression requires accurate setting of the coefficients.

### 5.2 The Effect of Mask Misalignment due to Skew

In the fabrication of s.a.w. devices masks are required to delineate the split electrode system for implementing the

weighting coefficients of the transversal filter and for defining the size of the input and output transducers. The fabrication of c.c.d.s[10,11] also requires several masks. The device engineer thus requires numerical data on the mask alignment required to produce a given filter performance.

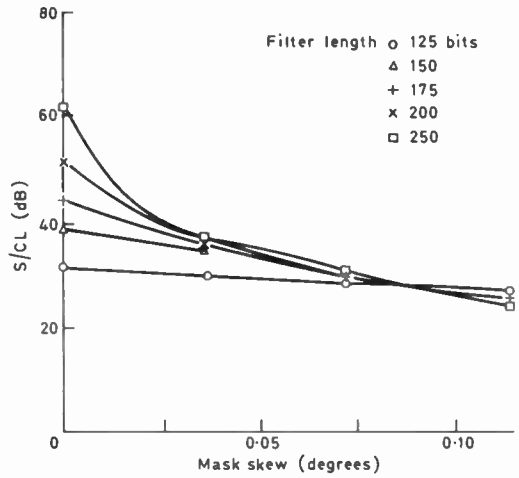


Fig. 12. The effect of mask skew on peak-to-sidelobe ratios of a 39-bit Barker word for filter lengths of 125 to 250 bits.

The present studies have found that the mask misalignment between the split electrode system and the direction of propagation of the s.a.w., or the direction of charge transfer for c.c.d.s, has a profound effect on the peak-to-sidelobe ratios obtainable from long filters, designed to give very high peak-to-sidelobe ratios ($> 50$ dB). The effects of errors in the coefficients of the transversal filter due to skew angle between masks may be seen in Figs. 12 and 13, where peak-to-sidelobe ratios and signal-to-selfclutter ratios are plotted against misalignment for filters which are 125, 150, 175, 200 and 250 bits respectively for the case of a 39-bit combined Barker word. Whilst the perfect 250-bit filter can give peak-to-sidelobe ratios of almost 70 dB, a mask misalignment of 0·04 degrees can reduce the ratio by almost 20 dB. However the shorter filters, such as the

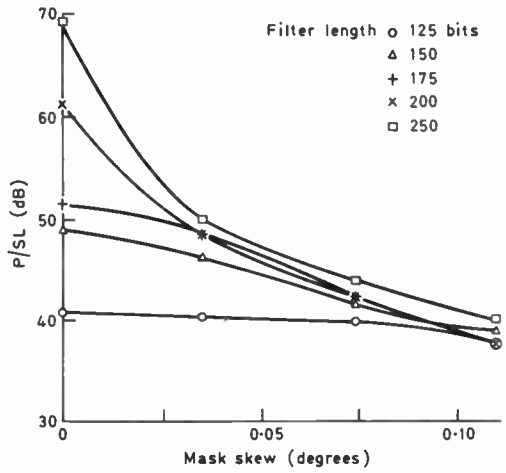


Fig. 13. As Fig. 12, but for signal-to-selfclutter ratios.

125-bit one, are fairly insensitive to mask misalignment. Similar remarks apply to the signal-to-selfclutter ratio.

## 6 An Improved Shaping Filter

Although the desired output of the optimum spiking filter should be a single spike, the actual output consists of a spike plus a set of finite valued sidelobes. The peak-to-sidelobe ratio is determined by the highest sidelobe, so that a further improvement can be obtained by specifically reducing the highest sidelobe, again keeping the total sidelobe energy to a minimum. In the shaping filter the desired output is taken as a variable parameter in the optimization and successively adjusted to improve the peak-to-sidelobe ratio. A flow diagram of the programme for doing this is given in Appendix 2. The sidelobes obtained for the spiking filter are gradually scaled down by a specified amount, 1 dB steps or so, until no further worthwhile improvement is realized ($< 0{\cdot}1$ dB).

Figure 14 shows the peak-to-sidelobe ratio and the signal-to-clutter ratio (S/CL) for 65 and 91 bit combined Barker words as a function of the number of delay stages of the shaping filter. The 65-bit word was composed of 13 sub-sets of 5 bits, whilst the 91-bit word had 13 sub-sets

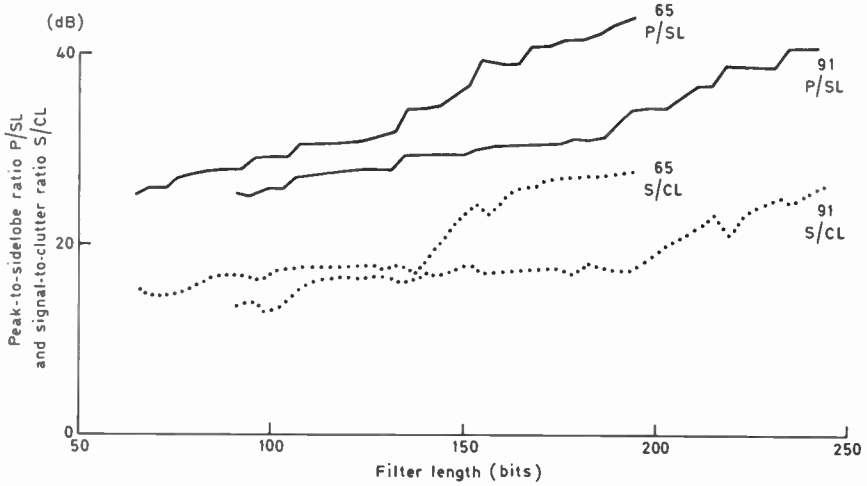


Fig. 14. Peak-to-sidelobe and signal-to-clutter ratios for combined Barker words and a shaping filter, as a function of filter lengths for 65- and 91-bit words.

of 7 bits. It can be seen by comparing Fig. 13 with Figs. 2 and 3 that the shaping filter offers an improvement over the spiking filter. For example, the 65-bit code has sidelobes that are 31 dB down at a filter length of 130 delays, whilst the sidelobes of the spiking filter of the same length were only 28·3 dB down on the peak signal. For the 91-bit word and a 182-bit delay the shaping filter had sidelobes which were 31 dB down as compared to the spiking filter having sidelobes which were 27·9 dB down. In each case the loss of signal detectability due to the mismatch of the shaping filter, compared to the matched filter, is about the same as for the spiking filter.

## 7 Conclusions

The combined Barker words when compressed in minimum square error transversal filters can give compression ratios of up to 169 with very low ($-40$ to $-50$) sidelobe levels in filters which are only several hundred bits in length. The loss in signal detectability which is inevitable due to the mismatched filter, is not significant. Doppler shift effects are very similar to those found when the combined Barker words are compressed in matched filters. Peak-to-sidelobe ratios are found to be very good once the signal-to-noise ratios are above a threshold (about 4 dB for the 39-bit word), and it was found that if very large peak-to-sidelobe ratios are required (50–60 dB) the tolerance on the coefficients of the filter are quite tight. A shaping filter, which specifically reduces the peak sidelobe, offers a worthwhile improvement over the spiking filter, and is no more complex.

## 8 References


1 'SAW/CCD update', *Microwave Systems News* **7**, October 1977.
2 Rihaczec, A. W. 'Principles of High Resolution Radar' (McGraw-Hill, New York, 1969).
3 Rihaczec, A. W. and Golden, R. M., 'Range sidelobe suppression for Barker codes', *IEEE Trans. on Aerospace and Electronic Systems*, **AES-7**, No. 6, pp. 1087–92, November 1971.
4 Dassanayake, P. and Morgan, G. B., 'Sidelobe reduction of pulses compressed from pseudorandom binary words', *Proc. IEE*, **122**, pp. 493–4, 1975.
5 Ackroyd, M. H. and Ghani, F., 'Optimum mismatched filters for sidelobe suppression', *IEEE Trans. on Aerospace and Electronic Systems*, **AES-9**, pp. 214–8, March 1973.
6 Rice, R. B., 'Inverse convolution filters', *Geophysics*, **27**, pp. 4–18, 1962.
7 Treitel, S. and Robinson, E. A.: 'The design of high resolution digital filters', *IEEE Trans. on Geoscience Electronics*, **GE-4**, no. 1, pp. 25–38, 1966.
8 Dassanayake, P., Ph.D. Thesis, University of Wales, 1974.
9 Wright, S. and Hammers, D. E., 'SAW sidelobe reduction filter for Barker codes', Radar 77, IEE Conference Publication No. 155, London 1977.
10 Baertsch, R. D., Engeler, W. E., Goldberg, H. S., Puckette, IV, C. M., and Tiemann, J. J., 'The design and operation of practical charge-transfer transversal filters', *IEEE J. Solid-State Circuits*, **SC-11**, no. 1, pp. 65–74, 1976.
11 Brodersen, R. W., Hewes, R. C. and Buss, D. D. 'A 500 stage c.c.d. transversal filter for spectral analysis', *IEEE J. Solid-State Circuits*, **SC-11**, no. 1, pp. 75–84, 1976.


## 9 Appendix 1: Coefficients of the minimum square error filter of length 200 bits for the combined Barker word of length 52 bits

| Coeff No. | | | | | | | | | | |
|---|---|---|---|---|---|---|---|---|---|---|
| 1- 10 | -0.0086 | -0.0117 | 0.0006 | -0.0023 | 0.0138 | 0.0164 | -0.0006 | 0.0034 | -0.0200 | -0.0225 |
| 11- 20 | -0.0008 | -0.0017 | 0.0234 | 0.0250 | 0.0002 | 0.0013 | -0.0255 | -0.0282 | 0.0015 | -0.0043 |
| 21- 30 | 0.0340 | 0.0355 | 0.0028 | -0.0012 | -0.0311 | -0.0226 | -0.0070 | 0.0154 | 0.0007 | -0.0162 |
| | 0.0011 | -0.0175 | 0.0353 | 0.0509 | 0.0020 | 0.0135 | -0.0624 | -0.0801 | 0.0042 | -0.0200 |
| | 0.1069 | 0.1246 | 0.0045 | 0.0132 | -0.1333 | -0.1280 | -0.0184 | 0.0237 | 0.0864 | 0.0655 |
| | -0.0027 | -0.0182 | -0.0499 | -0.0529 | 0.0212 | -0.0242 | 0.0981 | 0.1125 | 0.0098 | 0.0045 |
| | -0.1071 | -0.0987 | -0.0129 | 0.0214 | 0.0643 | 0.0692 | -0.0263 | 0.0313 | -0.1268 | -0.1275 |
| | -0.0306 | 0.0299 | 0.0669 | -0.0661 | 0.1030 | -0.2360 | 0.4051 | 0.6207 | 0.0203 | 0.1953 |
| | -0.7958 | -0.8824 | -0.1088 | 0.0222 | 0.7514 | 0.7673 | -0.0382 | 0.0541 | -0.8596 | -0.8844 |
| 91-100 | -0.0292 | 0.0044 | 0.8508 | 0.5744 | 0.2720 | -0.5484 | 0.2460 | 0.7087 | 0.0857 | 0.3770 |
| | -1.0000 | -0.9011 | -0.4759 | 0.5748 | -0.1496 | -0.5748 | -0.1497 | -0.2754 | 0.7005 | 0.5653 |
| | 0.4106 | -0.5458 | 0.3911 | 0.4887 | 0.4482 | -0.3507 | 0.3102 | 0.2786 | 0.3823 | -0.4138 |
| | 0.5174 | 0.5397 | 0.3914 | -0.3692 | 0.2209 | 0.3834 | 0.2068 | -0.0443 | -0.1324 | -0.0589 |
| | -0.0293 | 0.1027 | -0.0731 | -0.1068 | -0.0689 | 0.0353 | 0.0025 | 0.0024 | -0.0353 | 0.0352 |
| | -0.0729 | -0.0571 | -0.0508 | 0.0666 | -0.0604 | -0.0783 | -0.0488 | 0.0310 | -0.0014 | -0.0063 |
| | -0.0264 | 0.0214 | -0.0413 | -0.0204 | -0.0419 | 0.0628 | -0.0843 | -0.0812 | -0.0661 | 0.0691 |
| | -0.0538 | -0.0683 | -0.0543 | 0.0399 | -0.0259 | -0.0341 | -0.0319 | 0.0237 | -0.0212 | -0.0276 |
| | -0.0169 | 0.0107 | -0.0000 | -0.0109 | -0.0001 | -0.0108 | 0.0219 | 0.0174 | 0.0157 | -0.0201 |
| | 0.0184 | 0.0211 | 0.0171 | -0.0145 | 0.0109 | 0.0125 | 0.0132 | -0.0116 | 0.0121 | 0.0121 |
| 191-200 | 0.0116 | -0.0112 | 0.0113 | 0.0124 | 0.0093 | -0.0095 | 0.0065 | 0.0099 | 0.0097 | -0.0054 |

## 10 Appendix 2: Flow diagram of program to evaluate the minimum square error shaping filter

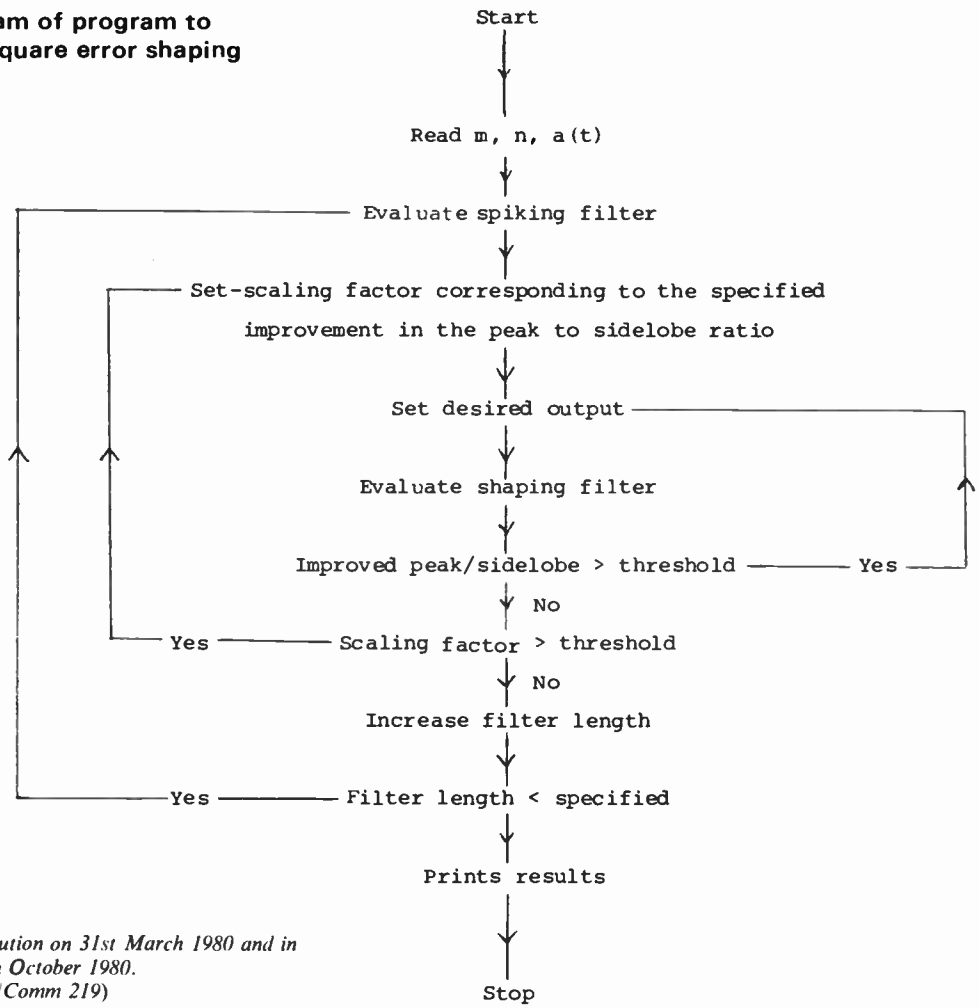


*Manuscript first received by the Institution on 31st March 1980 and in revised form on 24th October 1980.*
*(Paper No. 1990/Comm 219)*

# The Authors

**Oyvind Alv Liberg** received his B.Sc. in electronics from the University of Wales, Cardiff, in 1976 and his Ph.D. four years later for a thesis on digital pulse compression signals. His main interests continue to be in digital pulse compression and the simulation of the properties of such signals in a real physical environment. Dr Liberg is now with Standard Telefon and Kabelfabrik, Oslo, working on higher-order p.c.m. multiplexers.

**Gwyn Morgan** obtained the degrees of B.Sc. and Ph.D. at the University College of Swansea, Wales, where his researches were concerned with the high voltage electrical breakdown of air and oxygen. From 1964 to 1968 he was employed at the Royal Radar Establishment, Malvern, working initially on the $Q$ switching of high-power solid-state lasers and lidar, and subsequently on the microwave side of a high-power, multi-function search radar. From 1968 to 1970 he was at RCA, Burlington, Massachusetts, where he was concerned with electro-optic communication and radar systems. Dr Morgan lectures in electronics at the University of Wales Institute of Science and Technology, Cardiff, and his research interests are in microwave integrated circuits and digital pulse compression techniques, primarily for radar and communication systems.

**P. Dassanayake** lectures at the University of Moratuwa, Sri Lanka. He obtained the degree of B.Sc.(Eng.) in electrical engineering at the University of Sri Lanka and the degrees of M.Sc. and Ph.D. in electronics at the University of Wales Institute of Science and Technology, Cardiff. For his Ph.D. degree Dr Dassanayake studied phase coded pulse compression and impatt diode phase shifters. During 1979 and 1980 he was on leave of absence at the Electro-Medical Engineering Division, of the Department of Health Services, Colombo.

U.D.C. 621.374.4: 621.376.9
*Indexing Terms:* Delta-sigma modulation, Multipliers

# Multipliers of delta-sigma sequences

**D. LAGOYANNIS,** B.Sc., Ph.D.*
and
**K. PEKMESTZI,** B.Sc.*

**SUMMARY**

Multipliers of two delta-sigma sequences are proposed in this paper. These multipliers are very simple in circuitry and provide the product in delta-sigma sequence form, permitting simple further processing. The multipliers were constructed and their performance was experimentally measured. It was found that a certain type of multiplier with a relatively simple circuitry, provides a high signal-to-noise ratio. An application of this multiplier is given for the realization of a parallel type digital correlator.

* *National Research Centre Demokritos, Electronics Division, Aghia Paraskevi, Attiki, Greece.*

*The Radio and Electronic Engineer, Vol. 51, No. 6, pp. 281–286, June 1981*

## 1 Introduction

Delta-sigma modulation is a technique employed for coding an analogue signal into a sequence of binary digits.[1] Single digit representation simplifies analogue-to-digital conversion and also permits the realization of the basic arithmetic operations with simpler circuits than those required for pulse code modulation. Circuits of adders of two delta-sigma sequences (DSS) and multipliers of a DSS by a constant are to be found in the literature.[2–6,12] These circuits produce the results of the operations in DSS form and were proposed for the realization of digital filters.

The development of multipliers of DSS was necessary for the application of the delta-sigma modulation technique in the realization of correlators. Multipliers of the type already referred to provide the product either in analogue[7] or in p.c.m. form.[8–12]

In this paper a multiplier for DSS is proposed which delivers a DSS in its output, a property that permits simpler circuitry than p.c.m. and simpler further processing. More specifically, three such types of multipliers are proposed with varying circuit complexity and performance. The above multipliers were experimentally constructed and their signal-to-noise ratio (S/N) was measured. Finally, a certain multiplier was employed for the realization of a parallel type digital correlator.

## 2 Delta-Sigma Sequences

Consider two band-limited signals $x(t)$, $y(t)$ with bandwidths $B_x$ and $B_y$ respectively and both having the same maximum amplitude, for which the following relation holds

$$B_x \geqslant B_y \tag{1}$$

The signals $x(t)$ and $y(t)$ are coded by two delta-sigma coders DS-1 and DS-2, which have clock rates $f_x$ and $f_y$ respectively. The binary sequences $X_n$ and $Y_n$, $n = \ldots, -2, -1, 0, 1, 2, \ldots$, which take the values $+1$ or $-1$, will be obtained at the outputs of the above coders.

In the analysis which follows it is assumed that the coders DS-1 and DS-2 are not overloaded and that the signals $x(t)$ and $y(t)$ are normalized to their maximum amplitude.

Since the signal $x(t)$ is band-limited, there exist time intervals in which the amplitude variation of $x(t)$ is equal to a desired value $2/K$, where $K$ is a positive integer. If $\tau_x$ is the shortest of the above intervals, then the amplitude variation of $x(t) \leqslant 2/K$ is valid for every $t$ in the interval

$$\left[t_0 - \frac{\tau_x}{2}, t_0 + \frac{\tau_x}{2}\right].$$

Assume now that the clock rate $f_x$ is chosen so that the following relation holds

$$\tau_x = K\frac{1}{f_x} = KT_x \tag{2}$$

0033–7722/81/060281+06 £1.50/0

and that during $\tau_x$ the signal $x(t)$ is equal to

$$x(t) = x\left[\left(n+\frac{K}{2}\right)T_x\right].$$

Then the following relation is valid:[5,10]

$$x(t) \simeq \frac{1}{K}\sum_{i=0}^{K-1} X_{n+i} \text{ for } nT_x \leqslant t \leqslant (n+K)T_x \qquad (3)$$

where $nT_x$ is the $n$th sampling instant.

It is evident from (3) that $x(t)$ can be considered as amplitude quantized with quanta equal to $2/K$ and that within the time interval $\tau_x$ its approximation $x(t)$ is given by

$$\hat{x}(t) = \frac{1}{K}\sum_{i=0}^{K-1} X_{n+i} \text{ for } nT_x \leqslant t \leqslant (n+K)T_x \qquad (4)$$

It is evident that similar relations also hold for the sequence $Y_n$. As a matter of fact, $y(t)$ can be considered constant during a time interval $\tau_y$ such as

$$\tau_y = LT_y \qquad (5)$$

where $L$ is a positive integer and $T_y = 1/f_y$.

Since the bandwidth $B_y$ of the signal $y(t)$ is smaller than or equal to the bandwidth $B_x$ of $x(t)$ (eqn. (1)), the signal $y(t)$ is smoother than $x(t)$. Consequently $y(t)$ can be considered constant during the same time interval $\tau_x$, that is for $\tau_x = \tau_y$. From the above analysis it follows that the approximation of $y(t)$ during $\tau_x$ is given by the relationship

$$\hat{y}(t) = \frac{1}{L}\sum_{i=0}^{L-1} Y_{n+i} \text{ for } nT_x \leqslant t \leqslant (n+K)T_x \qquad (6)$$

Suppose now that

$$T_x = KT_y \qquad (7)$$

Then, from (2), (5), (7) and for $\tau_x = \tau_y$, it follows that

$$L = K^2 \qquad (8)$$

From equation (8) it follows that $y(t)$ can be approximated with the same accuracy as $x(t)$ provided that $y(t)$ is considered in the time interval $\tau = \tau_x/K$ (see Fig. 1). So, the signals $x(t)$ and $y(t)$ can be represented approximately by

$$\hat{x}(t) = \frac{1}{K}\sum_{p=0}^{K-1} X_{n+p} \qquad nT_x \leqslant t \leqslant (n+K)T_x \quad (9a)$$

$$\hat{y}(t) = \frac{1}{K}\sum_{m=0}^{K-1} Y_{(Kn+I)+m} \qquad nT_x \leqslant t \leqslant (n+K)T_x \quad (9b)$$

where $I = 0, 1, 2, \ldots, L-K$.

The new indices, $I, p, m$ have been introduced in order to facilitate the mathematical analysis which follows.

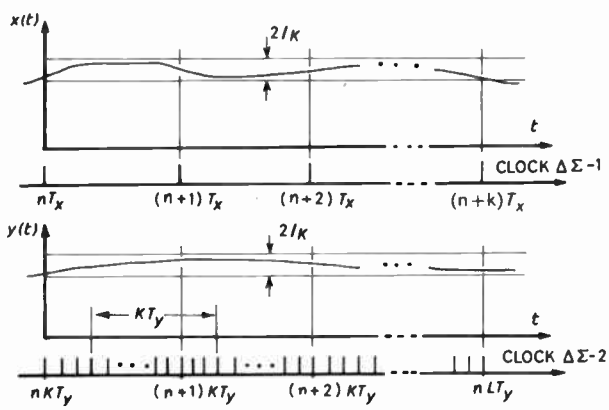


Fig. 1. The signals $x(t)$ and $y(t)$ within the time interval $[nT_x, (n+K)T_x]$.

## 3 The Multiplication

The approximated product of $x(t)$ and $y(t)$ is given by

$$p(t) = x(t)y(t) \simeq \frac{1}{K}\sum_{p=0}^{K-1} y(t)X_{n+p} \qquad (10)$$

Substituting the value of $\hat{y}(t)$ from (9b) into equation (10) the following relationship is derived:

$$p(t) \simeq \frac{1}{K}\sum_{p=0}^{K-1} X_{n+p}\left[\frac{1}{K}\sum_{m=0}^{K-1} Y_{(Kn+I)+m}\right] \qquad (10a)$$

where $I = 0, 1, 2, \ldots, L-K$.

Equation (10a) is valid for every value of $I = 0, 1, 2, \ldots, (K-1)K$ and consequently for all values of $Kp$. Therefore equation (10a) becomes

$$p(t) \simeq \frac{1}{K^2}\sum_{p=0}^{K-1}\sum_{m=0}^{K-1} X_{n+p}Y_{K(n+p)+m} \qquad (11)$$

If the integral part of $I/K$ is symbolized as $[I/K]$, equation (11) can be written

$$p(t) \simeq \frac{1}{L}\sum_{I=0}^{L-1} Y_{nK+I}X_{n+[I/K]} \qquad (12)$$

Since the variables $X_{n+[I/K]}$ and $Y_{nK+I}$ take the values $+1$ or $-1$, it is evident that the product $P_n = Y_{nK+I}X_{n+[I/K]}$ can be realized by an exclusive-NOR gate.[11] It can be seen from (12) that the sequence $P_n$, which appears at the output of the exclusive-NOR gate is a delta-sigma sequence which corresponds to the product $x(t)y(t)$. It is evident that, if $P_n$ is input to an analogue low-pass filter or to a corresponding digital one, an approximation of $p(t)$ will be obtained at its output (Fig. 2).

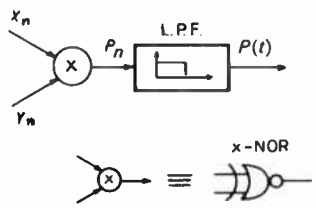


Fig. 2. Circuit for realizing equation (12).

In the above mentioned multiplier the clock rate $f_y$ is $K$ times higher than $f_x$ (eqn. (7)). Consequently, the clock rate of the coder DS-2 takes unacceptably high

values for large values of $K$. There exist, however, methods by which this problem may be overcome. It is for example possible to reduce the clock rate of the coder DS-2 by using the more complicated circuit of the multiplier shown in Fig. 3.

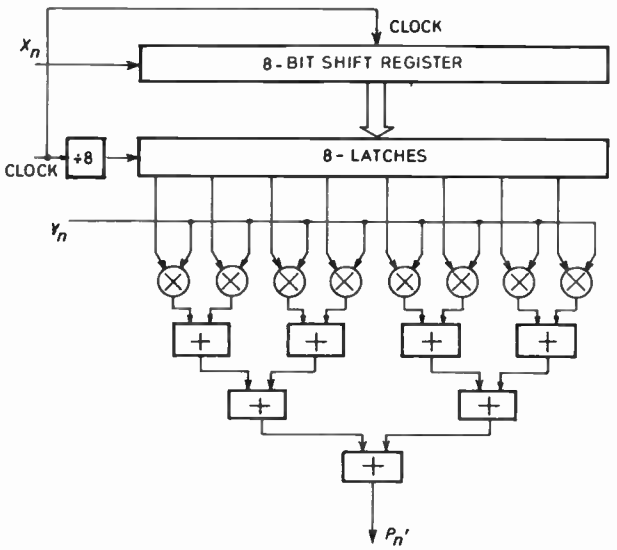


Fig. 3. Multiplier for delta-sigma sequences using a latch.

In this new circuit, the sequence $X_n$ is led to the $K$-bit shift-register (SR). The content of the SR is transferred to corresponding $K$-latch flip-flops with clock rate equal to $f_x/K$. The outputs of the exclusive-NOR gates form the inputs to a tree of $K$-1 delta adders.[4] At the output of the tree the sequence $P_n'$ is obtained.

Assume that

$$L = K = 2^m \tag{13}$$

where $m$ is a positive integer. From Fig. 3 and equation (13), it follows that

$$P_n' = \frac{1}{K}\sum_{i=0}^{K-1} Y_n X_{[n/K]K+i} \tag{14}$$

If the sum of the $K$-consecutive terms of $P_n'$ during the interval $[nT_x, (n+K)T_x]$ is taken into consideration, then

$$\sum_{n=I}^{I+(K-1)} P_n' = 1/K \sum_{n=I}^{I+(k-1)} Y_n \sum_{i=0}^{K-1} X_{[n/K]K+i} \tag{15}$$

where $I = 0, 1, 2, \ldots$

It follows from (4), (6) and (15) that

$$p(t) \simeq \sum_{n=I}^{I+(K-1)} P_n' = \hat{x}(t)\hat{y}(t) \tag{16}$$

As becomes evident from (16), $P_n'$ is a delta-sigma sequence which corresponds to the product $x(t)y(t)$. The multipliers shown in Figs. 2 and 3, represent two extreme cases. In one case, the clock rate is unacceptably high but the implementing circuit is simple. In the other case the clock rate is low but the implementing circuit is much more complex. A compromise solution however is possible so that $f_y$ is kept at acceptable values and at the same time the rather complicated circuit of Fig. 3 is simplified.

Another type of multiplier simpler than that of Fig. 3 and of higher performance is given in Fig. 4. This multiplier differs from that of Fig. 3 in that the latch F.F's are omitted. Assuming that equation (8) is valid, the output sequence $P_n^m$ is given by

$$P_n^m = Y_{Kn+m}\frac{1}{K}\sum_{p=0}^{K-1} X_{n+p} \tag{17}$$

The clock rate of the output sequence is $f_y$. The normalized sum $P_n$ of the $K^2$ successive terms of the $P_n^m$ will be equal to

$$P_n = \frac{1}{K^2}\sum_{\substack{q=n\\m=0}}^{\substack{m=K-1\\q=n+K-1}} P_n^m = \frac{1}{K^2}\sum_{q=n}^{n+K-1}\sum_{m=0}^{K-1} Y_{qK+m} \times \times\left\{\frac{1}{K}\sum_{p=0}^{K-1} X_{q+p}\right\} \tag{18}$$

From (9b) and for $I = 0$ it follows that

$$\frac{1}{K}\sum_{m=0}^{K-1} Y_{qK+m} = \hat{y}(t) \tag{19}$$

Equation (19) is valid for every $q$. From (18) and (19), it follows that

$$P_n = \hat{y}(t)\frac{1}{K^2}\left\{\sum_{q=n}^{n+K-1}\sum_{p=0}^{K-1} X_{q+p}\right\} \tag{20}$$

It is evident that the normalized double sum of (20) can be written in the form

$$\frac{1}{K^2}\sum_{q=n}^{n+K-1}\sum_{p=0}^{K-1} X_{q+p} = \frac{1}{K^2}\sum_{r=0}^{2(K-1)} W_r X_{n+r} \tag{21}$$

where

$$W_r = \begin{cases} r+1 & 0 \leqslant r \leqslant K-1 \\ 2K-(r+1) & K \leqslant r \leqslant (K-1) \end{cases} \tag{22}$$

It can be seen from equations (21) and (22) that the signal $x(t)$ is interpolated within the interval $[nT_x, (n+K-1)T_x]$ with triangular weights. It is known[13] that the triangularly weighted interpolation is much more accurate than the uniform one ($W_r = 1$) which is employed in the multiplier of Fig. 2 and its equivalent of Fig. 3. As a consequence the following relation is valid

$$\left|x(t) - \frac{1}{K^2}\sum_{r=0}^{2(K-1)} W_r X_{n+r}\right| \leqslant \left|x(t) - \frac{1}{K}\sum_{p=0}^{K-1} X_{n+p}\right| \tag{23}$$

and $P_n$ can therefore be written as

$$P_n = \hat{y}(t)\hat{x}(t) \simeq p(t) \tag{24}$$

Therefore, the sequence $P_n^m$ obtained at the output of the multiplier of Fig. 4 is the delta-sigma sequence which corresponds to the product $x(t)y(t)$. From the above it is evident that the signal-to-noise ratio of the multiplier of

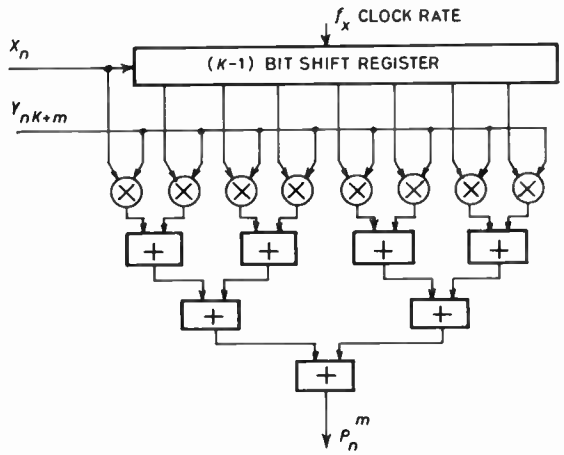


Fig. 4. Multiplier based on the triangularly weighted interpolation.

Fig. 4 is much higher than that of the two other multipliers proposed and has been experimentally confirmed.

## 4 Experimental Results

The three multipliers described above have been experimentally constructed in order to determine their accuracy. As a measure of the accuracy the S/N at their outputs was considered. Exponential delta-sigma modulators have been used as coders and the measurement has been carried out for sinusoidal input signals. The output sequence of each multiplier is filtered by an l.p.f. with a cut-off frequency of 3 kHz.

The S/N is defined as the ratio of the power of the ideal product of the two sinusoidal input signals divided by the power of the noise at the output of the l.p.f. Since the product $p(t)$ of two sinusoidal signals $x(t) = A_1 \sin \omega_1 t$ and $y(t) = A_2 \sin \omega_2 t$ is equal to

$$p(t) = \frac{A_1 A_2}{2}[\cos(\omega_1 - \omega_2)t - \cos(\omega_1 + \omega_2)t],$$

the measurement of S/N can be performed by means of the power density spectrum of the output. Another method could be the measurement of the power of the remaining signal, after rejecting the two sinusoidal terms of the product with angular frequencies $(\omega_1 + \omega_2)$ and $(\omega_1 - \omega_2)$ by means of two notch filters. Both methods were used and gave the same results.

Furthermore, the dependence of S/N on the value of $K$ was examined as well as on the kind of interpolation used (rectangular or triangular). The multiplier of Fig. 2 with rectangular interpolation is examined first. This multiplier realizes the expression (10a)

$$p(t) \simeq \frac{1}{K}\sum_{p=0}^{K-1} X_{n+p}\left[\frac{1}{K}\sum_{m=0}^{K-1} Y_{(Kn+l)+m}\right]$$

This expression is an approximation of the exact product $x(t)y(t)$ and the degree of approximation depends on the sum

$$\frac{1}{K}\sum_{m=0}^{K-1} Y_{(Kn+1)+m}$$

as can be easily seen. The above sum represents the approximation of $y(t)$ within a clock period $T_x$ and depends on the value of the constant $K = f_y/f_x$. So, for increasing $K$, the accuracy of the multiplier increases (finer quantization of the signal $y(t)$).

It has been shown in Sections 2 and 3 that the relation (10a) holds for every $\tau_x$ obeying the inequality $\tau_x \geqslant KT_x = K/f_x$. The value of $\tau_x$ for which $\tau_x = KT_x = K/f_x$ constitutes a limiting case and the corresponding clock frequency $f_x$, for a given $K$, becomes the critical frequency $f_{xc}$ of the system. For $f_x < f_{xc}$, relation (10a) does not hold anymore and the accuracy of the approximation of $p(t)$ deteriorates.

The above theoretical conclusions have been verified experimentally by measuring the S/N of the multiplier of Fig. 2. In Fig. 5 the S/N of the multiplier is plotted against clock frequency $f_x$ with parameter the values of $K = f_y/f_x = 2$, $K = 4$, $K = 8$.

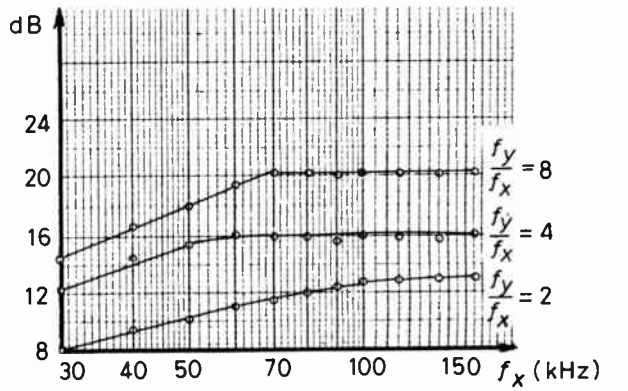


Fig. 5. Measured S/N ratio against $f_x$ of the multiplier of Fig. 2 for various ratios $f_y/f_x$.

Consider next the multiplier of Fig. 4. In this multiplier the triangular interpolation was used, the signal $x(t)$ being approximated by the sum

$$\frac{1}{K^2}\sum_{r=0}^{2(K-1)} W_r X_{n+r}$$

where the weights $W_r$ are triangularly distributed as can be seen from (22).

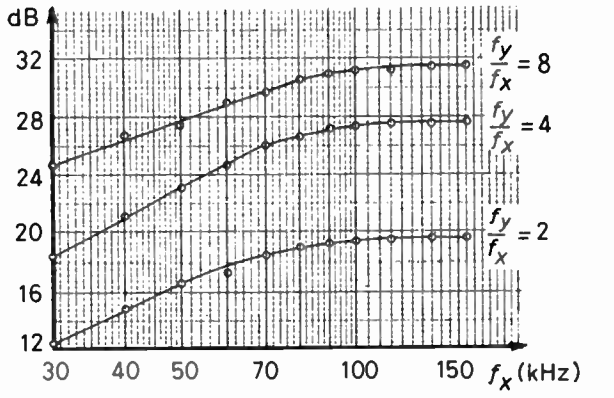


Fig. 6. Measured S/N ratio against $f_x$ of the multiplier of Fig. 4 for various ratios $f_y/f_x$.

Because of the relation (23), the S/N of this multiplier is expected to be higher than the corresponding S/N of the previous multiplier for the same values of $K$ and clock frequency $f_x$. This has been verified experimentally as can be seen from the curves of Fig. 6.

The measurement of the S/N ratio at the output of the multiplier shown in Fig. 3 has yielded the same results as those obtained for the multiplier of Fig. 5. This was expected after what has been explained in the previous Section. It should also be noted that the S/N ratio does not depend on the frequency of the input signals.

It must be noted here that, if $x(t) = y(t)$, the S/N of the product deviates by $-5$ dB with respect to that for which $x(t) \neq y(t)$. No plausible explanation of this discrepancy can be given at present.

Finally Figs. 7 and 8 illustrate the product of the signals $x(t) = A \sin 2\pi f_1 t$ and $y(t) = A \sin 2\pi f_2 t$, for $f_1 = 2$ kHz and $f_2 = 125$ Hz at the outputs of the multipliers of Figs. 2 and 4 respectively. Trace (a) shows the unfiltered product, when the output sequence of the multiplier is input to an up–down counter and is transformed into p.c.m. Trace (b) shows the product, when the same sequence is filtered by an l.p.f. with a bandwidth of 3 kHz.

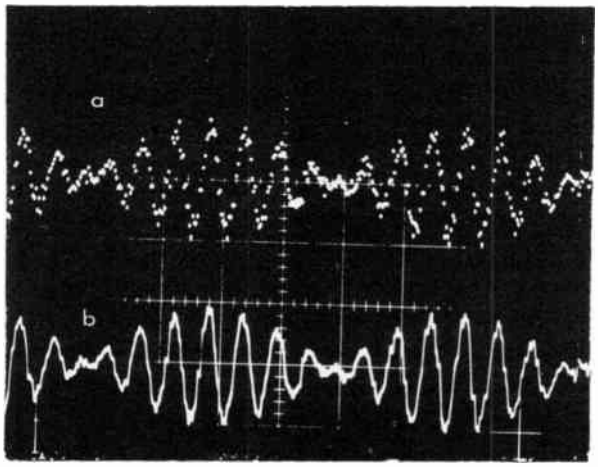


**Fig. 7.** The product of two sinusoids obtained at the output of the multiplier of Fig. 2: (a) In unfiltered p.c.m. form. (b) In filtered form obtained through an l.p.f. with 3 kHz cut-off frequency.
Vert.: 5V/div, Hor.: 1 ms/div.

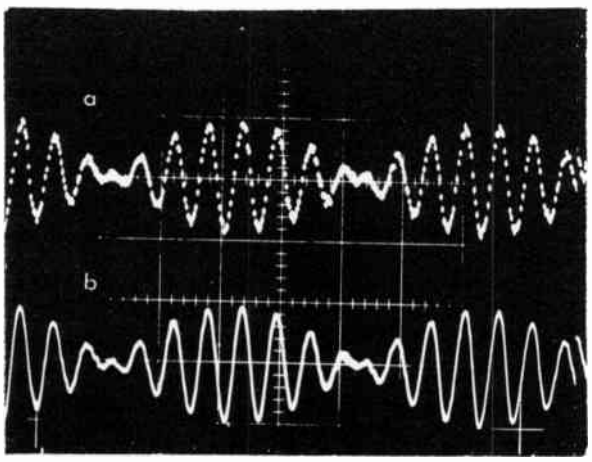


**Fig. 8.** The product of two sinusoids obtained at the output of the multiplier of Fig. 4. (a) In unfiltered p.c.m. form. (b) In filtered form obtained through an l.p.f. with 3 kHz cut-off frequency.
Vert.: 5V/div, Hor.: 1 ms/div.

## 5 Applications

The circuit simplicity of the proposed multipliers and their satisfactory performance at rather low clock rates make them very suitable for digital processing systems as parallel-type correlators. These correlators simultaneously provide at their output the values of the correlation function $\phi_{xy}(\tau)$ of two signals, for several values of the variable $\tau$.[14] This implies a number of multipliers equal to the number of values of $\phi_{xy}(\tau)$ and therefore the circuitry of the multipliers must be simple. Thus, given that the required accuracy of the multiplication for the determination of the correlation function is not high, the use of multipliers like those shown in Fig. 4 is ideal. Moreover, the integration required for the determination of the correlation function can be easily achieved by an up–down counter, since the output of each multiplier is a delta-sigma sequence.

It is known that the correlator is a system, which realizes the following expression

$$\phi_{xy}(\tau) = \lim_{T \to \infty} \frac{1}{T} \int_{-T/2}^{T/2} x(t) y(t-\tau)\, d\tau \qquad (25)$$

where $x(t)$ and $y(t)$ are stationary signals. In practice, $T$ is limited and integration is done mostly digitally. In the case of parallel type correlators the value of $\phi_{xy}(\tau)$ is calculated simultaneously for several values of the time variable $\tau$. The outline of such a system is given in Fig. 9.

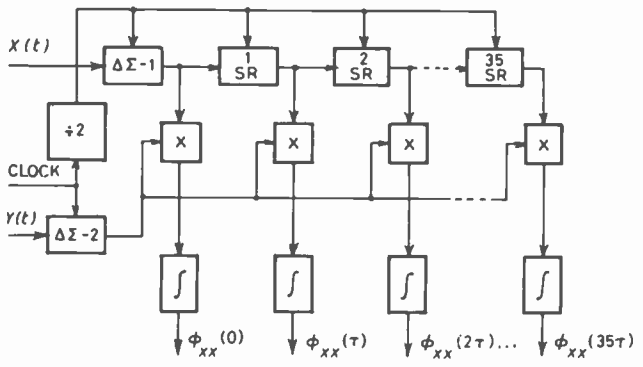


**Fig. 9.** Block diagram of the correlator.

The multiplier employed in the correlator is shown in Fig. 10 and the integrator is an up–down counter. The correlator has been experimentally constructed and provides $\phi_{xy}(\tau)$ for 36 values of time variable $\tau$ at its output. Some examples of its use as an autocorrelator are given in Figs. 11 and 12. Specifically, Fig. 11 shows the autocorrelation function $\phi_{xx}(\tau)$ of a train of rectangular pulses with 60 Hz pulse rate and Fig. 12 the autocorrelation function $\phi_{hh}(\tau)$ of band-limited white noise with 20 kHz bandwidth.

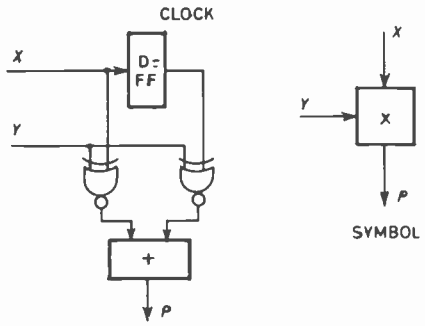


**Fig. 10.** The multiplier used in the correlator of Fig. 9.

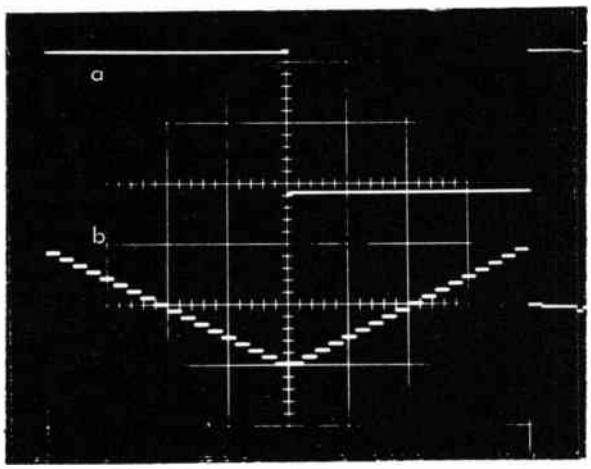


**Fig. 11.** The autocorrelation function of a square pulse.
Trace a: The signal.
Vert.: 5V/div, Hor.: 2 ms/div.
Trace b: The autocorrelation function.
Vert.: $\phi_{xx}(\tau)/\phi_{xx}(0)$, Hor.: delay $\tau$ (2 ms/div.)

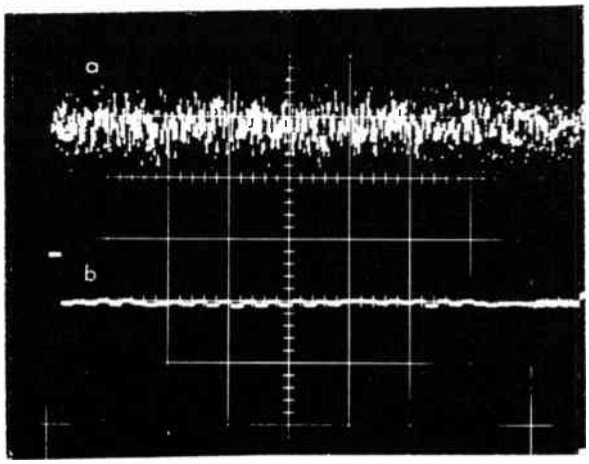


**Fig. 12.** The autocorrelation function of bandlimited white noise.
Trace a: The signal.
Vert.: 10V/div, Hor.: 1 ms/div.
Trace b: The autocorrelation function.
Vert.: $\phi_{hh}(\tau)/\phi_{hh}(0)$, Hor.: delay $\tau$ (1 ms/div.)

## 6 Conclusions

Multipliers of two delta-sigma sequences have been developed and tested. These multipliers deliver at their outputs delta-sigma sequences while their implementation is relatively simple. One type of the proposed multiplier is particularly promising because of the high S/N ratio in relation to its simplicity.

It has been proved theoretically that the high S/N ratio which was obtained is due to the inherent triangular interpolation property that takes place in the multiplication process. Finally, this type of multiplier has been used for the realization of a parallel type digital correlator.

## 7 Acknowledgments

Many thanks are due to Dr C. Laskaris for many useful discussions and suggestions during the development of the ideas presented in this paper.

## 8 References

1 Steele, R., 'Delta Modulation Systems' (Pentech Press, London, 1975).
2 Lockhart, G. B., 'Implementation of delta modulators for digital inputs', *IEEE Trans. on Acoustics, Speech and Signal Processing*, **ASSP-22**, no. 6, pp. 453–6, December 1974.
3 Engle, L. and Steenaart, W., 'Digital summation of delta modulation signals', Canadian Communications and Power Conf., Montreal 1976, pp. 245–8.
4 Kouvaras, N., 'Operations on delta-modulated signals and their application in the realization of digital filters', *The Radio and Electronic Engineer*, **48**, no. 9, pp. 431–8, September 1978.
5 Lagoyannis, D., 'Multiplier for delta-modulated signals', *Electronics Letters*, **14**, no. 19, pp. 615–16, September 1978.
6 Lockhart, G. B., 'Digital encoding and filtering using delta modulation', *The Radio and Electronic Engineer*, **42**, no. 12, pp. 547–51, December 1972.
7 Lagoyannis, D., 'Correlator based on delta-sigma modulation', *Electronics Letters*, **12**, no. 10, pp. 253–4, 13th May 1976.
8 Nakamura, S., 'A digital correlator using delta modulation', *IEEE Trans. on Acoustics, Speech and Signal Processing*, **ASSP-24**, no. 3, pp. 238–43, June 1976.
9 LoCicero, J., Schilling, D. and Garodnick, J., 'Realization of adm arithmetic signal processors', *IEEE Trans. on Communications*, **COM-27**, no. 8, pp. 1247–54, August 1979.
10 Ashouri, M., 'A new approach to the implementation of signal processors', Fourth Intl. Symp. on Network Theory, Ljubljana, Yugoslavia, September 1979.
11 Lockhart, G. B. and Babary, S. P., 'Binary transversal filters using recirculating shift registers', *The Radio and Electronic Engineer*, **43**, no. 3, pp. 224–6, March 1973.
12 Lockhart, G. B., 'Modular networks for direct processing of delta-modulated signals', *Computer and Digital Techniques*, **2**, no. 6, pp. 237–43, December 1979.
13 Candy, J., Ching, Y. and Alexander, D., 'Using triangularly weighted interpolation to get 13-bit p.c.m. from a sigma-delta modulator', *IEEE Trans. on Communications*, **COM-24**, no. 11, pp. 1268–75, November 1976.
14 Max, J., 'Traitement du Signal' (Masson, Paris, 1972).

*Manuscript first received by the Institution on 28th December 1979 and in revised form on 7th July 1980.*
*(Paper No. 1991/CC338)*

UDC 621.317.34.029.62: 621.316.313: 681.32
*Indexing Terms:* Measurement, Attenuation/phase constants, Microwave measurements, Network analysers, Electronic applications of computers

# A flexible microwave automatic network analyser system

**H. V. SHURMER,** Ph.D., D.Sc.(Eng.), C.Eng., F.I.E.E.*

**SUMMARY**

This paper describes the microwave automatic network analyser system which has been established at the University of Warwick over the last decade. The different systems of correction which have been utilized are explained in detail, followed by an account of the system development, interfacing units and some new calibration test pieces. A description of the software precedes an outline of various applications. Finally, the advantages of this particular facility are stated and new developments of the system are indicated.

* *Department of Engineering, University of Warwick, Coventry CV4 7AL.*

*The Radio and Electronic Engineer, Vol. 51, No. 6, pp. 287–298, June 1981*

## 1 Introduction

An automatic network analyser system (A.N.A.) was first described by Hackborn a decade ago.[1] Such systems are now adopted, most notably by major standards laboratories throughout the world, enabling a reduction of at least a hundred-fold in measurement times over the procedures previously necessary for comparable accuracy and resulting in far more rigorous characterization of passive components. Semiconductor manufacturers are also benefitting through the rapid availability of parameter data during device development, particularly when the devices are intended for strip-line applications where conventional measuring techniques are inapplicable.

Whilst the standards laboratories invariably use packaged systems, which include a dedicated computer and involve very high capital outlay, for device development there is scope for employing more flexible yet less expensive techniques by augmenting conventional basic facilities and accepting some appropriate relaxation in specification tolerances. It is this latter approach which we have primarily in mind with the present paper, with emphasis on the work carried out at the University of Warwick since the initial development in 1969 of an elementary system linking a Hewlett–Packard 8410 network analyser to a GEC 90/2 digital computer,[2] which was indeed the first A.N.A. system in the UK.

## 2 Basic Principle

The underlying principle common to all these systems is that errors arising internally (e.g. due to variations of coupler directivity or amplifier gain with frequency), together with those arising from transitions, mounting arrangements, etc., are evaluated and stored by the computer via a series of preliminary calibration runs in which standard terminations are used, such as a short-circuit or a matched load. During each of these runs, either the reflection or transmission coefficient of the standard termination, as measured by the network analyser, is first recorded by the computer for a succession of precise frequency steps over the pre-selected bandwidth. Since the true reflection or transmission coefficients of these terminations are accurately known, from the stored calibration data, the overall effect of errors at each frequency can be computed, provided that there are sufficient independent runs to cater for all of the sources of error.

Subsequent runs, using the test items which are to be characterized, are carried out for the same discrete frequency steps. The previously computed error data, evaluated and stored immediately following the calibration procedures, can be effectively subtracted from the measured data to give corrected results over the required bandwidth. With the aid of a visual display unit the results pertaining to a test run may be displayed immediately afterwards in any preferred form, e.g. as the

0033–7722/81/060287+12 $1.50/0

magnitude or phase of selected parameters, using either rectangular or polar co-ordinates.

## 3 Theory of Correction Procedures

### 3.1 Use of Bilinear Transformations

For the determining of reflection coefficient in loss-less systems it is possible to eliminate the effect of transitions between a plane of measurement and the desired reference plane of a test piece or device by utilizing the bilinear relationship which exists between a reflection coefficient as seen in the measuring line ($\sigma$-plane) and the corresponding value appropriate to the desired plane in the terminating feeder ($\rho$-plane).

Thus, immediately

$$\sigma = \frac{a\rho + b}{c\rho + 1} \tag{1}$$

where $a$, $b$ and $c$ are in general complex constants.

By choosing the reference planes such that $\rho = -1$ when $\sigma = -1$ (short-circuit planes corresponding) it can readily be shown[3] that the terminating feeder reflection coefficient is given by

$$\rho = \frac{(-\sigma + b)(\bar{b} + 1)}{(\bar{b}\sigma - 1)(b + 1)}. \tag{2}$$

This expression involves only one of the above complex constants, $b$, which may be found by measuring $\sigma$ with the feeder terminated in a matched load, making $\rho = 0$. The corresponding value $\sigma_0$ for $\sigma$ is thus equal to $b$.

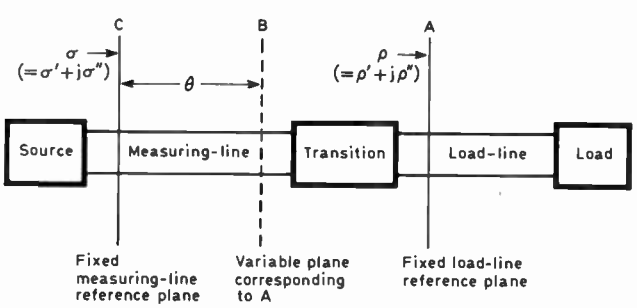


Fig. 1. Location of reference planes.

The desired plane in the feeder is at a fixed position, whereas the corresponding short-circuit plane in the measuring line changes position with frequency, as illustrated in Fig. 1. A further transformation is therefore required between the two planes of interest in the measuring line, i.e. the one just indicated and the actual plane of measurement. This transformation, however, represents simply a rotation of the reflection coefficient by an angle $\theta$, which depends on frequency and is obtainable during a calibration run using a short-circuit as the feeder termination.

Thus, if $b = b' + jb''$, it follows that

$$\left.\begin{aligned} b' &= b'_m \cos\theta - b''_m \sin\theta \\ b'' &= b''_m \cos\theta + b'_m \sin\theta \end{aligned}\right\} \tag{3}$$

where $b_m = b'_m + jb''_m$ is the reflection coefficient at the fixed plane in the measuring line under matched conditions at the terminating feeder.

Apart from the calibration run mentioned above, only one other is necessary, provided that an adequately good matched termination is available, this enabling the value of $b$ to be determined for each frequency of measurement.

### 3.2 One-port Correction (incorporating losses)

To take into account losses when determining corrected reflection coefficients it is necessary to employ a different approach and represent the total errors by a general 2-port $s$-parameter error network, as shown in Fig. 2. Here $S_{11}$ mainly represents directivity errors of the couplers and imperfect test-to-reference channel isolation, $S_{22}$ covers mismatch errors and $S_{21}S_{12}$ represents variations in the gain of both signal and reference channels (due mainly to the frequency converter and directional coupler). However, within these parameters may also be incorporated mismatch and loss errors due to imperfect transitions between the network analyser measuring port and the load, which is a matter of extreme advantage.

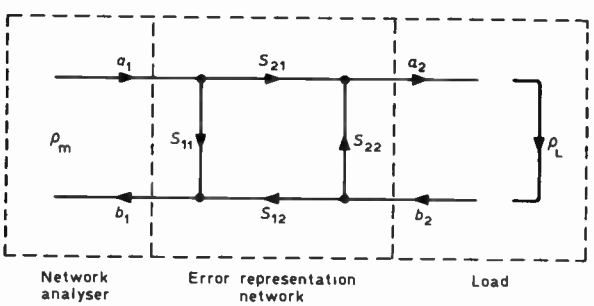


Fig. 2. $s$-parameter representation of errors.

By using flow-diagram analysis[4] it may readily be shown that

$$\rho_m = S_{11} + \frac{S_{21}S_{12}\rho_L}{1 - S_{22}\rho_L}. \tag{4}$$

Although there are four unknowns in equation (4) the two transmission $s$-parameters occur in the subsequent analysis only in the form of a product, so that only three calibration runs are required for determining the correction constants. One possible set of standard terminations for this purpose would comprise a matched load ($\rho = 0$), a short-circuit ($\rho = -1$) and an off-set short-circuit ($\rho = -e^{-j\theta}$). Substituting each of these three values in turn into equation (4) gives the following:

MATCHED LOAD

$$\rho_{m1} = S_{11}. \tag{5}$$

SHORT-CIRCUIT

$$\rho_{m2} = S_{11} - \frac{S_{21}S_{12}}{1 + S_{22}}. \tag{6}$$

OFF-SET SHORT-CIRCUIT

$$\rho_{m3} = S_{11} - \frac{S_{11}S_{12}\,e^{-j\theta}}{1 + S_{22}\,e^{-j\theta}}. \tag{7}$$

Hence

$$S_{22} = \frac{(S_{11} - \rho_{m2}) - (S_{11} - \rho_{m3})\, e^{j\theta}}{\rho_{m2} - \rho_{m3}} \qquad (8)$$

and

$$S_{21} S_{12} = (S_{11} - \rho_{m2})(1 + S_{22}). \qquad (9)$$

Using equations (5), (8) and (9) to determine the error *s*-parameters from the three calibration runs, the corrected reflection coefficient $\rho_L$, for an arbitrary terminating load whose reflection coefficient at the measuring port is $\rho_m$, is given by

$$\rho_L = \frac{\rho_m - S_{11}}{S_{22}\rho_m + S_{21}S_{12} - S_{11}S_{22}}. \qquad (10)$$

One of the difficulties in applying the above method stems from the problem of making a matched termination which has no measurable reflection from its absorbent element. For waveguide or coaxial line the difficulty is often obviated by arranging for a sequence of several measurements to be made in determining $\rho_{m1}$, using a sliding load at different settings, from which the effect of reflection can be eliminated. Frequently it is not feasible to use a matched termination at all, mainly because of dimensional restrictions, a situation often met in strip-line applications. Here, alternative calibration procedures are used, e.g. two short-circuited terminations, together with a third which may be either short- or open-circuited.[5,6] Also, certain advantages have recently been claimed for procedures requiring four test pieces with identical terminations.[7,8]

### 3.3 Two-port Correction

For general purposes transmission properties are important, particularly when dealing with amplifiers or filters, when it is necessary to characterize the unknown component or device in terms of all four *s*-parameters, which require to be appropriately corrected. This necessitates a much more elaborate approach, involving the representation of both ports of the measuring system by an equivalent error parameter network, each component of which has to be evaluated from the calibration data. Any leakage paths must similarly be represented and evaluated as error parameters. In essence, one establishes a set of simultaneous equations, equal in number to the postulated error parameters, which are related to a similar number of calibration runs. The computer solves these equations on completion of the calibration runs, storing a complete set of error parameters for each frequency of measurement. An appropriate correction routine is applied after a test run on an unknown component to eliminate from the measurement of each *s*-parameter the effects of these error parameters. The system of correction currently used at Warwick, detailed below, is based on an approach first indicated by B. P. Hand.[9] One major difference is that we have chosen to ignore the noise contribution to errors in the analysis, but each recorded measurement is the average of ten readings. The r.m.s. noise voltage is somewhat less than 0·1% of the maximum reading for any *s*-parameter.

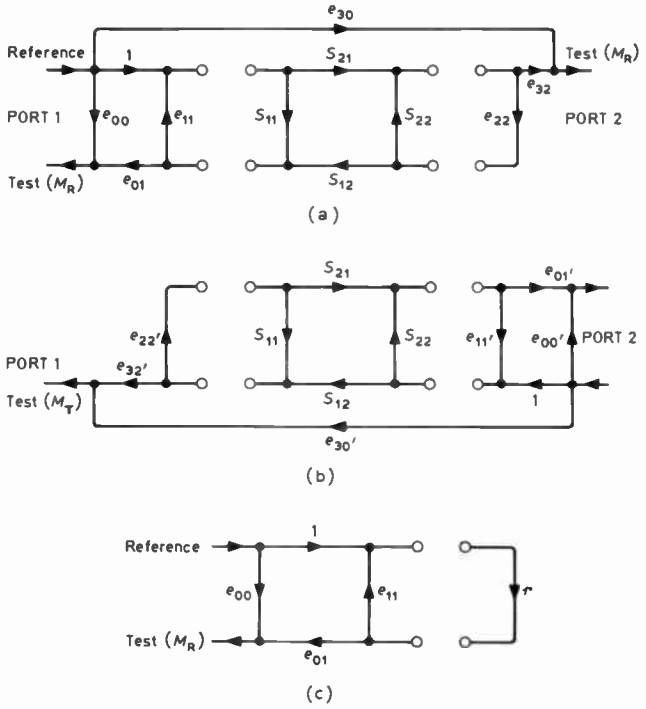


Fig. 3. Signal flowgraphs.

The signal flow-graphs representing the complete system are shown in Fig. 3.

The *s*-parameters of any device connected between the two ports are represented by $S_{11}$, $S_{21}$, $S_{12}$, $S_{22}$. The properties of the test unit, plus some of the errors due to transmissions and mounting arrangements, are represented by the *e*-parameters, which are not assumed to be independent of the reference port. Flowgraph analysis results in the following general expressions for the measured values of reflection and transmission coefficients:

$$M_R = e_{00} + \frac{S_{11}e_{01}(1 - S_{22}e_{22}) + S_{21}S_{12}e_{22}e_{01}}{1 - S_{11}e_{11} - S_{22}e_{22} - S_{21}S_{12}e_{11}e_{22} + S_{11}e_{11}S_{22}e_{22}}$$

$$M_T = e_{30} + \frac{S_{21}e_{32}}{1 - S_{11}e_{11} - S_{22}e_{22} - S_{21}S_{12}e_{11}e_{22} + S_{11}e_{11}S_{22}e_{22}}$$

$$M'_R = e'_{00} + \frac{S_{22}e'_{01}(1 - S_{11}e'_{22}) + S_{12}S_{21}e'_{22}e'_{01}}{1 - S_{22}e'_{11} - S_{11}e'_{22} - S_{12}S_{21}e'_{11}e'_{22} + S_{22}e'_{11}S_{11}e'_{22}}$$

$$M'_T = e'_{30} + \frac{S_{12}e_{32}}{1 - S_{22}e'_{11} - S_{11}e'_{22} - S_{12}S_{21}e'_{11}e'_{22} + S_{22}e'_{11}S_{11}e'_{22}}$$

The calibration process involves making sufficient measurements with standard terminations and under definable conditions to determine all of the $e$-parameters.

3.3.1 *Calibration*

The calibration measurements involve the following:

(1) Reflection with a sliding load. The computer measures the reflection three times, instructing the user to slide the load between measurements. It then constructs a circle passing through the three values and finds the centre of the circle. Thus

$$S_{11} = S_{21} = S_{12} = S_{22} = 0.$$

Hence,

$$M_1 = e_{00}, \quad M'_1 = e'_{00}$$
(first port) (second port)

(2) Transmission without a 'through connection', both measurements ports terminated.

$$S_{11} = S_{21} = S_{12} = S_{22} = 0.$$

Hence

$$M_2 = e_{30}, \quad M'_2 = e'_{30}.$$

(3) Reflection with a short circuit or off-set short circuit.

$$S_{11} = -e^{-j2\beta l},$$

where $l$ is the length of the off-set short circuit.

Again,

$$S_{21} = S_{12} = S_{22} = 0$$

and it follows that

$$M_3 = e_{00} + \frac{Ae_{01}}{1 - Ae_{11}},$$

where

$A = -e^{-j2\beta l}$ for an off-set short circuit

$A = -1$ for a short circuit ($l = 0$).

Similarly, for

$$S_{22} = -e^{-j2\beta l'}, \quad S_{21} = S_{12} = S_{11} = 0$$

leads to

$$M'_3 = e'_{00} + \frac{A'e'_{01}}{1 - A'e'_{11}}.$$

(4) Reflection with an off-set short or open circuit. Here

$$S_{21} = S_{12} = S_{22} = 0,$$

$S_{11} = -e^{-j2\beta l}$ for an off-set short circuit

$= e^{-j2\theta}$ for an open circuit, where $\theta = \tan^{-1}(\omega C Z_0)$.

Hence

$$M_4 = e_{00} + \frac{Be_{01}}{1 - Be_{11}},$$

where

$B = -e^{-j2\beta l}$ for an off-set short circuit

$= e^{-j2\theta}$ for an open circuit.

Similarly, for

$$S_{22} = -e^{-j2\beta l'} \text{ or } e^{-j2\theta'},$$

$$S_{21} = S_{12} = S_{11} = 0$$

and one obtains

$$M'_4 = e'_{00} + \frac{B'e'_{01}}{1 - B'e'_{11}},$$

(5) Reflection with a 'through' connection. Here

$$S_{11} = S_{22} = 0, \quad S_{21} = S_{12} = e^{-j\beta l}$$

where $l$ is the 'through' length. Letting

$$L = e^{-j\beta l} \quad (L = 1 \text{ if } l = 0)$$

leads to

$$M_5 = e_{00} + \frac{L^2 e_{22} e_{01}}{1 - L^2 e_{11} e_{22}}$$

and

$$M'_5 = e'_{00} + \frac{L^2 e'_{22} e'_{01}}{1 - L^2 e'_{11} e'_{22}}.$$

(6) Transmission with a 'through' connection. Now

$$S_{11} = S_{22} = 0, \quad S_{21} = S_{12} = e^{-j\beta l}$$

where again $l$ is the 'through' length. Hence

$$M_6 = e_{30} + \frac{Le_{32}}{1 - L^2 e_{11} e_{22}}$$

and

$$M'_6 = e'_{30} + \frac{Le'_{32}}{1 - L^2 e'_{11} e'_{22}}.$$

The equations for $M_1 \to M_6$ and $M'_1 \to M'_6$ can be solved to give the desired $e$-parameters:

Letting

$$X_1 = M_3 - M_1$$
$$X_2 = M_4 - M_1$$
$$X_3 = M_4 - M_3$$
$$X_4 = M_5 - M_1$$
$$X_5 = M_6 - M_2,$$

it follows that:

$$e_{00} = M_1$$

$$e_{11} = \frac{AX_2 - BX_1}{ABX_3}$$

$$e_{01} = \frac{X_1 X_2 (B - A)}{ABX_3}$$

$$e_{30} = M_2$$

$$e_{20} = \frac{X_4}{L^2(e_{01} + X_4 e_{11})}$$

$$e_{32} = \frac{X_5(1 - L^2 e_{11} e_{22})}{L}.$$

Similar equations can be obtained for $e'_{00}$, $e'_{11}$, $e'_{01}$, $e'_{30}$,

$e'_{22}$, $e'_{32}$. Different $e$-parameters are obtained for each frequency point and used by the computer for correcting all subsequent measurements at that frequency. Values for $A$, $B$ and $L$ are computed from information provided by the user.

3.3.2 *Device measurements*

When a device of unknown parameters is connected to the system, reflection and transmission measurements are made at each port. Re-writing the expressions for $M_R$ and $M_T$:

$$M_R = e_{00} + \frac{S_{11}e_{01} + e_{01}e_{22}(S_{21}S_{12} - S_{11}S_{22})}{D}, \quad (11)$$

$$M_T = e_{30} + \frac{S_{21}e_{32}}{D}, \quad (12)$$

where

$$D = 1 - S_{11}e_{11} - S_{22}e_{22} - e_{11}e_{22}(S_{21}S_{12} - S_{11}S_{22}).$$

Similarly,

$$M'_R = e'_{00} + \frac{S_{22}e'_{01} + e'_{01}e'_{22}(S_{21}S_{12} - S_{11}S_{22})}{D'}, \quad (13)$$

$$M'_T = e'_{30} + \frac{S_{12}e'_{32}}{D'}, \quad (14)$$

where

$$D' = 1 - S_{22}e'_{11} - S_{11}e'_{22} - e'_{11}e'_{22}(S_{21}S_{12} - S_{11}S_{22}).$$

Letting $Q = S_{21}S_{12} - S_{11}S_{22}$, it follows from equations (1) . . . (4) that

$$S_{11} = \frac{(M_R - e_{00})D}{e_{01}} - e_{22}Q, \quad (15)$$

$$S_{21} = \frac{(M_T - e_{30})D}{e_{32}}, \quad (16)$$

$$S_{22} = \frac{(M'_R - e'_{00})D'}{e'_{01}} - e'_{22}Q, \quad (17)$$

$$S_{12} = \frac{(M'_T - e'_{30})D'}{e'_{32}}. \quad (18)$$

An explicit solution to equations (15) . . . (18), although theoretically feasible, is unnecessary and an iterative method of solution is used, which has been shown to have negligible error. The procedure is as follows:

Initially set

$$\hat{S}_{11} = M_R, \quad \hat{S}_{21} = M_T, \quad \hat{S}_{22} = M'_R, \quad \hat{S}_{12} = M'_T.$$

Then:

(1) Calculate $Q$, $D$, $D'$ from $\hat{S}_{11}$, $\hat{S}_{21}$, $\hat{S}_{22}$, $\hat{S}_{12}$ and the $e$-parameters.

(2) Calculate new values for $\hat{S}_{11}$, $\hat{S}_{21}$, $\hat{S}_{22}$, $\hat{S}_{12}$ as follows:

$$\hat{S}_{11} = \frac{(M_R - e_{00})D}{e_{01}} - e_{22}Q,$$

$$\hat{S}_{21} = \frac{(M_T - e_{30})D}{e_{32}},$$

$$\hat{S}_{22} = \frac{(M'_R - e'_{00})D'}{e'_{01}} - e'_{22}Q,$$

$$\hat{S}_{12} = \frac{(M'_T - e'_{30})D'}{e'_{32}}.$$

(3) Return to (11).

This cycle is repeated until a convergence is obtained.

The final values for $\hat{S}_{11}$, $\hat{S}_{21}$, $\hat{S}_{22}$ and $\hat{S}_{12}$ are the corrected $S$-parameters for the unknown device.

3.3.3 *Relationships between measurement parameters*

The relationship between the reading sequence of the 2-port correction program and the measurement parameters is as follows:

| Program $K$ setting | Type of measurement | Device to be measured | Equation parameters |
|---|---|---|---|
| 1 | $S_{11}$ | sliding load | $M_1$ |
| 2 | $S_{11}$ | | |
| 3 | $S_{11}$ | | |
| 4 | not used | | |
| 5 | $S_{22}$ | sliding load | $M'_1$ |
| 6 | $S_{22}$ | | |
| 7 | $S_{22}$ | | |
| 8 | not used | | |
| 9 | $S_{21}$ | matched termination | $M_2$ |
| 10 | $S_{12}$ | matched termination | $M'_2$ |
| 11 | $S_{11}$ | short- or offset short-circuit | $M_3$ |
| 12 | $S_{22}$ | offset- or open-circuit | $M_4$ |
| 13 | $S_{22}$ | offset- or open-circuit | $M'_3$ |
| 14 | $S_{11}$ | short- or offset short-circuit | $M_4$ |
| 15 | $S_{11}$ | 'through' connection | $M_5$ |
| 16 | $S_{21}$ | | $M_6$ |
| 17 | $S_{22}$ | | $M'_5$ |
| 18 | $S_{12}$ | | $M'_6$ |
| 19 | $S_{11}$ | device under test | $M_R$ |
| 20 | $S_{21}$ | | $M_T$ |
| 21 | $S_{22}$ | | $M'_R$ |
| 22 | $S_{12}$ | | $M'_T$ |

The $K$ setting relates to the software (Sect. 7).

3.3.4 *Accuracy and repeatability*

Questions of accuracy and repeatability are of major importance in relation to calibration techniques, accuracy in particular being dependent on many factors. For comparability with a standards laboratory, a frequency synthesizer is probably essential, and this has not been available to us. However, for test specimens whose parameters are only slowly varying functions of frequency, corrected values for each of the four $s$-parameters can be achieved with accuracy of the order 0·01, even with a system in which the source frequency is set from data stored in the form of a calibration table in the computer, giving an absolute frequency of no better than 1 part in $10^4$. An improvement by two orders of

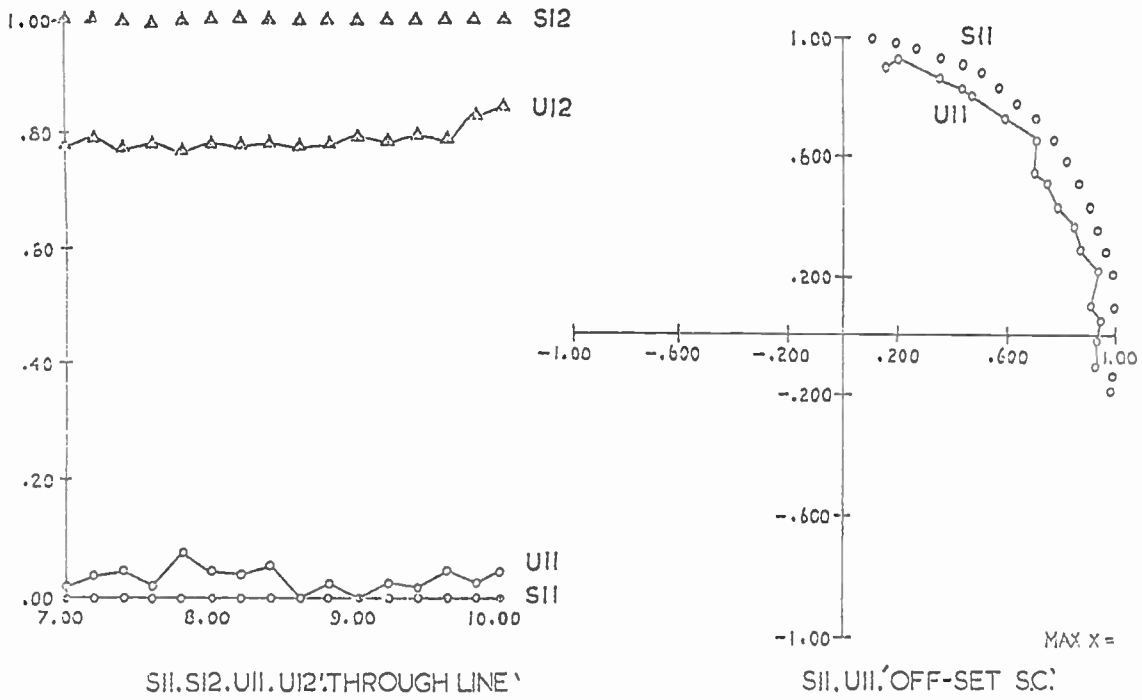


**Fig. 4.** Examples of displays on v.d.u. (off-set short circuit and 'through' line).

magnitude in this accuracy over pre-selected 40% bandwidths has been obtained by adding a phase-locked loop facility.

In Fig. 4 are illustrated examples which were produced without phase-locking and it is seen that, even here, errors in the corrected results are barely discernible for normal graphical plotting. The facility has been applied primarily to active device characterization, where residual errors have been of negligible consequence.

The effects of variations in physical lengths for off-set short-circuits and also the effects of errors in the estimated discontinuity capacitance of open-circuit calibration pieces have been studied by the author's colleague, Dr M. K. McPhun, and former colleague, Dr E. F. Da Silva.[8] The same pair of researchers also studied the repeatability of measurements of reflection coefficients and concluded that accuracies of about $\pm 1\%$ for phase angle and $\pm 1{\cdot}5\%$ for amplitude were obtainable, when referred to reflection from a short-circuited termination.[10]

## 4 System Development

### 4.1 Basic Hardware

The correction procedures described in Sections 3.1 and 3.2 belong to the initial phase of development associated with a GEC 90/2 computer, programmed in a low-level language and which has been reported in some detail.[2] The system now described is of a subsequent phase, referred to in Section 3.3. Figure 5 shows a photograph of the equipment, excluding the computer.

The network analyser Type 8410 was retained but linked now to a much more powerful computer (XDS Sigma 5). The original separate reflection and

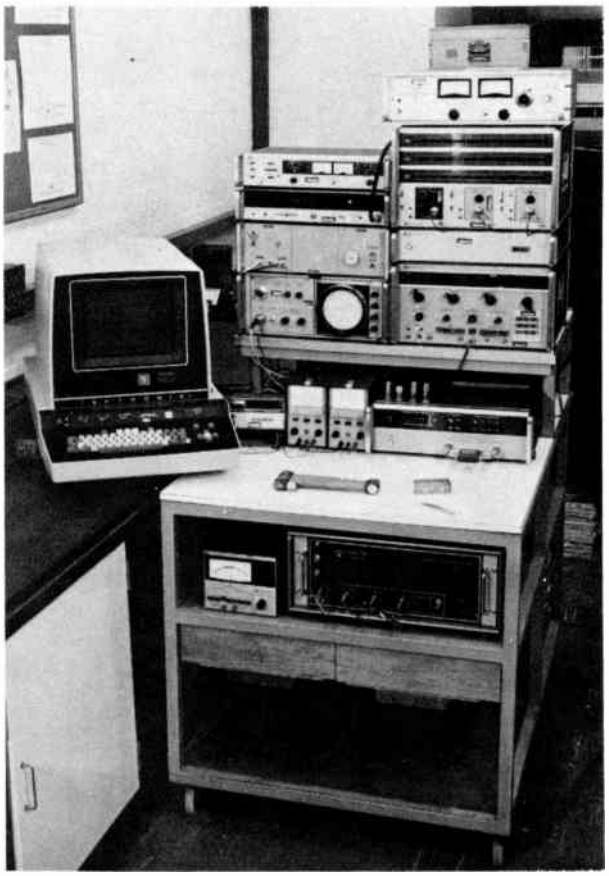

**Fig. 5.** The microwave equipment.

transmission test units were replaced by a single high-frequency *s*-parameter unit and a multiplexer provided, enabling three octave-bandwidth sweepers to be fed sequentially into the system under computer control. A further major item introduced at this stage was a self-tracking frequency counter, giving a continuous digital read-out up to 18 GHz, together with feedback to the computer for the automatic elimination of frequency errors. Shortly afterwards, a phase-lock loop system was provided, enabling the frequency to be set at a value determined by the accuracy of a reference crystal oscillator, frequency coverage being available from 100 MHz to 18 GHz, although not with phase-locking capabilities over the whole of this range.

### 4.2 Control of Network Analyser

The computer fulfils three basic requirements in the system:

(1) Control of the measurement procedure.
(2) Storage and presentation of data to obtain the corrected results.
(3) Presentation of output data.

Operations are performed by the computer as instructed by the operator via a graphics terminal (v.d.u. with input keyboard), situated remotely from the computer. A typical question and answer routine through which control is achieved is illustrated in Fig. 6, which is taken directly from the v.d.u.

```
2-PORT FULL CORRECTION PROGRAM.

VERSION OL2/3
INITIALISATION REQUIRED ? TYPE Y OR N >YES
USE OF DATA TAPE REQUIRED ? TYPE Y OR N >NO
ARE AMPLIFIERS IN USE ? TYPE Y OR N (YES
WAVEGUIDE OR COAX - TYPE W OR C  (COAX

STANDARD CALIBRATION USES SLIDING LOAD, SHORT AND OFFSET SHORT.
STANDARD CALIBRATION REQUIRED ? (TYPE Y OR NO> (YES
LENGTH OF OFFSET SHORT (CM) = 0.3
JOYSTICK IS NOT IN USE.
NO. OF READINGS PER POINT =10
TIMING INTERVAL ( M40.01 SEC). N=30
INPUTS TAKEN FROM POLAR DISPLAY OR PHASE GAIN UNIT ?
TYPE LOG,LIN,OR POL (!! POL
CENTRE BEAM WHILE TYPING ANY CHARACTER Y
MAXIMUM FREQUENCY (GHZ) = 12.0
MINIMUM FREQUENCY (GHZ) = 8.0
NO. OF POINTS = 11
SWITCH TOLEC RESET TO 3U.
MINIMUM FREQUENCY SET UP
CORRECTION TO FREQ. IN MHZ = 0.0
K=1   CONNECT MATCHED LOAD ON PORT 1>YES
K=2   SLIDE LOAD                    >YES
K=3   SLIDE LOAD                    >YES
K=4   SLIDE LOAD                    >YES
K=5   CONNECT MATCHED LOAD ON PORT 2>YES
K=6   SLIDE LOAD                    >YES
K=7   SLIDE LOAD                    >YES
K=8   SLIDE LOAD                    >YES
K=9   FWD TRANSM  2 MATCHED LOADS   >YES
K=10  REV TRANSM  2 MATCHED LOADS   >YES
K=11  SHORT CIRCUIT ON PORT 1       >YES
K=12  OFFSET SHORT 1 ON PORT 2      >YES
K=13  SHORT CIRCUIT ON PORT 2       >YES
K=14  OFFSET SHORT 1 ON PORT 1      >YES
K=15  CONNECT THROUGH LINE          >YES

NEW DEVICE ? >YES
TYPE DEVICE IDENTIFICATION & TERMINATE WITH CR
TEST RUN
K=19  CONNECT DEVICE                >YES
```

**Fig. 6.** Typical question and answer routine from v.d.u.

Upon receipt of the appropriate command, the computer selects the *s*-parameter corresponding to the desired reflection or transmission measurement. It then sets the frequency and reads the output from the network analyser. These functions are accomplished by the aid of interface units described in Section 5.

The procedure is repeated at a sequence of discrete frequency points over the pre-selected bandwidth. This is first done for a series of calibration runs, as described in Section 3.3 from which the errors of the system are evaluated. Subsequently the unknown device is connected to the terminals of the *s*-parameter test set and the appropriate *s*-parameters are read at each frequency point, the results stored, corrected, and the output data made ready for display.

### 4.3 Presentation of Results

Unlike the GEC 90/2 computer, which had to be programmed in assembly language, high-level languages may be used with the Sigma 5. Based on the mathematical procedures of Section 3, two powerful programs in FORTRAN have been developed, one giving the full two-port correction facility for all four scattering parameters, the other being limited to reflection parameters. Into each of these have been incorporated a wide range of options covering calibration and test procedures, as well as numerous formats for the results. These include print-outs in tabular form from the line printer and graphical displays in polar or rectangular form (with the facility for enlargement between any selected limits) using the computer graphics terminal, from which hard copies may be obtained.

Up to four variables may be plotted at once and any combination of four corrected *s*-parameters with four uncorrected *s*-parameters is possible. Examples of such displays achieved for a 'through line' and for an off-set short-circuit are shown in Fig. 6 in which the continuous curves $U_{11}$, $U_{22}$, represent uncorrected results and the discrete points, $S_{11}$, $S_{22}$, give corrected values.

At frequencies above 15 GHz accuracy becomes limited owing to the large errors arising due to the present network analyser and associated mixer not having been designed to operate much above 12 GHz.

It has been demonstrated that the computerized system can be controlled from a distant terminal via telephone lines. The present system has been controlled from the University of Sussex, where corrected graphical displays of *s*-parameters have been received on-line from the Warwick equipment.

## 5 Interfacing of the Network Analyser to the Computer

Selection of the *s*-parameters and the control of frequency are performed via five interface units, as illustrated in Fig. 7.

### 5.1 Serializer

As each particular frequency is set up, it is read by the automatic frequency counter, which has now replaced the earlier counter requiring semi-manual tuning and for

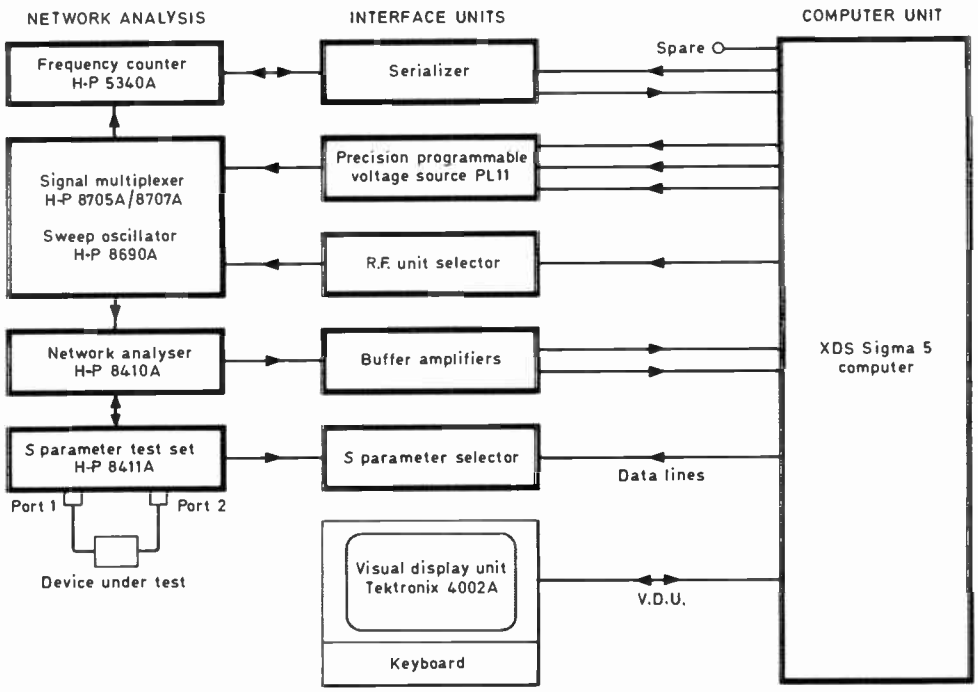


Fig. 7. Interface units.

which a servo control system was developed. The reading from the automatic counter is fed back to the computer along a single channel, after conversion of the counter output by a 'serializer' from eight parallel bits into a serialized form. By using both positive and negative analogue voltages, a second channel serves to carry either clock pulses for the serializer or control instructions for the computer.

### 5.2 Programmable Voltage Source

The particular step of voltage which is required to provide the next frequency, at any stage of the calibration or testing, is determined by data stored in the computer and is accomplished via a programmable voltage source. The data are obtained from preliminary calibration of the swept oscillators. Operation of this unit requires three separate lines from the computer, which permit initialization, output and cancellation of the tuning voltage, respectively.

The programmable voltage source was developed from a stabilized power unit whose output was originally controlled by manual decade switching. In the present unit, the switching is accomplished electronically and the voltage increased progressively in steps of 1 mV over the range 3 V to 73 V, corresponding to the full frequency range of each of the swept oscillators. Each step requires one voltage pulse from the computer and the rate at which these are supplied is 30000 p/s.

### 5.3 R.F. Unit Selector

The swept oscillators are multiplexed in groups of three, which can be changed at will. Selection of a particular unit is effected via the r.f. unit selector, using a direct voltage which is interpreted as a 4-bit binary word.

### 5.4 Buffer Amplifiers

The output from the network analyser to the computer comprises two analogue voltages, which correspond to the real and imaginary parts, respectively, of the *s*-parameter being measured. These voltages are stepped up via buffer amplifiers before being transmitted, in order to give improved signal-to-noise ratios at the analogue inputs of the computer.

### 5.5 *s*-Parameter Selector

The *s*-parameter test set is controlled through the application of a direct voltage to the *s*-parameter selector, whose level it interprets as a 4-bit binary word.

## 6 Calibration Test Pieces

Several ranges of coaxial and strip-line test pieces were produced, examples of which are shown in Fig. 8. At (a) are shown various short-circuits, off-set short-circuits and a 'through line' constructed for use in the transistor strip-line mount shown in Fig. 9(a). At (b) are shown examples of test elements prepared on alumina ceramic for use in conjunction with the test jig shown in Fig. 9(b).

The units shown at (c), (d) and (e) (Fig. 8) were constructed for use in coaxial line corrected measurements involving connectors of the OSM-, N- and APC/7-types, respectively.

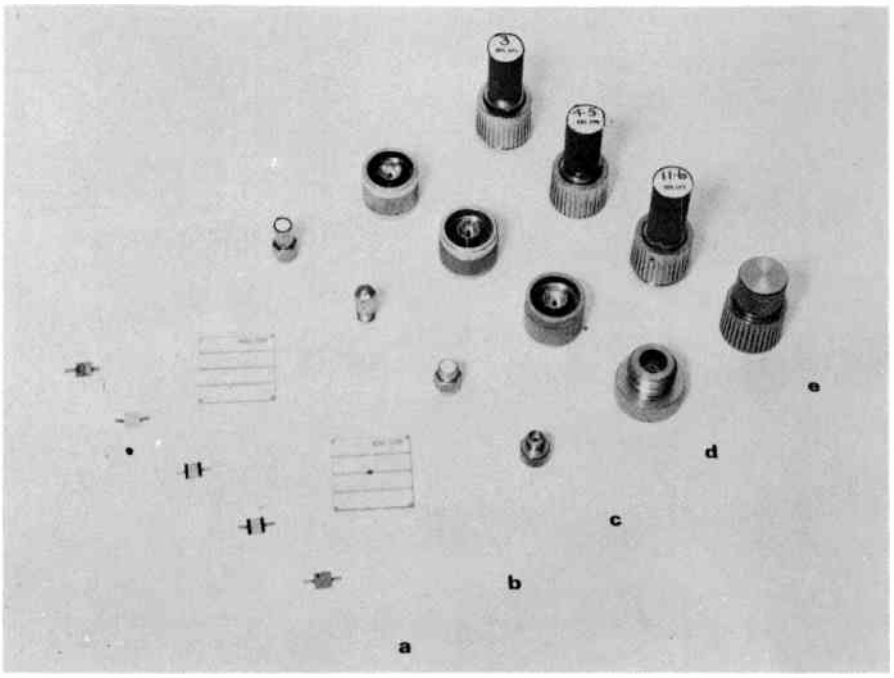


**Fig. 8.** Examples of calibration test pieces.

## 7 Development of Software

The Sigma 5 computer has 32K storage capacity, backed by a rapid access disk of 1·5 megabytes, each byte being one-quarter of a 32-bit computer word. The core storage is divided between foreground and background areas. Tasks in the foreground are executed according to a priority interrupt system, whereas the background is used for batch processing.

The programming associated with the present work has been almost entirely in FORTRAN IV, together with minor injections of machine code. The programs have been written as a series of subroutines, prepared on punched cards and then transferred to magnetic tape. The user controls the program by means of a series of questions or instructions, together with answers or responses, the former being posed on the v.d.u. and the operator replying via the keyboard. After each question, the computer waits until a suitable reply has been received before proceeding. There are four main sections to each program:

(1) *Initialization*. This part poses a series of questions to the operator, so as to allow the setting up of hardware required for that particular run and the specification of calibration options and frequency ranges.

(2) *Calibration*. The operator is requested to connect a series of standard terminations. Measurements for each termination are then made over the specified frequency ranges and the results stored by the computer.

(3) *Measurement, Correction and Display*. On completion of the calibration procedures the operator is requested to connect the test device. This is then measured, the results corrected in accordance with the calibration data and displayed either graphically on the v.d.u. or in tabular form via the line printer. This stage may be repeated for any number of test devices.

(4) *Task Facility*. This allows flexibility in running the program. A list of options is offered permitting parameters to be changed, calibration data to be re-read and basic sequences to be re-entered at various points. A facility is provided whereby the results may be dumped on to magnetic tape in a 'photographic' manner, i.e. a complete image of the data store is copied. This can be re-loaded remotely from the network analyser system, enabling facilities to be used which core limitations have precluded from the main program, thus permitting more sophisticated graphical plots or tabulations of results. The complete set of Task options is shown in Fig. 10.

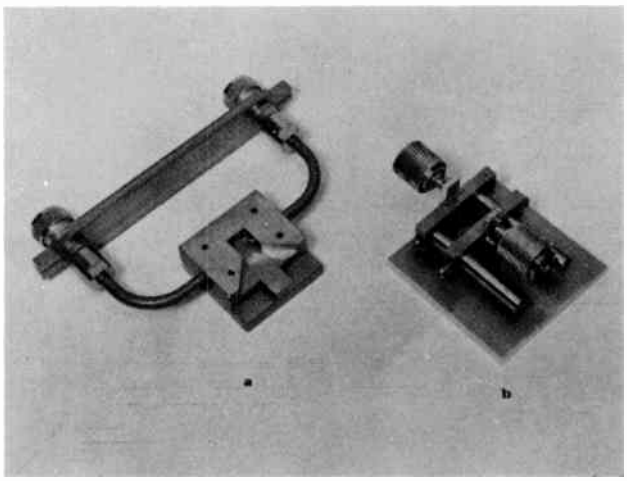


**Fig. 9.** Examples of test mounts.

```
TASK ? (TYPE LI FOR LIST OF OPTIONS)  !!
TASK OPTIONS - TWO LETTER KEYS REQUIRED
LI  LIST OPTIONS              ZE  RESTART PROGRAM
BG  RESTART CALIBRATION       RE  REPEAT LAST READING
SK  RESET K (SEE BELOW)       ND  GO TO NEW DEVICE
CA  CALCULATE                 PR  PRINT
DI  ENTER DISPLAY             DU  DUMP READINGS
UD  UNDUMP READINGS           ST  RELEASE PROGRAM
CO  INSERT COMMENT            CE  CENTRE BEAM
AM  RESET AMPLIFIERS          IN  RESET INPUT TYPE
WA  WAVEGUIDE OR COAX         CL  DEFINE CALIB PIECES
JO  JOYSTICK SWITCH           FR  RESET FREQ RANGE
MF  CORRECT MIN FREQ          NO  RESET NO. READINGS
TI  RESET TIMING INT          TF  UPDATE TAPE FORMAT
DC  DISC FILE CLEAR           LT  LOAD DATA TAPE
UT  UNLOAD DATA TAPE          RS  RESTORE CALIB. DATA

SETTINGS FOR K IN SK OPTION
K=1   CONNECT MATCHED LOAD ON PORT 1
K=2   SLIDE LOAD
K=3   SLIDE LOAD
K=4   SLIDE LOAD
K=5   CONNECT MATCHED LOAD ON PORT 2
K=6   SLIDE LOAD
K=7   SLIDE LOAD
K=8   SLIDE LOAD
K=9   FWD TRANSM  2 MATCHED LOADS
K=10  REV TRANSM  2 MATCHED LOADS
K=11  SHORT CIRCUIT ON PORT 1
K=12  OFFSET SHORT 1 ON PORT 2
K=13  SHORT CIRCUIT ON PORT 2
K=14  OFFSET SHORT 1 ON PORT 1
K=15  CONNECT THROUGH LINE


K=19  CONNECT DEVICE
```

**Fig. 10.** Task operations.

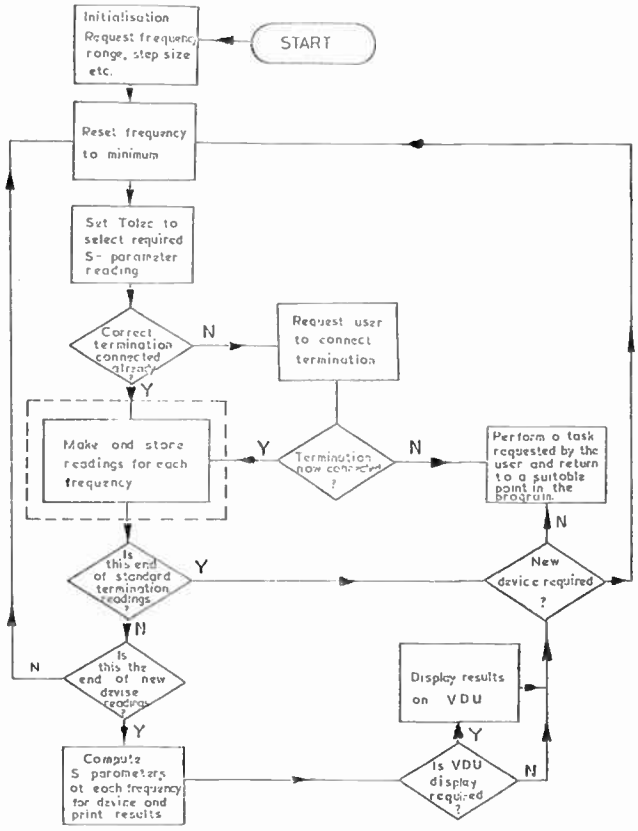


**Fig. 11.** General flow-chart of scattering parameters measurement.

### 7.1 Flow-chart

A general flow chart of the routine for *s*-parameter measurements is shown in Fig. 11. That part of it which relates to the setting up of each frequency and the recording of network analyser readings is shown in Fig. 12.

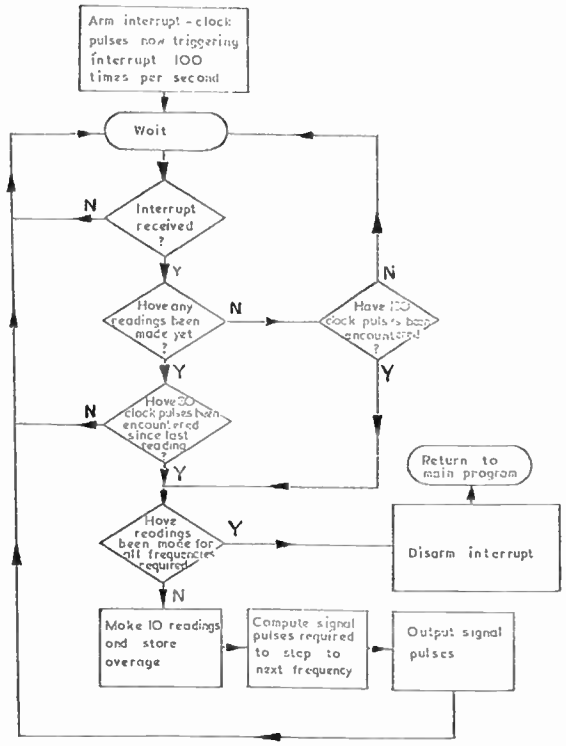


**Fig. 12.** Frequency storage procedure and signal measurement.

### 7.2 Overlaying

The programs as originally written occupied most of the core store but were subsequently re-written to facilitate their use in a time-sharing environment, reducing the core storage and allowing extended running time. By constructing the programs as a series of subroutines this requirement has been met, using a hierarchical structure of control and functional parts. A secondary benefit has been to allow greater flexibility in program content, as demanded by a research environment. One specific example is the ability to substantiate one calibration routine for another, dependent on the particular circuit environment of the test device.

The overlay structure enables the 2-port correction program to be operated within 8K of core storage, including a section reserved for data. The main control or root section branches into four sub-sections, as indicated below.

*Calibration and Reading Control.* Calls the correction and reading sub-routines.

*Line Printer Sub-routine.* Available for results which are to be printed in tabulated form.

*V.D.U. Display Control.* Calls the graph plotting sub-routines.

*Initialization and Task Control.* Calls data set-up, initialization, tape dumping routines, etc.

## 8 Applications

### 8.1 Device Development

A major application of the facility so far has been in developing microwave f.e.t.s for use in microstrip transmission lines. Accurate measurements would be impossible without such a system of correction because of the difficulties of characterizing the transitions to the transistor mounts, the labour involved otherwise being prohibitive.

In addition to the general advantages, the system offers some especially attractive features in relation to the characterization of f.e.t.s. For instance, the effects of cross-coupling between ports of the test fixtures may be eradicated, which is particularly advantageous in measuring reverse transmission, important in relation to stability. The definition of reference-plane positions is facilitated, a provision which is extremely valuable when using asymmetric mounts or a coaxial 'flexible arm'. The rapid comparison of test devices has been facilitated by the addition of sub-routines to calculate gain and stability, a straightforward matter with the present programme structure.

### 8.2 Amplifiers and Oscillators

The facility has been extensively used in the development of a wide range of f.e.t. and bipolar amplifiers over a bandwidth of 2–12 GHz, mainly using transistors mounted on alumina substrates but also using standard packages. Much of the work has been in the field of computer-aided design, incorporating optimization programs.[11] A second major interest to date has involved the development of circuits for microwave oscillators over a bandwidth from 3 GHz to 15 GHz, which represents the upper frequency limit at which the facility can be usefully applied in its present form.

### 8.3 C.A.D. and Optimization

A further significant field of application is in computer-aided design, enhanced by advances in optimization and analysis procedure.[12] The ability to characterize an unknown component or device, exclusive of system hardware errors, then to represent and store the results in any desired mathematical form, would be virtually impossible without an automatic network analyser system. Particularly valuable results have been obtained with the present system in characterizing strip-line parameters.[13]

## 9 Conclusions and Future Work

A unique and versatile facility has been created whose major features are as follows:

- Automatic operation of the microwave equipment by the computer with a correction capability from 500 MHz to approximately 15 GHz.
- Calibration of both measurement ports, obviating the need for device reversal.
- Facility for calibrating each port independently, using different types of standard termination.
- Display of results as *s*-parameters or in various other forms, e.g. as *y*-parameters.
- Storage of data on magnetic tape for subsequent display or analysis.

Up to four variables may be plotted at once and any combination of four uncorrected *s*-parameters with four corrected *s*-parameters is possible over the bandwidth of any one of the swept frequency sources, starting at 100 MHz and continuing with effective correction up to at least 15 GHz. Polar or rectangular plots may be displayed and amplitude or phase may be shown separately. In all cases selected parts of the displays may be expanded and hard copies taken. The results may alternatively be obtained in tabulated form via a line printer or 'dumped' on to magnetic tape for storage or further processing.

Calibration procedures have been devised and standard terminations appropriate to these procedures have been produced in a variety of forms, e.g. for coaxial line terminated in connectors of APC/7, OSM- or 'N'-type and for microstrip on alumina.

The facility is currently being applied to the automatic control and correction of amplifier noise figure measurements. Here the computer measures the noise figure at various known source admittances, which are automatically set up, subsequently embarking on a curve-fitting procedure for optimum results.[14]

Proposals are in hand to apply microcomputing techniques to the facility in several successive stages, whilst maintaining a capability for continuing operation.

## 10 Acknowledgments

The author is indebted to H. E. G. Luxton and D. A. Abbott, formerly of the Allen Clark Research Centre, Plessey Research (Caswell), for much assistance in setting up and operating the facility. Thanks are also due to Mrs C. A. Stoneman and to A. J. Hulme at Warwick University for computing assistance. The work has received substantial support, especially in its early stages, from A.E.I. Semiconductors, also from the Ministry of Science and Higher Education of Iran and, continuously, from the UK Science Research Council.

## 11 References

1 Hackborn, R. A., 'An automatic network analyser system', *Microwave J.*, **11**, no. 5, pp. 45–52, 1968.
2 Shurmer, H. V., 'Low-level programming for the on-line correction of microwave measurements', *The Radio and Electronic Engineer*, **41**, no. 8, pp. 357–64, 1971.
3 Shurmer, H. V., 'Correction of a Smith-chart display through bilinear transformations', *Electronics Letters*, **5**, no. 10, p. 209, 1969.
4 Abrahams, J. R. and Coverley, G. P., 'Signal Flow Analysis' (Pergamon, Oxford, 1965).
5 da Silva, E. F. and McPhun, M. K., 'Calibration of microwave network analyser for computer-corrected *s*-parameter measurements', *Electronics Letters*, **9**, no. 6, pp. 126–8, 1973.

6 Shurmer, H. V., 'Calibration procedure for computer-corrected *s*-parameter characterization of devices mounted in microstrip', *Electronics Letters*, **9**, no. 14, pp. 323–4, 1973.
7 da Silva, E. F. and McPhun, M. K., 'Calibration techniques for one port measurement', *Microwave J.*, **21**, no. 6, pp. 97–100, 1978.
8 da Silva, E. F. and McPhun, M. K., 'Calibration of an automatic network analyser using transmission lines of unknown characteristic impedance, loss and dispersion', *The Radio and Electronic Engineer*, **48**, no. 5, pp. 227–34, 1978.
9 Hand, B. P., 'Developing accuracy specifications for automatic network analyser systems', *Hewlett-Packard J.*, **21**, no. 6, pp. 16–19, 1970.
10 da Silva, E. F. and McPhun, M. K., 'Repeatability of computer-corrected network analyses measurements of reflection coefficients', *Electronics Letters*, **14**, no. 25, pp. 832–4, 1978.
11 Hosseini, N. M. and Shurmer, H. V., 'Computer-aided design of microwave integrated circuits', *The Radio and Electronic Engineer*, **48**, no. 1/2, pp. 85–8, 1978.
12 Hosseini, N. M., Shurmer, H. V. and Soares, R. A., 'OPTIMAL: a program for optimizing microstrip networks', *Electronics Letters*, **12**, no. 8, pp. 190–2, 1976.
13 Hosseini, N. M. and Shurmer, H. V., 'MICPA: evaluation of microstrip-line parameters', *Electronics Letters*, **12**, no. 19, pp. 596–7, 1976.
14 Abbott, D. A. and Shurmer, H. V., 'Computer control and correction of microwave noise figure measurements', XIXth General Assembly of U.R.S.I., Helsinki, 1978.

*Manuscript received by the Institution on 6th August 1980*
*(Paper No. 1992/MI20)*

UDC 621.371.029.55: 621.376: 621.394: 681.32
*Indexing Terms:* H.f. radio communication systems, Modems, Microprocessor application

# Bit-slice microprocessors in h.f. digital communications

**S. D. SMITH,** B.Sc.,*
**P. G. FARRELL,** B.Sc., Ph.D., C.Eng., M.I.E.E.*,
**K. R. DIMOND,** B.Sc., Ph.D., C.Eng., M.I.E.E.*

*Based on a paper presented at the IERE Conference on Microprocessors in Automation and Communications held in London in January 1981*

**SUMMARY**

A 2·4 kbit/s baseband modem is being designed for use at h.f., incorporating modulation/demodulation techniques that are matched to those frequencies and the problems associated with them. Fed by a continuous serial data stream, the modulator functions are implemented wholly by a bit-slice microprocessor, and controlled by another more conventional microprocessor. Analogue output waveforms are generated in a d/a converter, which is driven by the bit-slice machine. Demodulation is performed in a similar device, using an a/d input and giving a serial output.

* *Electronics Laboratories, University of Kent at Canterbury, Canterbury, Kent CT2 7NZ*

## 1 Introduction

Over the past ten years, devices for transmission and reception of data have become more digital in their realization. Not only are these devices constructed with more digital circuitry, but also signals hitherto transmitted on analogue schemes have been modulated digitally. This mode of transmission requires a modem which will convert the baseband signal into a form suitable for transmission. Design of modulators/demodulators which convert between data streams and waveforms suitable for specific types of channel has accelerated in recent years, one such channel being h.f. radio.

This paper describes a modem of this type, which has been designed at the University of Kent for use specifically on voiceband channels at h.f, and also discusses methods of realization. The modem is fed by a serial data stream at 2·4 kbits per second, which it modulates into a 3 kHz baseband channel. In the receiver, after mixing down to baseband, the second half of the modem uses the incoming signal to synchronize, and demodulates it back into a serial data stream (Fig. 1). The modulation technique employed for this system is multi-channel four-phase differential p.s.k.,[1] both with and without pilot synchronization tones inserted in the band. Although other modulation schemes are under consideration to demonstrate the versatility of the modem, this technique is the one to be used at h.f. trials.

H.f. transmission and reception have special problems associated with them. This is because h.f. channels are usually ionospheric and therefore suffer from multi-path propagation and both man-made and natural interference, properties which can cause unpredictable loss of data and synchronization. Unless modem parameters such as data rate or bandwidth are altered, little can be done to prevent loss of data. Loss of synchronization on the other hand results in an additional increase in data errors which can to some extent be controlled. Hence synchronization and the approach for its implementation have been under careful scrutiny in the design of the demodulator.

Until quite recently, nearly all modems would have consisted largely of analogue circuitry with a digital interface to the data source or sink. Utilizing microprocessors enables the construction of modems which are completely digital with just an analogue interface to the communication channel. The most obvious advantage in this case is the increased versatility of the modem. Whereas before, to change modulation type would have needed a major reconstruction of the hardware, the microprocessor realization reduces the problem to a modification in the program which it executes.

## 2 Operation

In the modulator, incoming data are packed into bytes which are used two or four at a time to provide sixteen or



0033–7722/81/060299+03 $1.50/0

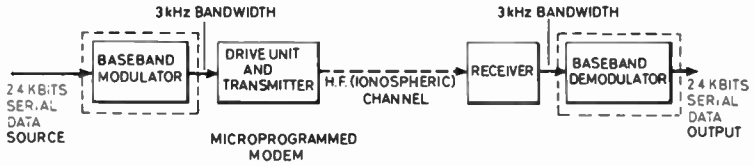


Fig. 1. Schematic diagram of the modem.

thirty-two channels of parallel information. These blocks of data are modulated by a repeating real-time programme with period $\tau$ equal to 1/16th or 1/32nd of the incoming serial data rate, into sixteen or thirty two parallel q.d.p.s.k. channels all placed side-by-side in the 3 kHz baseband. Each channel is separated from its neighbour by $2/\tau$ Hz and is also at a multiple of the frequency $2/\tau$. In the 16-channel case, eight carriers each at multiple of the frequency 300 Hz are phase modulated, carrying two bits of information on each of four 90° spaced phases (Fig. 2). In the thirty-two-channel case, sixteen carriers are modulated at a time, but the period $\tau$ is doubled too.

The individual carrier signals are generated from sine look-up tables, similar to those described in Ref. 2. These tables are sampled, scaled and summed, depending on the required frequency and phase, every 1/9600th of a second. 128 samples at each frequency of the carriers are derived from the tables at the requisite phases, and summed to obtain 128 samples for transmission. Another two or four bytes are taken from the incoming data stream and used to calculate the new phases for each carrier, so that the whole cycle may begin again. The resultant samples are clocked through a d/a converter to produce the baseband modulated waveform (Fig. 3).

The demodulator, which has to contend with synchronization and error decisions, is more complex than the modulator. (Error decisions consist of resolving the polarity of incoming data into its most likely state, and possibly implementing any error detection/correction that might have been coded into the data.) The noise-corrupted incoming signal is sampled by an a/d converter at 9·6 kbaud. Samples are used in a synchronization algorithm which is arranged to provide the start pulses to a Fast Fourier Transform (F.F.T.) routine. Output from this gives the phase and amplitude of each carrier, which may be compared with the previous phase and amplitude of the same carrier to regenerate the two bits of data.

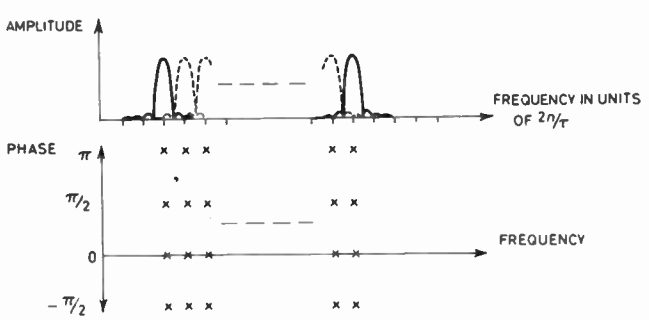


Fig. 2. Amplitude and phase spectrum for multi-channel 4-phase d.p.s.k.

Consider the sixteen carrier situation.

The incoming data from the a/d converter consist of amplitudes of an analogue waveform sampled at discrete intervals of 1/9600th of a second. Without noise, this analogue signal is a sum of sixteen sine waves of equal amplitudes at four possible discrete phases. At intervals of 1/32nd of the data rate (i.e. 75 Hz) the phase of each carrier might change by multiples of 90°, depending on the two new bits of data it carries. Assuming it is highly probable that at least one of the carriers will change phase at every discontinuity, it is possible to gain data synchronization from the phase transitions. An output from this synchronization is used to keep an F.F.T. in step with the incoming data. A double 64-point radix-2 F.F.T. routine[3,5] is applied to each block of 128 samples to produce two frequency domain samples for each carrier frequency. These are averaged and converted from complex coordinates to amplitude and phase coordinates from which not only the data may be determined, but also the rate of fading of the incoming signal and the frequency/phase shift caused by h.f. interference.

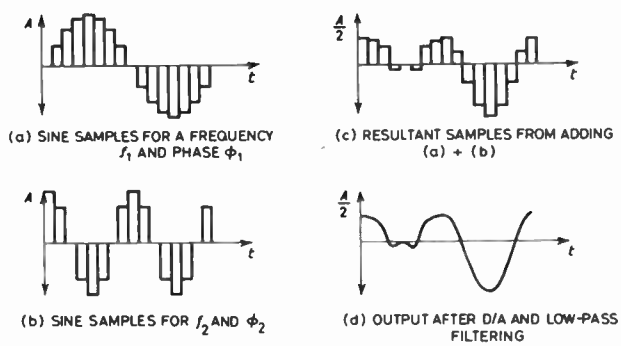


Fig. 3. Example of sine sample summation for two carriers.

Were the F.F.T. to take its 128 samples so that a phase discontinuity boundary was somewhere in the middle, the resulting data would be completely useless. In fact the errors rise fairly quickly with the number of samples at the wrong side of a phase transition, so it is essential that there is good data synchronization. This requires accurate data rate recovery from the incoming signal, which is achieved by a sliding filter algorithm in association with a local 'flywheel' clock. Whether this local clock or the generated synchronization pulses are used to synchronize the transform depends on the depth of fade or the frequency/phase error, as ascertained from previously decoded data blocks.

An additional technique is available for improving

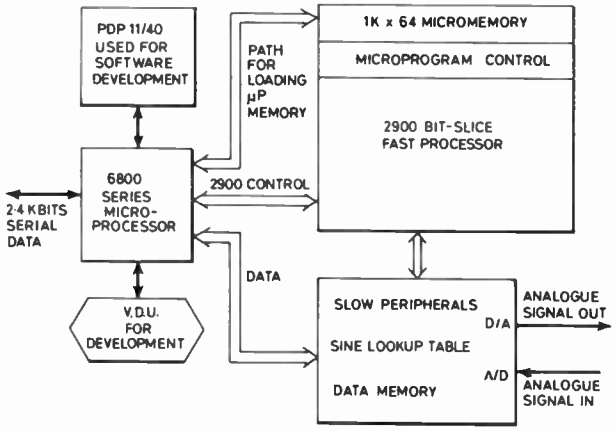


Fig. 4. Modem structure (block diagram).

synchronization, and for minimizing the possibility of performing an F.F.T. across a discontinuity. This involves spreading the carrier frequencies out so that they cover the complete bandwidth of the voice channel, rather than their frequencies being integral multiples of the data rate. The sampling frequency of the receiver is increased proportionately so that it is still an integral multiple of the carrier frequencies. However, the period between phase discontinuities in the transmitted signal remains a simple fraction of the data rate. Hence the period during which the 128 samples are taken for the F.F.T. is shorter than the time between discontinuities by approximately 16% for a data rate of 2·4 kHz in a 3 kHz bandwidth.[4] This means that there is a fairly long period of time, across the phase transition, over which no samples are taken for use in the F.F.T. This is advantageous for two reasons: (a) to allow a greater margin for synchronization error before trans-discontinuity samples cause errors in the F.F.T. algorithm, and (b) the F.F.T. does not employ samples near to the discontinuity where the 3 kHz bandlimiting causes 'rounding' of the signal on either side.

## 3 The Modem Structure

In both the modulator and the demodulator there are two microprocessors. A slower, one-chip microprocessor from the 6800 family is used to interface the modem to the serial data source or sink. Its responsibility is for the slower data processing, such as packing the incoming serial data into bytes and encoding it, some of the synchronization mechanism in the demodulator, and the control functions for the fast processor. (Fig. 4.)

This fast processor consists of a 2900-series bit-slice microprocessor to perform the modulation and demodulation of data, and is connected directly to the analogue port via its data bus. Its purpose is to convert data to samples of summed sine waves at the correct phases in the modulator, and to perform the F.F.T. and clock recovery in the receiver. Since as a modulator/demodulator it is repeatedly executing a dedicated routine of known duration, there is no need for macro-coding and a mapping p.r.o.m. as in the conventional bit-slice machine.[6] Hence all programming is at the microcode level. Microcode is bootstrapped into the writable microcode memory on power-up by the 6800 processor, which in turn is fed by a host mainframe computer during microprogram development. For a completed portable modem, the bootstrapping is from e.p.r.o.m.s in the 6800's memory map.

All data/address buses on the bit-slice are 12 bits wide, together with the a/d, d/a converters, while the width of the microprogram word is 64 bits. Two-level pipelining and parallel hardware stacks, together with fast data paths and devices isolated from slow data buses by registers allow minimization of processor cycle times. The bit-slice machine is connected to the slow processor by an 8-bit bidirectional data register which is directly addressable in the memory map of each machine.

## 4 Conclusions

This paper describes a modem which uses only digital processing to accomplish its operation. When used for h.f. trials the modem demonstrates the viability of microprocessor controlled modulation and demodulation. It also reveals its versatility to be reprogrammed with ease to a completely different modulation scheme.

## 5 Acknowledgments

S. D. Smith would like to acknowledge the support of the S.R.C. and of the Ministry of Defence (Procurement Executive); the authors are grateful for helpful discussions with Mr J. Pennington (A.S.W.E.)

## 6 References

1 Ziemer, R. E., and Tranter, W. H., 'Principles of Communication: Modulation and Noise', Sect. 7.5 (Houghton Mifflin, Boston, 1976).
2 Gorski-Popiel, J. (Ed.), 'Frequency Synthesis: Techniques and Applications' (IEEE Press, New York, 1975).
3 Rabiner, L. R., and Gold, B., 'Theory and Application of Digital Signal Processing' (Prentice Hall, Englewood Cliffs, N.J., 1975).
4 Riley, G. I., 'Error Control for Data Multiplex Systems', Ph.D. Thesis, University of Kent at Canterbury, 1975.
5 Brigham, O., 'The Fast Fourier Transform' (Prentice Hall, Englewood Cliffs, N.J., 1974)
6 'Build a Microcomputer', Advanced Micro Devices, Sunnyvale, Cal., 1979

*Manuscript received by the Institution in final form on 27th March 1981*
*(Paper No. 1993/Comm 220)*

# Contributors to this issue

**K. Pekmestzi** received his Diploma of Electrical Engineering from the National Technical University in Athens, Greece. He is currently a research fellow in the Electronics Department of the Nuclear Research Centre Demokritos while at the same time he is working towards his Ph.D. in the area of digital signal processing.

**Charles Jones** did his National Service in the RAF and in 1950 he entered the Scientific Civil Service at the Signals Research and Development Establishment (now part of the Royal Signals and Radar Establishment) to work on military communications. He graduated in 1964 in electrical engineering, receiving the external B.Sc. honours degree of London University. Mr Jones worked for several years in the fields of design and of failure analysis of micro-electronics, and he contributed a paper to the Journal in April 1972 on aspects of this work. His present interests are in the design of ground stations for satellite communications.

**Patrick Farrell** received the B.Sc. degree in electrical engineering at the City University, London, in 1965. He then undertook post-graduate research in the Engineering Laboratories of the University of Cambridge and in 1969 was awarded his Doctorate for a thesis on aspects of data transmission. From 1965–1969, Dr Farrell was Development Engineer with AEI at Woolwich and in 1968 he joined the Electronics Laboratories at the University of Kent as a lecturer. He was promoted to Senior Lecturer in 1974 and subsequently became Head of the Digital Communications Research Group in the Electronics Laboratories. His appointment to the Chair of Electrical Engineering at the University of Manchester has recently been announced. Dr Farrell has research interests in digital communications, in particular in error-control, signal design, and signal processing for h.f. and other channels.

**Harold Shurmer** received the M.Sc. degree from the University of Wales in 1948, followed by the degrees of Ph.D. and D.Sc.(Eng.) from London University. He worked on semiconducting devices at the former AEI Research Laboratory at Rugby until his move to Warwick University in 1969, where he is currently Reader in Electronics and Deputy Chairman of the School of Electronics. He has contributed numerous papers to the technical press including two in *The Radio and Electronic Engineer* and is author of a book 'Microwave Semiconductor Devices'.

**Sean Smith** received his first degree in electronics from the University of Kent at Canterbury in July 1975. He is currently studying for a Ph.D. in digital communications at Kent, designing and implementing microcoded modems for use at h.f.

**Dimitri Lagoyannis** graduated first from the Athens Higher School of Electronics Engineering, after which he attended the Faculty of Mathematics of the University of Athens and obtained his B.Sc. degree in mathematics. Later on he obtained his Ph.D. degree. In 1960 he joined the Electronics Department of Demokritos Nuclear Research Centre where he has been involved in research and development work on digital systems and delta modulation.

**Keith Dimond** graduated from UMIST in 1965 where he remained as a research student and Demonstrator until 1969 when he was awarded the degree of Ph.D. He then joined the Government Communications Headquarters at Cheltenham where he worked on a variety of projects. He was appointed a Lecturer at the University of Kent in October 1971, where his interests are in the applications of digital systems in industrial control and communications; Dr Dimond is currently involved in developing techniques and tools for implementing systems in v.l.s.i. He is at present a Senior Lecturer in the Electronics Laboratory at the University of Kent.

(See also page 280)